Electrochemical Fragmentation

of Proteins

A thesis

submitted in partial fulfillment

of the requirements for the Degree of

Masters of Science in Chemistry

at the

University of Canterbury

by

Paul Robertson

UNIVERSITY OF CANTERBURY
Te Whare Wānanga o Waitaha
CHRISTCHURCH NEW ZEALAND

2012

Acknowledgments

Abstract

This thesis presents a study of three electrochemical methods applied to the fragmentation of proteins. Direct electrochemical oxidation at graphite electrodes, production of hydroxyl radicals on lead dioxide electrodes and electro-Fenton methods were each investigated as methods for fragmenting proteins. A key objective of this project was to achieve specific fragmentation, meaning that fragmentation would only occur at defined sites on each protein molecule and that this process may provide a new pathway to producing useful protein fragments.

Protein fragments produced by electrochemical means were detected using mass spectroscopy and gel electrophoresis techniques.

Direct electrochemical oxidation of the target proteins was studied at a graphite rod electrode in a solution containing acetonitrile, water and formic acid. β-lactoglobulin fragmentation was detected by mass spectroscopy, but fragmentation did not occur to an extent where fragments were observable by gel electrophoresis. It was evident that most of the electrolysis products appear to arise from non-cleavage oxidation reactions.

The use of PbO_2 electrodes to generate hydroxyl radicals was thoroughly investigated in this work. For the first time, specific fragmentation of proteins has been achieved by direct electrochemical generation of hydroxyl radicals on the electrode surface. The pH

Abstract

and the chemical composition of the protein solutions were found have a strong influence on the extent of fragmentation.

Electro-Fenton chemistry was conducted on a woven carbon fibre electrode. The electrode successfully reduced dissolved oxygen to produce H_2O_2 and regenerated Fe(II) from Fe(III). Cell conditions were optimized for applied current, method of oxygen delivery and cell division. The Fenton reaction between H_2O_2 and Fe(II) produced hydroxyl radicals that were able to specifically fragment proteins. It was not possible to increase the concentration of these protein fragments by increasing the H_2O_2 concentration, as the fragmentation products were also further fragmented.

Electrochemical protein fragmentation was achieved in all three electrochemical systems, however the most promising results were achieved by electrochemical generation of hydroxyl radicals on a lead dioxide electrode. This work has the potential to become a fast and cost effective method for the fragmentation of proteins required for nutrition and medical purposes or for use in protein identification analysis with mass spectroscopy.

Table of Contents

Abbreviations

BSA	Bovine Serum Albumin
BDD	Boron doped diamond
Bis-Tris	2-[Bis-(2-hydroxyethyl)-amino]-2-hydroxymethyl-propane-1,3-diol
CV	Cyclic voltammogram
DTT	Dithiothreitol
GC	Glassy carbon
HEPES	(4-(2-hydroxyethyl)-1-piperazineethanesulfonic acid)
LDS	Lithium dodecyl sulfate
MES	2-(N-morpholino)ethanesulfonic acid
MS	Mass spectroscopy
NTA	Nitrilotriacetic acid
PEG	Polyethylene glycol
RNO	N,N-dimethyl-4-nitrosoaniline
SEM	Scanning electron microscope
Tris	2-Amino-2-hydroxymethyl-propane-1,3-diol
UV	Ultraviolet
SCE	Saturated calomel electrode
Vis	Visible

Chapter 1. Introduction

1.1. Applications for protein hydrosylates

The chemical modification of proteins often gives new products that are significantly more valuable, or have new and useful properties compared to the raw materials. One very useful modification to proteins is hydrosylation, which is the chopping up of proteins into smaller fragments. Hydrosylation of globular proteins such as whey has been occurring for many years, especially in the food industry where high nutritive value food products[1] are required. Protein hydrosylates have become an important component of nutritional supplements for athletes,[2] and have particular importance in medicine to treat patients with food allergies. For example, whey protein hydrosylates have been used to develop hypoallergenic baby formula.[3] Another important use is for digestive disorders, conditions that diminish the body's ability to absorb nutrients in the gastrointestinal tract. Medical conditions that can affect the body's ability to cover its basic protein requirements include severe burns, unconscious states, pancreatitis and Crohn's disease. In these cases artificial feeding maybe important, either through a tube directly into the gastrointestinal tract or intravenously. In both cases the protein administered must be in a hydrolyzed form.[4]

Electrochemistry offers many advantages over the more traditional chemical and enzymatic techniques. It is a cleaner method of modifying proteins compared to existing

chemical methods because there are minimal or no reagents that need to be separated from the products. Importantly from an industrial viewpoint, there is a reduction in the amount of chemicals needing to be disposed of, stored or recycled. Additionally, the electrochemical route may offer a cheaper and more robust alternative to enzymatic cleavage of proteins as enzymes can be expensive and sensitive to some chemical environments.

1.2. Review of current enzyme & chemical methods for protein cleavage

A review of the current enzyme and chemical methods of protein fragmentation is provided in this section for comparison to electrochemical methods used in this thesis.

1.2.1. Specific and Non-specific fragmentation

There are important uses for both specific and non-specific methods of protein fragmentation. Specific fragmentation means that the protein will be cleaved at specific amino acid residues or points in the protein and will cleave each protein molecule in the same way. Non-specific means that cleavage sites will occur at random amino acids and will produce a large number of different sized fragments. The methods most commonly used to achieve fragmentation are mainly enzymatic and chemical methods. The driving force for research in the field at this time is protein cleavage for protein analysis and sequencing with mass spectrometry.

1.2.2. Enzymatic cleavage

Nature has developed many enzymes that are very good at digesting proteins. Some of them are specific for one or several amino acid residues and some are completely non-specific. Thousands of specific proteases found in nature have been identified and expressed. The list of enzymes available to most chemists is limited, but includes a selection of proteases with desirable properties such as high specificity of cleavage site, readily available and good stability.

1.2.2.1. Trypsin

Trypsin is by far the most widely used protease in preparation of proteins for mass spectral analysis. Trypsin is usually extracted from bovine or porcine pancreas and is easily purified. It is a well-characterized serine protease that cleaves proteins at the lysine and arginine residues, unless either of these is followed by a proline residue at the c-terminal end. Trypsin is most active in the pH range of 7-9 and reversibly inactivated at pH 4.[5] It is most effective at a temperature of 37° C and needs to be stored between -20° C and -80° C. A catalytic triad of histadine-57, aspartate-102 and serine-195 achieves trypsin's mechanism of action.[6] These residues combine to form a charge relay, which makes the active site serine nucleophilic. An oxyanion hole in trypsin stabilizes negative charge that develops on the carbonyl oxygen of the cleaved amide. An aspartate residue that stabilizes positive charge is responsible for the peptide being cleaved between lysine and arginine.

1.2.2.2. Other proteases

There are several other proteases commonly used for protein digestion. These are Glu-C, Lys-C, chymotrypsin and Asp-N.[7] Glu-C is isolated from Staphylococcus aureus. It cleaves on the carboxyl side of glutamate residues in acetate or ammonium bicarbonate buffer, but cleaves at both glutamate and aspartate residues in sodium phosphate buffer. Lys-C specifically cleaves at lysine. Chymotrypsin selectively catalyzes the hydrolysis of peptide bonds on the C-terminal side of tyrosine, phenylalanine, tryptophan, and leucine. A secondary hydrolysis will also occur on the C-terminal side of methionine, isoleucine, serine, threonine, valine, histidine, glycine, and alanine.[8] Asp-N specifically cleaves peptide bonds on the N-terminal side of aspartic and cysteic acid.[9] Common non-specific proteases are pepsin, subtilysin, proteinase-K and pronase. These proteases tend to cleave proteins randomly. Digestion time is an important factor with these non-specific proteases, as proteins will be broken down to very small fragments and individual amino acids at long digestion times.

1.2.3. Chemical methods

1.2.3.1 Cyanogen Bromide

Some chemical methods can also be used to cleave proteins. Cyanogen bromide is the most widely used chemical for achieving this. Cyanogen bromide cleaves specifically at methionine residues in the protein backbone. Its mechanism of action involves the electrophilic carbon atom of cyanogen bromide being attacked by the sulfur atom in methionine, which acts as the nucleophile. The bromine atom leaves and a five membered ring is formed when the carbonyl oxygen attacks the carbon atom beside the sulfur atom,

liberating thiocyanide. The iminolactone formed is then nucleophilically attacked by water leading to hydrolysis of the protein backbone.[10] This method is highly specific but the relative infrequency of methionine residues in most proteins limits its usefulness. Cyanogen bromide is highly toxic and moisture sensitive during storage which also limits its potential applications.

1.2.3.2. Other Chemical methods

There are several other chemical methods used to cleave proteins. BNPS-skatole (3-bromo-3-methyl-2-(2-nitrophenyl)thiol-3H-indole) cleaves at tryptophan residues.[11] Hydroxylamine cleaves between asparagine and glycine peptide bonds,[12] 2-nitro-5-thiocyanobenzoic acid (NTCB) cleaves at cysteine residues[13] and formic acid cleaves at aspartic acid residues.[14] Because the above cleavage locations occur at relatively low frequency in most proteins, long peptides chains are usually obtained with use of these chemical agents.

1.3. Description of proteins to be studied

Protein electrochemistry is influenced by individual protein structure and properties. A description of the structure and properties of the target proteins is provided in this section.

1.3.1. Whey

Modifications of whey proteins via hydrolysis have a broad potential for designing functionality for applications in food, medicine and cosmetics industries.[3] The major protein fractions in whey are β-lactoglobulin, α-lactalbumin, bovine serum albumin (BSA) and immunoglobulins.[15] β-lactoglobulin makes up approximately 65 % of whey protein and α-lactalbumin makes up approximately 25 %. β-lactoglobulin is a relatively small soluble protein that usually exists as a dimer with each monomer containing 162 amino acids. It has one free cysteine and two disulphide bridges.[16] One of the main differences structurally between β-lactoglobulin and α-lactalbumin is that α-lactalbumin does not have a free thiol group.

1.3.2. Casein

The family of proteins known as caseins are a group of phosphorylated proteins which exist in milk as casein micelles.[17] Their main function in nature is transporting important nutrients (calcium and phosphorous) to newborns. High proline content, no disulphide bridges, high heterogeneity and temperature-dependent self-association makes structure elucidation of caseins very difficult.[18] Caseins can be thought of approximately as amphiphilic block co-polymers with regions that have high concentrations of either hydrophilic or hydrophobic amino acid residues.[19] The isoelectric point of casein is 4.6 and it becomes increasingly insoluble close to this pH and even more so in the presence of salt.[20] Increasing salt concentrations in protein solutions decreases the solubility of proteins as bulk water required for the solvation layers of individual protein molecules becomes associated with the salt ions. This can expose hydrophobic regions of the protein

surface. Hydrophobic interactions may then cause protein aggregation leading to precipitation of the protein from solution.

1.3.3. Bovine serum albumin

In this thesis work, BSA is used in initial studies as a model for the proteins of interest, as casein and whey are both mixtures of several different proteins. BSA is well characterized and its use removes the complexity of dealing with several different proteins at once. BSA accounts for roughly 8 % of whey proteins, so it is also of interest in that regard. BSA contains 585 amino acids and has a molecular weight of 66776 Da. It contains 17 disulfide bridges throughout the protein and a free sulfhydral group at cys34.[21] BSA is very soluble and stable in a wide range of pH conditions and at temperatures up to 60° C,[21] making it a suitable protein for studying the electrochemical reactions of casein and whey type proteins.

1.4. Direct electrochemical modification of proteins

Electrodes have the ability to accept or donate electrons, so they are able to oxidize or reduce molecules capable of donating or accepting electrons. Proteins contain within them electroactive groups on amino acid side chains, capable of exchanging electrons. When a positive potential is applied to an electrochemical cell, the amino acid residues in the protein most susceptible to direct oxidation are tyrosine, tryptophan, histadine, cysteine and methionine.[22] At negative potentials it is also possible to reduce disulfide

bridges in proteins.[23] Oxidation of aromatic amino acids can lead to reactive intermediates that can be hydroxylated by reaction with water. Sulfur containing cysteine can be oxidized by insertion of up to three oxygen atoms or by forming disulfide bridges with other cysteine residues.

There are problems associated with direct electron-transfer between an electrode and the protein that arise from, irreversible adsorption of proteins to the electrode surface[24] or the electroactive groups in the protein residing in pockets or locations that are buried in the protein making them inaccessible to the electrode surface. However, electron transfer to small proteins and peptides has revealed direct electron transfer induced cleavage of the protein backbone can be initiated by the oxidation of electroactive amino acid residues.[25, 26]

1.4.1. Direct electrochemical cleavage of proteins on platinum and graphite electrodes

Electrochemical oxidation of peptides and proteins has been shown to lead to main chain cleavage next to tyrosine and tryptophan residues on platinum[27, 28] and graphite[25, 26] electrodes. Oxidation of tyrosine and tryptophan can lead to the formation of intermediates that can undergo further reactions with some reaction pathways leading to cleavage of the protein backbone. Figure 1.1 shows a proposed reaction mechanism for an oxidized tryptophan residue that can lead to protein backbone cleavage.[26]
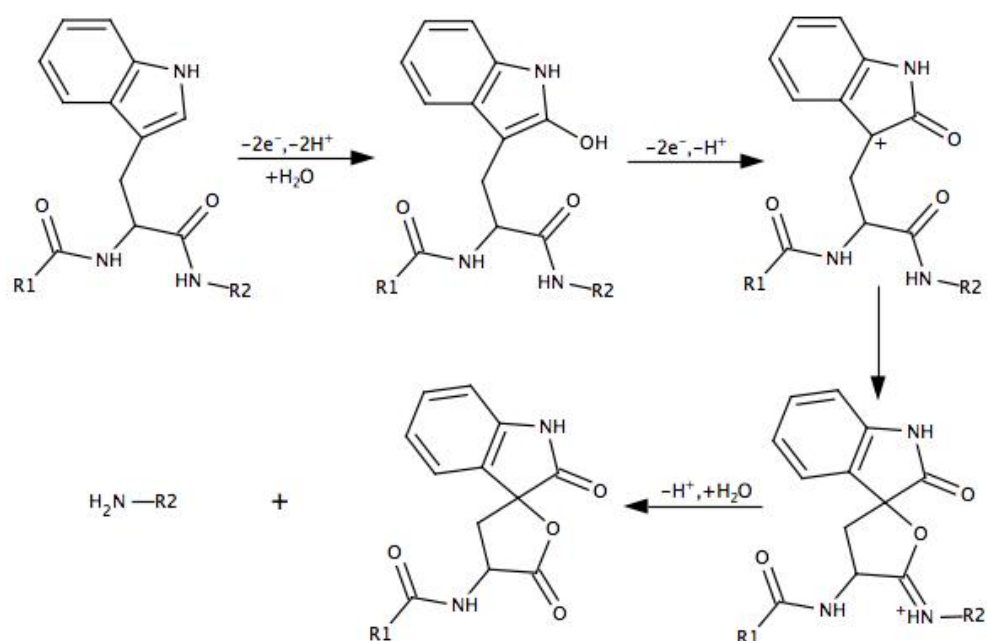
Figure 1.1. Proposed reaction pathway that a tryptophan residue can follow leading to protein backbone cleavage. R1 and R2 represent the rest of the protein on either side of the tryptophan residue.

Once tryptophan or tyrosine are electrochemically oxidized, there is a number of competitive processes, giving multiple reaction pathways and products, which means that not all oxidized tryptophan or tyrosine residues will lead to backbone cleavage in the protein. Figure 1.2 outlines some of the possible reaction pathways that a tyrosine residue can take after oxidation.[26] Products 1, 2 and 3 in figure 2 are tyrosine oxidation products that result in no protein backbone cleavage, but result in a change in mass of the original protein material. Products 4 and 5 are the result of backbone cleavage, which is the target in this project.

9
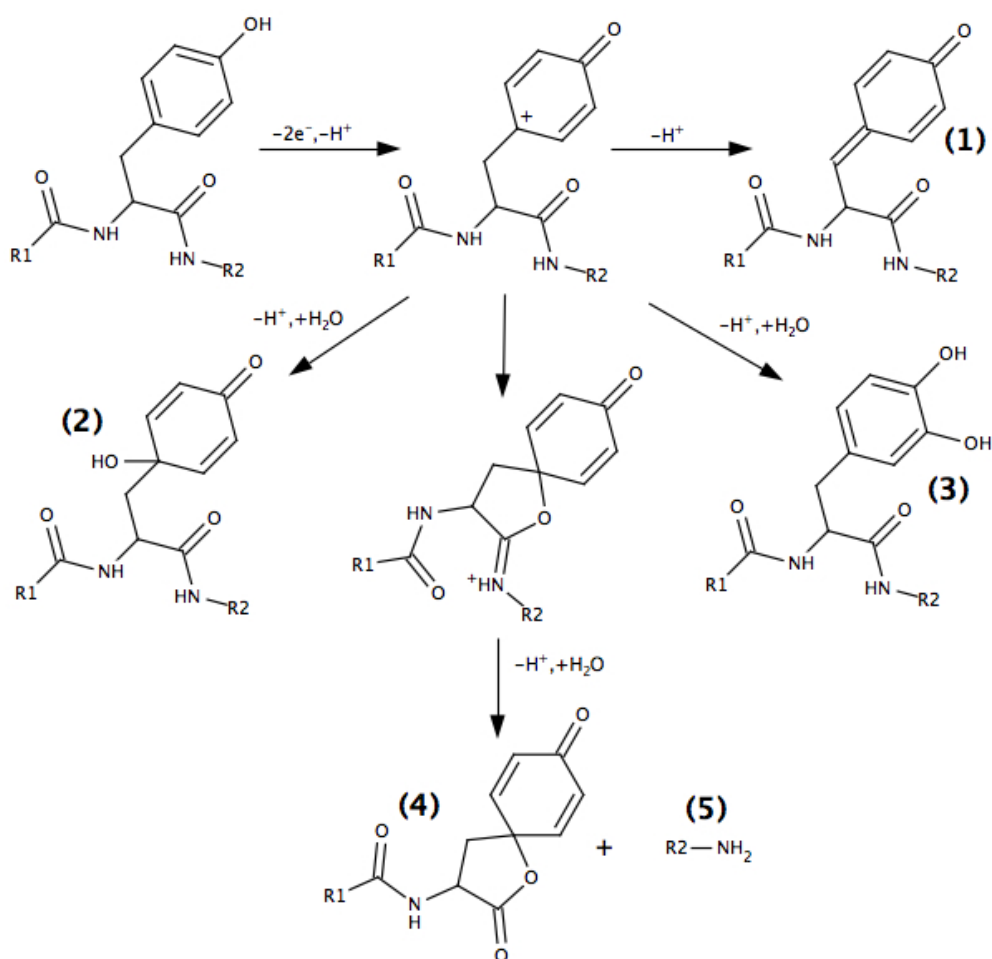
Figure 1.2. Proposed reaction pathways a tyrosine residue. Products 4 and 5 are the successfully cleaved products. R1 and R2 represent the rest of the protein on either side of the tyrosine residue.

Cleavage of tripeptides with either tyrosine or tryptophan in the middle of the sequence has been demonstrated by Roeser et al.[25] They showed that the best cleavage yields (40-80 %) occurred in acidic conditions (pH 1.9-3.1) and little or no cleavage occurred under basic conditions. The adjacent residues to tyrosine and tryptophan in the tripeptides also strongly affected the oxidation products. Their highest cleavage percentage was from the glycine-tyrosine-glycine tripeptide. The low steric hindrance from the glycine residues was thought to be a major factor in this result. Permentier et al were able to demonstrate fragmentation in a range of proteins in solutions of acetonitrile, water and formic acid using a porous flow through graphite electrode, connected directly to a mass

spectrometer.[22] They were able to see cleavage at all possible tyrosine and tryptophan residues in some small proteins (sizes between 6 and 14 kDa). But in larger proteins only some or none of the possible fragments were able to be detected. The main products of their experiments were oxidation products without cleavage, caused mainly by oxidation of cysteine and methionine or oxidation of tyrosine and tryptophan without cleavage. Their work demonstrated that not all proteins would behave in the same manner in relation to cleavage products. But the method is feasible and can be optimized to some extent, for individual proteins.

1.4.2. Disulfide bonds

Disulfide bonds are an important aspect of this project, as disulfide bonds within a protein could hold cleavage products together. Disulfide bonds may also induce a protein structure that makes potential cleavage sites inaccessible, hence reducing the effectiveness of the cleavage process. Various methods can be employed for reducing disulfide bonds. Usually agents such as mercaptoethanol, dithiothreitol (DTT), hydride donors such as sodium borohydride or alkali metals are used to reduce disulfide bonds. The mechanism for DTT reduction of disulfide bonds is shown in figure 1.3.[29]
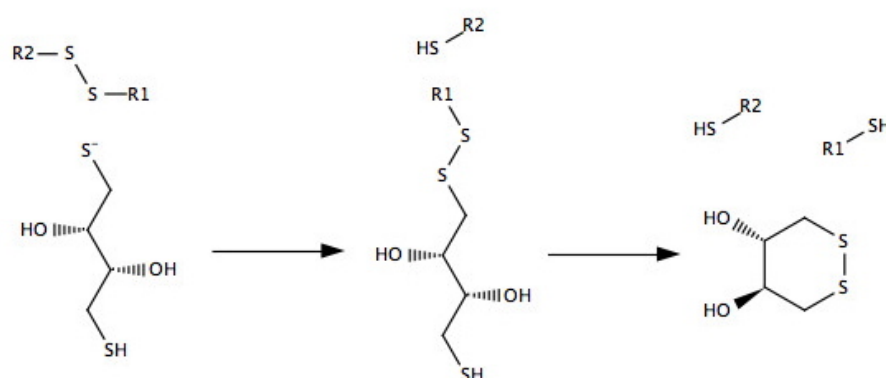
Figure 1.3. Mechanism of disulfide bond reduction by the chemical DTT. R1 and R2 represent the rest of the protein linked by the disulfide bridge.

Electrochemical reduction of disulfides is possible and occurs between -1 and -2 V depending on the environment of the disulfide. This has been demonstrated on mercury and glassy carbon electrodes.[30, 31] However the process is not yet as efficient as chemical methods, because not all the disulfide bonds in the protein may be electrochemically accessible. This can be enhanced by introduction of denaturing agents and high pH, but this also removes some of the value of a clean electrochemical process. If the electrochemical reduction of disulfide bonds could be done more efficiently, it would offer some advantages over chemical methods, because chemical reducing agents can be toxic or difficult to handle. It is also often necessary to separate the excess reagent and byproducts (under anaerobic conditions) to obtain the protein products.[22, 31]

1.4.3. Protein adsorption processes

Proteins spontaneously adsorb to many types of surfaces. This may be considered beneficial or problematic in regard to this project. Typically, protein adsorptions need to be controlled in some way. Since the main aim of this project is to cleave proteins and collect the products, understanding surface desorption phenomena of the proteins (and any fragments) is of importance. Generation of useful protein cleavage products requires the protein fragments to reside in solution rather than fouling the electrode surface.

Protein adsorption is governed by solution conditions, surface properties, individual protein properties and transport conditions.[32] Most proteins are amphiphilic molecules, meaning that they have both hydrophilic and hydrophobic regions. This makes them very surface active. These surface interactions arise from intermolecular forces such as Lewis

acid-base forces, coulombic forces, van der Waals forces and hydrophobic interactions. Hydrophobic interactions could be one of the most useful methods to control adsorption processes, for example, it has been shown that BSA adsorbs less to hydrophilic saccharide modified latex particles than the more hydrophobic unmodified particles.[33] Protein adsorption onto surfaces is usually easy to achieve, however controlling their desorption can be problematic.[24] Intramolecular forces within the protein molecule can alter once the protein is adsorbed, changing the protein conformation and exposing different regions of the protein to the surface after initial adsorption. This can potentially cause more adsorption interactions between the surface and the protein. This means that there can be a large difference between protein adsorption and desorption behaviour. This difference in adsorption and desorption behavior can lead to a perceived irreversibility of the adsorption process.[24]

1.5. Direct electrochemical generation of hydroxyl radicals for cleaving proteins

In this section an outline will be given for the electrochemical generation of hydroxyl radicals on an electrode surface and also how these generated radicals react with proteins.

Fragmentation of proteins has been demonstrated to occur by hydroxyl radicals generated by several methods including, Fenton type reactions[34] and the radiolysis of water in the presence of oxygen[35]. The mechanism of fragmentation by hydroxyl radicals is a result

of the hydroxyl radical's ability to abstract a proton from a saturated carbon site or add to unsaturated carbon atoms or aromatic rings. This gives rise to a radical species that can undergo further reactions, which depend upon the environment of the newly formed radical. Some of these reactions can lead to cleavage of the protein backbone.[36]

1.5.1. Mechanism of protein reactions with hydroxyl radicals

The hydroxyl radical has been shown to be weakly electrophilic so will attack electron rich carbons preferentially. Other factors that affect the position of attack are the strength of the C-H bond in the hydrogen abstraction mechanism, stability of the organoradical that is created and steric effects. Furthermore, the hydroxyl radical will preferentially add to a double bond rather than abstract a proton from a saturated carbon site.[37] All of these factors contribute to the site of hydroxyl reaction.

Hydroxyl radicals can abstract a hydrogen directly from the protein backbone or from aliphatic amino acid side chains. There are four proposed mechanisms that explain hydroxyl radical initiated protein backbone cleavage. Mechanism (a) (figure 1.4): Direct attack at the α-carbon of the protein backbone, usually at glycine because there is less steric hindrance.[38] The radical generated on the α-carbon then undergoes a reaction with oxygen, which leads to peroxyl radical formation and loss. This is followed by hydrolysis of the imine formed cleaving the protein backbone. Mechanism (b) (not shown): Direct attack on the proline side chain may also result in backbone cleavage.[38] Schuessler and Schilling observed that the number of protein residues after fragmentation was approximately equal to the number of prolines in the protein in their radiolysis

experiments.[39] Mechanism (c) (not shown): Main chain cleavage can occur via oxidation

at γ-carbon on the side chain occurs via free radical transfer from side chain to backbone,

which can result in cleavage of the backbone. Mechanism (d) (not shown): Main chain

cleavage can occur via radical transfer from the β-carbon in the side chain. Initial

hydroxyl radical attack at the β-carbon can lead to the formation of a radical on the α-

carbon, which can lead to main chain scission.[38]
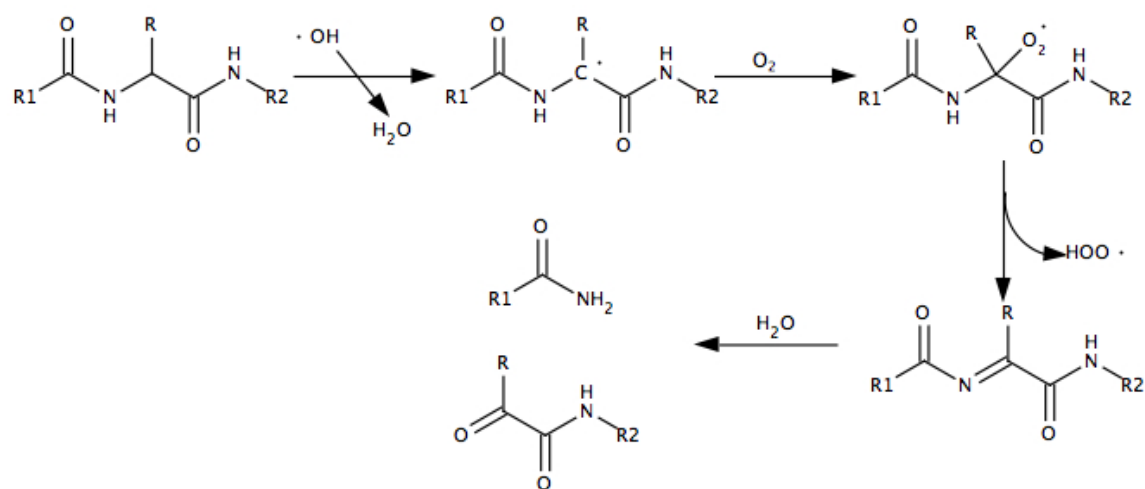
Figure 1.4. Proposed mechanism showing the direct attack at the α-carbon of the protein
backbone by the hydroxyl radical.

1.5.2. Electrochemical generation of hydroxyl radicals on lead dioxide electrodes

Two of the most common anodes for oxidation of organic species are lead dioxide (PbO_2)

and boron doped diamond (BDD).[40-45] These two electrodes have high oxidation power,

because they generate hydroxyl radicals that are physisorbed to the surface.[46, 47] Once

generated, the radicals are able to react with organic molecules that are in the vicinity of

the electrode. BDD electrodes can achieve higher mineralisation rates of organics than

PbO_2 electrodes, however PbO_2 electrodes are much cheaper and easier to produce

making them more suitable for a commercial setting. PbO_2 is a material that is often used

when high anodic potentials are required as it is a stable low cost material with good electrocatalytic activity.

Cong et al showed that hydroxyl radicals could be generated electrochemically from water using a standard cell design and commonly available electrolytes.[48] A basic undivided cylindrical cell was used for the electrochemical production of the hydroxyl radical. The anode was a β-PbO_2 electrode doped with fluorine, and was chosen because it has a high oxygen overpotential and good electro-catalytic activity for effective generation of the hydroxyl radicals instead of oxygen evolution. The solution containing deionised water and Na_2SO_4 as supporting electrolyte was electrolysed at 7.5 V. Electron spin resonance was used to successfully detect the hydroxyl radical created in solution.

This approach offers several advantages over chemical methods of hydroxyl radical generation, the major one being that is an environmentally friendly process. It could prove to be a useful method for cleaving the target proteins as it has a very simple cell setup and generates the reactive species from water and common electrolytes with no need for additional chemicals.

1.5.3. PbO_2 electrode preparation

There is a vast amount of literature on the deposition of PbO_2 films on many different substrates including platinum,[49] titanium,[50] gold,[51] tin dioxide[52] and glassy carbon.[53] There can be some confusion surrounding optimum deposition conditions because there

are many parameters that can be altered to give PbO_2 coatings with different characteristics and morphologies. PbO_2 is a polymorphic substance with two allotropic forms known as α-PbO_2 and β-PbO_2. α-PbO_2 has an orthorhombic structure and β-PbO_2 is tetragonal. α-PbO_2 has a compact structure whereas β-PbO_2 has a much more open structure which is more porous and provides a higher surface area.[54, 55] β- PbO_2 is generally preferable as an electrode material as it is a factor of 10 more conductive than α-PbO_2.[56, 57] The conductivity of β-PbO_2 is similar to that of titanium or mercury and higher than most forms of carbon.[58] PbO_2 electrodes are often written as PbO_2, but the actual ratio of oxygen to lead is close to 1.94-1.96 to 1 depending on the method of preparation.[59] There are also a variable number of water molecules throughout the crystal structure of PbO_2.[60] The deficiency in oxygen gives PbO_2 its metallic-like conductivity.[61]

1.5.4. Synthesis of PbO$_2$ electrodes

Deposition conditions are very important as they can control several important characteristics of PbO_2 films. Film adhesion to the conducting substrate, surface morphology, α and β ratio and catalytic activity can all be affected by varying different parameters including:

- The substrate.

- The pH of plating solution.

- Anionic species present in the electrolyte.

- The concentration of Pb^{2+} in the plating solution.

- The current density of the deposition, which is the amount of current applied/area of

electrode (A/cm^2). This determines the rate of deposition.

- Potential of deposition. This determines the rate of any competing reactions that are taking place, especially the O_2 evolution reaction.

- Mass transport in the plating bath, determined by rate of stirring, ultrasound or other methods.

The deposition conditions determine the quality of the PbO_2 film, but from the literature, no clear conclusions can be made about the optimum conditions required to give the best film. There are several reasons for this: not all of the conditions used in various laboratories are controlled or stated in papers. The large number of adjustable variables for deposition means that there are many possible combinations of conditions that can be used. This makes it difficult to reproduce results from the literature. Another reason is that different laboratories value different qualities in their PbO_2 films, so films are not evaluated in the same way, for example, it is difficult to compare a film that has been evaluated based only on mechanical strength with one that has only been evaluated based on overpotential for oxygen evolution.

1.5.5. Mechanism of PbO_2 deposition

Valichenko et al have proposed a mechanism (equations 1-4) for the deposition of PbO_2 onto an electrode surface.[62-65]

(1) $H_2O \rightarrow OH_{ads} + H^+ + e^-$

(2) $Pb^{2+} + OH_{ads} \rightarrow Pb(OH)^{2+}$

(3) $Pb(OH)^{2+} + H_2O \rightarrow Pb(OH)_2^{2+} + H^+ + e^-$

(4) $Pb(OH)_2^{2+} \rightarrow PbO_2 + 2H^+$
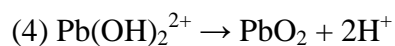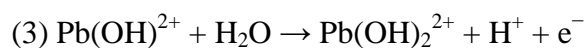
The mechanism has been proposed to proceed in four stages. In the first stage water is oxidised on the anode to give OH_{ads} chemisorbed to the electrode surface. The second step involves a chemical reaction between Pb^{2+} and OH_{ads} to form a soluble intermediate product $Pb(OH)^{2+}$. This species is oxidised on the electrode surface forming an oxygenated soluble Pb(IV) compound $Pb(OH)_2^{2+}$, which then decomposes chemically in the final step to form a hydrated Pb(IV) species in solution that crystallizes on the electrode surface as PbO_2. At low current density the rate limiting step is step 3, but at high current density the rate is controlled by diffusion of Pb^{2+} to the electrode surface.[66]

1.5.6. Doping of PbO$_2$ films

Important properties of PbO_2 films can be improved by inclusion of dopants in the deposition bath, which can be incorporated into the deposited film. Introducing dopants such as fluorine,[67, 68] bismuth[69, 70] and iron[71] during the deposition can alter important properties, such as: mechanical strength,[72] surface area[73] and the oxygen evolution potential.[74]

1.5.7. How PbO$_2$ electrodes generate radicals

The exact mechanism by which PbO_2 electrodes generate hydroxyl radicals is not well understood and could be quite complex. Johnson and co-workers propose that there are surface sites on PbO_2 capable of adsorbing hydroxyl radicals produced during the hydrolysis of water.[75, 76] Possible reactions that can occur are outlined in equations 5-8 below. $PbO_2[]$ represents an unoccupied surface site on the PbO_2 electrode and

$PbO_2[OH\bullet]$ indicates an $OH\bullet$ adsorbed to a surface site. R represents an organic species that is oxidized upon reaction with the hydroxyl radical species.

(5) $PbO_2[] + H_2O \rightarrow PbO_2[OH\bullet] + H^+ + e^-$

(6) $PbO_2[OH\bullet] + R \rightarrow PbO_2[] + RO + H^+ + e^-$

(7) $PbO_2[OH\bullet] + H_2O \rightarrow PbO_2[] + O_2 + 3H^+ + 3e^-$

(8) $2\ PbO_2[OH\bullet] \rightarrow 2PbO_2[] + O_2 + 2H^+ + 2e^-$
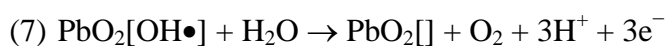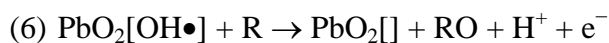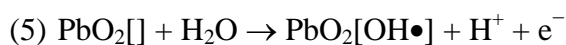
In the absence of organic species to react with the hydroxyl radicals, and also as competitive processes in the presence of organic species, reactions 7 and 8 occur producing oxygen. An efficient electrode must optimize reactions 5 and 6 while minimizing reactions 7 and 8.

1.6. Electrochemical generation of H_2O_2 for use in the Fenton reaction

In the following section the process of electrochemically generating H_2O_2 for use in the Fenton reaction to produce hydroxyl radicals will be explained. The hydroxyl radicals produced will be used to fragment proteins as outlined in section 1.5.

1.6.1. Generation of hydroxyl radicals by the Fenton reaction

The Fenton reaction was discovered by H. J. H. Fenton during the 1890s when he realised that he could oxidise tartaric acid after activating H_2O_2 with Fe(II) salts.[77] In 1934 Haber and Weiss proposed that the active oxidant generated in the Fenton reaction was the hydroxyl radical.[78] The classical mechanism for the reaction between H_2O_2 and an iron

catalyst in acidic solution and in the absence of any organic compounds to produce

hydroxyl radicals was proposed in 1949 by Barb et al, as outlined in equations 9-15.[79]

(9) $Fe^{2+} + H_2O_2 \rightarrow Fe^{3+} + OH\bullet + OH^-$

(10) $Fe^{3+} + H_2O_2 \rightarrow Fe^{2+} + OOH\bullet + H^+$

(11) $OH\bullet + H_2O_2 \rightarrow OOH\bullet + H_2O$

(12) $OH\bullet + Fe^{2+} \rightarrow Fe^{3+} + OH^-$

(13) $Fe^{3+} + OOH\bullet \rightarrow Fe^{2+} + O_2 + H^+$

(14) $Fe^{2+} + OOH\bullet + H^+ \rightarrow Fe^{3+} + H_2O_2$

(15) $OOH\bullet + OOH\bullet \rightarrow H_2O_2 + O_2$
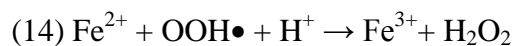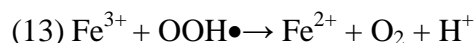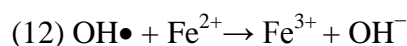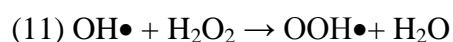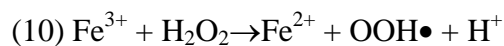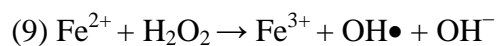
The reaction between Iron(II) and H_2O_2 can proceed at stoichiometric concentrations of

H_2O_2 and Fe(II) salts but a stoichiometric amount of Fe(III) will result eventually,

leading to insoluble Fe(III) oxyhydroxides as the pH increases from acidic to neutral. The

Fe(III) precipitates are collectively referred to as 'iron sludge' and are undesirable in most

applications of the Fenton reaction. Fe(II) can be regenerated according to equation 10,

so Fe(II) can be used in catalytic quantities reducing the amount of iron sludge formed.

However, reaction 10 is several orders of magnitude slower reaction 9. The rate constant

for equation 9 is 76 $M^{-1}s^{-1}$ and the rate constant for equation 10 is 0.01-0.02 $M^{-1}s^{-1}$. [80, 81]

The difference in the rates of reactions 9 and 10 reduces the efficiency of the reaction,

however there are other methods of reducing Iron(III) to Iron(II), which will be discussed

later. Another advantage of using iron in catalytic amounts, at a molar ratio of between

100-1000 for peroxide to iron, is that it limits hydroxyl radical scavenging by iron according to equation 12.

The initiation of the Fenton reaction can be achieved by adding Fe(II) or Fe(III) to H_2O_2. In the case of adding Fe(II), all of the Fe(II) will be quickly oxidized to Fe(III) so after the initial burst of activity, the system will behave in the same manner regardless of the initial oxidation state of the iron. The initial burst phase that occurs as a result of adding Fe(II) can be used to promote a rapid initial phase of degradation of the target compound.[82, 83] On the other hand it may also be desirable to have a slow rate at the beginning of the reaction which can be achieved by using Fe(III) to initiate the reaction.

1.6.2. Influence of pH

The Fenton reaction has been found to be most efficient at pH 2.8-3.[84-87] This is mainly due to the speciation of Fe(II) and Fe(III), which is controlled in part by the pH and the effectiveness of these iron species at participating in the Fenton reaction.

Fe(II) exists largely as $Fe(H_2O)_6^{2+}$ below pH 3. As the pH increases it becomes increasingly hydrolysed to $Fe(H_2O)_5OH^+$ and $Fe(H_2O)_4(OH)_2$. Note: the water ligands will be dropped from now on when referring to these compounds. $Fe(OH)_2$ reacts approximately 7 times faster than Fe^{2+} in the reaction shown in equation 9. $Fe(OH)_2$ becomes more prevalent and it's concentration reaches a plateau as the pH increases from pH 3 to 4.[88, 89] This means that the rate of reaction 9 is optimum above pH 3. Since the

optimum pH for the Fenton reaction is usually pH 2.8-3, it can be concluded that Fe(III) speciation determines the optimum pH for the reaction. Above pH 3, Fe(III) becomes extensively hydrolysed according to equation 16[90] and begins to precipitate in the form of insoluble oxyhydroxides which are much less Fenton reactive and do not easily redissolve.[91]

$$(16) \ Fe^{3+} \leftrightharpoons Fe(OH)^{2+} \leftrightharpoons Fe(OH)_2^+ \leftrightharpoons Fe(OH)_2^{4+} \rightarrow \rightarrow \rightarrow Fe_2O_3$$
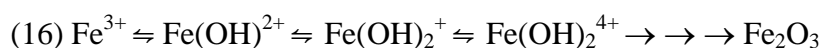
1.6.3. Ligand influence on pH dependence

Attempts have been made to extend the pH range in which the Fenton reaction can operate in, by adding chelating agents to bind Iron(III), competing against the formation of insoluble oxyhydroxides.[92] Suitable iron complexes formed by chelating agents need to be capable of producing hydroxyl radicals upon reaction with H_2O_2, and be resistant to oxidation by the oxidising species present during the reaction. Pignatello et al[93] studied the decomposition of the pesticide 2,4-D by the Fenton reaction at pH 6 by adding a range of iron complexing ligands. They established a list of ligands capable of producing a similar rate of decomposition as unchelated Fe(III) at pH 2.8. The list included nitrilotriacetic acid (NTA), rhodizonic acid, gallic acid, hexaketocyclohexane, picolinic acid, and tetrahydroxy-1,4-quinone. All of the organic ligands tested were eventually oxidised in the medium, but the formation of insoluble iron oxyhydroxides was able to be prevented for periods of hours to days. Inorganic iron complexing agents such as pyrophosphate have also been used to stop Fe(III) from precipitating at higher pH.[94] Pyrophosphate has the added advantage that it cannot be oxidized by the Fenton reaction.

1.6.4. Metal binding ability of proteins

Some proteins have the ability to bind metal ions, such as copper and iron, at specific sites in the protein structure that can be used to initiate the Fenton reaction. This property has been proposed to lead to a site-specific generation of hydroxyl radicals upon reaction of the bound metal ion and H_2O_2 at the metal binding sites in the protein. This phenomenon has been described as a 'cage-like' effect,[35] where the radicals generated are confined to reacting preferentially with the amino acid residues nearby in the metal binding pocket of the protein and are less able to diffuse into solution and react with other parts of the protein. In proteins with metal binding sites, radical scavengers have much less effect in slowing down the oxidation of the protein compared with proteins that don't have metal binding sites. Radical scavengers must enter the 'cage' to compete for the radicals that are generated in situ inside the cage like structure; this is an inefficient process. For proteins that do not have the ability to bind metal ions at specific sites, it may be possible to chelate the metal ion with ligands in a way that makes it able to be bound by the protein. For example, some proteins have hydrophobic binding pockets, which may be able to bind a metal ion chelated by hydrophobic ligands.

1.6.5. Electro-Fenton reaction

The electro-Fenton reaction is a process in which one or both of the species required for the Fenton reaction are electrochemically generated. [95, 96] In general this process can be divided into 4 categories.[97] In category 1 H_2O_2 is generated electrochemically from reduction of oxygen at the cathode and iron is added to the solution externally. In this system it may also be possible to regenerate Iron(II) at the cathode depending on the cathode material and type.[98, 99] In type 2, a sacrificial anode made of iron is used to

provide the Iron(II) and H_2O_2 is externally applied.[100, 101] In type 3, H_2O_2 is generated on the cathode electrochemically and iron is supplied by a sacrificial anode. In the fourth category iron is regenerated from Iron(III) in solution on the cathode and H_2O_2 is externally applied.[102, 103]

1.6.6. Electrochemical generation of H_2O_2

H_2O_2 is an excellent oxidiser that is environmentally friendly, since it leaves no hazardous residues, such as other oxidants. It is commercially produced by the autooxidation of 2-alkyl anthrahydroquinones.[104]

On site electrochemical production of H_2O_2 through the reduction of dioxygen has gained a lot of interest recently as it eliminates the potential hazards associated with transport, handling and storage of such a strong oxidising agent. This has led to numerous studies relating to the electrochemical production of H_2O_2.

1.6.7. Electrode materials for H_2O_2 production

The cathode materials used for H_2O_2 electrosynthesis are carbon-based cathodes such as bulk graphite, reticulated vitreous carbon, carbon or graphite felt or carbon polytetrafluroethylene (PTFE) gas diffusion electrodes (GDE). The anode materials used are Pt-wire or dimensionally stable anodes (titanium coated with RuO_2).[105, 106] GDEs work by passing the oxygen required for the reaction across the back of the electrode. They have been shown to be more efficient in producucing H_2O_2 than graphite electrodes

where oxygen is sparged into solution near the electrode surface.[107] However the usable lifetime of GDEs is much shorter than bulk graphite.

1.6.8. Cell design for H_2O_2 production

A comparison of H_2O_2 production in divided and undivided cells showed that membrane-separated cells achieve a much higher performance.[108] This is mainly because divided cells prevent the decomposition of H_2O_2 that occurs at the anode in the undivided cell. Cells can be divided by the use of a cation exchange membrane, which prohibits the transfer of H_2O_2 molecules and anions between the cell compartments. Protons generated at the anode are electrically driven through the membrane into the catholyte, partially supplementing the protons consumed at the cathode.

1.7. Aims and scope of this work

The aim of this project is to use electrochemical techniques to cleave globular proteins from milk (casein and whey) into smaller fragments using three separate electrochemical techniques. A key objective of this project is to achieve specific fragmentation, meaning that fragmentation would only occur at defined sites on each protein molecule. This process may provide a new pathway to producing useful protein fragments. Direct electrochemical oxidation at graphite electrodes, production of hydroxyl radicals on lead dioxide electrodes and electro-Fenton methods will each be investigated as methods for fragmenting proteins.

Protein fragments produced by electrochemical means were detected using mass spectroscopy and gel electrophoresis techniques. UV-VIS spectroscopy, cyclic voltammetry, electrochemical impedance spectroscopy and scanning electron microscopy techniques are also used for evaluation of the three electrochemical methods of protein fragmentation used in this work.

Initially, direct electrochemical oxidation of proteins at carbon electrodes will be undertaken in order to investigate the potential of the method for fragmentation of proteins. These studies will also give an understanding of adsorption processes of proteins in general at carbon.

Electrochemical generation of hydroxyl radicals as reactive intermediates to initiate protein cleavage will be investigated in two ways: by using direct electrochemical generation of hydroxyl radicals from water on PbO_2 electrodes and by using electro-Fenton generation of hydroxyl radicals using woven carbon fibre electrodes to produce the H_2O_2 required for the Fenton reaction. Electrochemical protein fragmentation in all three systems will be compared to determine the most promising system.

References

1. Hauser, B., U. Blecker, B. Suys, and S. Peeters, *The Nutritional Value of a Whey Hydrolysate Formula Compared with a Whey-Predominant Formula in Healthy Infants.* Journal of pediatric gastroenterology and nutrition, 1993. **17**(1): p. 92-96.

2. Frokjaer, S., *Use of Hydosylates for Protein Supplementation.* Food technology (Chicago), 1994. **48**(10): p. 86-88.

3. Foegeding, E.A., J.P. Davis, D. Doucet, and M.K. McGuffey, *Advances in modifying and understanding whey protein functionality.* Trends in Food Science & Technology, 2002. **13**(5): p. 151-159.

4. Neklyudov, A., A. Ivankin, and A. Berdutina, *Properties and uses of protein hydrolysates (Review).* Applied Biochemistry and Microbiology, 2000. **36**(5): p. 452-459.

5. Beynon, R. and J.S. Bond, *Commercially Available Proteases*, in *Proteolytic Enzymes: A Practical Approach*, R. Beynon and J.S. Bond, Editors. 1989, IRL Press: Oxford, UK.

6. Polgár, L., *The catalytic triad of serine peptidases.* Cellular and Molecular Life Sciences, 2005. **62**(19): p. 2161-2172.

7. Wood, E.J., *Enzymes of molecular biology volume 16.* Biochemical education, 1993. **21**(4): p. 221-221.

8. Burrell, M.M.e., *Enzymes of Molecular Biology*. 1993, Humana Press: Totowa, NJ. p. 277-281.

9. Drapeau, G.R., *Substrate specificity of a proteolytic enzyme isolated from a mutant of Pseudomonas fragi.* Journal of Biological Chemistry, 1980. **255**(3): p. 839-840.

10. Kaiser, R. and L. Metzka, *Enhancement of Cyanogen Bromide Cleavage Yields for Methionyl-Serine and Methionyl-Threonine Peptide Bonds.* Analytical Biochemistry, 1999. **266**(1): p. 1-8.

11. Rahali, V. and J. Gueguen, *Chemical Cleavage of Bovine β-Lactoglobulin by BNPS-Skatole for Preparative Purposes: Comparative Study of Hydrolytic Procedures and Peptide Characterization.* Journal of Protein Chemistry, 1999. **18**(1): p. 1-12.

12. Saris, C.J.M., J. van Eenbergen, B.G. Jenks, and H.P.J. Bloemers, *Hydroxylamine cleavage of proteins in polyacrylamide gels.* Analytical Biochemistry, 1983. **132**(1): p. 54-67.

13. Eshdat, Y. and A. Lemay, *Specific fragmentation of human erythrocyte spectrin by chemical cleavage at cysteine residues.* Biochimica et Biophysica Acta (BBA) - Protein Structure, 1979. **577**(2): p. 360-370.

14. Piszkiewicz, D., M. Landon, and E.L. Smith, *Anomalous cleavage of aspartyl-proline peptide bonds during amino acid sequence determinations.* Biochemical and Biophysical Research Communications, 1970. **40**(5): p. 1173-1178.

15. Haug, A., A. Hostmark, and O. Harstad, *Bovine milk in human nutrition--a review.* Lipids in health and disease, 2007. **6**: p. 25.

16.   Brownlow, S., J.o.H.M. Cabral, R. Cooper, D.R. Flower, S.J. Yewdall, I. Polikarpov, A.C.T. North, and L. Sawyer, *Bovine β-lactoglobulin at 1.8Å resolution - still an enigmatic lipocalin.* Structure, 1997. **5**(4): p. 481-495.

17.   Horne, D.S., *Casein structure, self-assembly and gelation.* Current Opinion in Colloid & Interface Science, 2002. **7**(5-6): p. 456-461.

18.   Bansal, P.S., P.A. Grieve, R.J. Marschke, N.L. Daly, E. McGhie, D.J. Craik, and P.F. Alewood, *Chemical synthesis and structure elucidation of bovine [kappa]-casein (1-44).* Biochemical and Biophysical Research Communications, 2006. **340**(4): p. 1098-1103.

19.   Liu, Y. and R. Guo, *pH-dependent structures and properties of casein micelles.* Biophysical Chemistry, 2008. **136**(2-3): p. 67-73.

20.   Strange, E.D., D.L. Van Hekken, and V.H. Holsinger, *Effect of Sodium Chloride on the Solubility of Caseins.* Journal of Dairy Science, 1994. **77**(5): p. 1216-1222.

21.   Peters, T., *Serum Albumin.* Advances in Protein Chemistry, 1985. **37**: p. 161-245.

22.   Permentier, H.P. and A.P. Bruins, *Electrochemical oxidation and cleavage of proteins with on-line mass spectrometric detection: Development of an instrumental alternative to enzymatic protein digestion.* Journal of the American Society for Mass Spectrometry, 2004. **15**(12): p. 1707-1716.

23.   Rivat, C., M. Fontaine, C. Ropartz, and C. Caullet, *Electrochemical reduction of immunoglobulins specific reduction of the inter-heavy chain disulfide bridges of igg.* European Journal of Immunology, 1973. **3**(9): p. 537-542.

24.   Hlady, V. and J. Buijs, *Protein adsorption on solid surfaces.* Current Opinion in Biotechnology, 1996. **7**(1): p. 72-77.

25.   Roeser, J., H.P. Permentier, A.P. Bruins, and R. Bischoff, *Electrochemical Oxidation and Cleavage of Tyrosine- and Tryptophan-Containing Tripeptides.* Analytical Chemistry, 2010. **82**(18): p. 7556-7565.

26.   Permentier, H.P., U. Jurva, B. Barroso, and A.P. Bruins, *Electrochemical oxidation and cleavage of peptides analyzed with on-line mass spectrometric detection.* Rapid Commun Mass Spectrom, 2003. **17**(0951-4198).

27.   Iwasaki, H. and B. Witkop, *New Methods for Nonenzymatic Peptide Cleavage. Electrolytic, Differential, and Solvolytic Cleabage of the Antibiotic Cyclopeptide Rufomycin.* Journal of the American Chemical Society, 1964. **86**(21): p. 4698-4708.

28.   Cohen, L.A. and L. Farber, *Cleavage of tyrosyl-peptide bonds by electrolytic oxidation.* Methods Enzymol., 1967. **11**: p. 299-308.

29.   Cleland, W.W., *Dithiothreitol, a New Protective Reagent for SH Groups*.* Biochemistry, 1964. **3**(4): p. 480-482.

30.   Honeychurch, M.J., *The reduction of disulfide bonds in proteins at mercury electrodes.* Bioelectrochemistry and Bioenergetics, 1997. **44**(1): p. 13-21.

31.   Cayot, P., H. Rosier, L. Roullier, T. Haertlé, and G. Tainturier, *Electrochemical modifications of proteins: disulfide bonds reduction.* Food Chemistry, 2002. **77**(3): p. 309-315.

32.   Santos, O., T. Nylander, M. Paulsson, and C. Trägårdh, *Whey protein adsorption onto steel surfaces--effect of temperature, flow rate, residence time and aggregation.* Journal of Food Engineering, 2006. **74**(4): p. 468-483.

33.   Revilla, J., A. Elaïssari, P. Carriere, and C. Pichot, *Adsorption of Bovine Serum Albumin onto Polystyrene Latex Particles Bearing Saccharidic Moieties.* Journal of Colloid and Interface Science, 1996. **180**(2): p. 405-412.

34.   Hunt, J.V., J.A. Simpson, and R.T. Dean, *Hydroperoxide-mediated fragmentation of proteins.* Biochemical Journal, 1988. **250**(1): p. 87-80.

35.   Stadtman, E.R., *Oxidation of Free Amino Acids and Amino Acid Residues in Proteins by Radiolysis and by Metal-Catalyzed Reactions.* Annual Review of Biochemistry, 1993. **62**(1): p. 797-821.

36.   Xu, G. and M.R. Chance, *Hydroxyl Radical-Mediated Modification of Proteins as Probes for Structural Proteomics.* Chemical Reviews, 2007. **107**(8): p. 3514-3543.

37.   Pignatello, J.J., E. Oliveros, and A. MacKay, *Advanced Oxidation Processes for Organic Contaminant Destruction Based on the Fenton Reaction and Related Chemistry.* Critical Reviews in Environmental Science and Technology, 2006. **36**(1): p. 1-84.

38.   Headlam, H.A. and M.J. Davies, *Beta-scission of side-chain alkoxyl radicals on peptides and proteins results in the loss of side-chains as aldehydes and ketones.* Free Radical Biology and Medicine, 2002. **32**(11): p. 1171-1184.

39.   Schuessler, H. and K. Schilling, *Oxygen Effect in the Radiolysis of Proteins -- Part 2 Bovine Serum Albumin.* International Journal of Radiation Biology, 1984. **45**(3): p. 267-281.

40.   Luong, J.H.T., K.B. Male, and J.D. Glennon, *Boron-doped diamond electrode: synthesis, characterization, functionalization and analytical applications.* analyst, 2009. **134**(10): p. 1965-1979.

41.   Karolina, P., J. Musilova, and J. Barek, *Boron-Doped Diamond Film Electrodes - New Tool for Voltammetric Determination of Organic Substances.* Critical Reviews in Analytical Chemistry, 2009. **39**(3): p. 148-172.

42.   Kapalka, A., G. Foti, and C. Comninellis, *The importance of electrode material in environmental electrochemistry: Formation and reactivity of free hydroxyl radicals on boron-doped diamond electrodes.* Electrochimica Acta, 2009. **54**(7): p. 2018-2023.

43.   Liu, Y. and H. Liu, *Comparative studies on the electrocatalytic properties of modified PbO2 anodes.* Electrochimica Acta, 2008. **53**(16): p. 5077-5083.

44.   Cong, Y. and Z. Wu, *Electrocatalytic Generation of Radical Intermediates over Lead Dioxide Electrode Doped with Fluoride.* The Journal of Physical Chemistry C, 2007. **111**(8): p. 3442-3446.

45.   Velichenko, A.B., R. Amadelli, G.L. Zucchini, D.V. Girenko, and F.I. Danilov, *Electrosynthesis and physicochemical properties of Fe-doped lead dioxide electrocatalysts.* Electrochimica Acta, 2000. **45**(25-26): p. 4341-4350.

46.   Comninellis, C., *Electrocatalysis in the electrochemical conversion/combustion of organic pollutants for waste water treatment.* Electrochimica Acta, 1994. **39**(11-12): p. 1857-1862.

47.   Panizza, M., I. Sirés, and G. Cerisola, *Anodic oxidation of mecoprop herbicide at lead dioxide.* Journal of Applied Electrochemistry, 2008. **38**(7): p. 923-929.

48.   Cong, Y., Z. Wu, and Y. Li, *Hydroxyl radical electrochemically generated with water as the complete atom source and its environmental application.* Chinese Science Bulletin, 2007. **52**(10): p. 1432-1435.

49.   Hwang, B.J., R. Santhanam, and Y.W. Chang, *Mechanism of Electrodeposition of PbO2 at a Pt Sheet/Rotating Disk Electrode.* Electroanalysis, 2002. **14**(5): p. 363-367.

50.   Ghasemi, S., M.F. Mousavi, and M. Shamsipur, *Electrochemical deposition of lead dioxide in the presence of polyvinylpyrrolidone: A morphological study.* Electrochimica Acta, 2007. **53**(2): p. 459-467.

51.   Mohd, Y. and D. Pletcher, *The Influence of Deposition Conditions and Dopant Ions on the Structure, Activity, and Stability of Lead Dioxide Anode Coatings.* Journal of The Electrochemical Society, 2005. **152**(6): p. D97-D102.

52.   Nan Ho, C. and B. Joe Hwang, *Effects of copper cation and acetate anion on the growth of PbO2 on a SnO2/Ti substrate.* Electrochimica Acta, 1993. **38**(18): p. 2749-2757.

53.   González-García, J., V. Sáez, J. Iniesta, V. Montiel, and A. Aldaz, *Electrodeposition of PbO2 on glassy carbon electrodes: influence of ultrasound power.* Electrochemistry Communications, 2002. **4**(5): p. 370-373.

54.   Shen, P.K. and X.L. Wei, *Morphologic study of electrochemically formed lead dioxide.* Electrochimica Acta, 2003. **48**(12): p. 1743-1747.

55.   Abaci, S. and A. Yildiz, *Electropolymerization of thiophene and 3-methylthiophene on PbO2 electrodes.* Journal of Electroanalytical Chemistry, 2004. **569**(2): p. 161-168.

56.   Mindt, W., *Electrical Properties of Electrodeposited PbO2 Films.* Journal of The Electrochemical Society, 1969. **116**(8): p. 1076-1080.

57.   Inguanta, R., F. Vergottini, G. Ferrara, S. Piazza, and C. Sunseri, *Effect of temperature on the growth of [alpha]-PbO2 nanostructures.* Electrochimica Acta, 2010. **55**(28): p. 8556-8562.

58.   Li, X., D. Pletcher, and F.C. Walsh, *Electrodeposited lead dioxide coatings.* Chemical Society Reviews, 2011. **40**(7): p. 3879-3894.

59.   Munichandraiah, N., *Physicochemical properties of electrodeposited β-lead dioxide: Effect of deposition current density.* Journal of Applied Electrochemistry, 1992. **22**(9): p. 825-829-829.

60.   Trasatti, S., *Electrodes of conductive metallic oxides.* 1981: Elsevier Scientific Pub. Co.

61.   Barak, M., *Electrochemical power sources: primary and secondary batteries.* 1980: P. Peregrinus on behalf of the Institution of Electrical Engineers.

62.   Velichenko, A.B., R. Amadelli, E.V. Gruzdeva, T.V. Luk'yanenko, and F.I. Danilov, *Electrodeposition of lead dioxide from methanesulfonate solutions.* Journal of Power Sources, 2009. **191**(1): p. 103-110.

63.   Velichenko, A.B., E.A. Baranova, D.V. Girenko, R. Amadelli, S.V. Kovalev, and F.I. Danilov, *Mechanism of Electrodeposition of Lead Dioxide from Nitrate Solutions.* Russian Journal of Electrochemistry, 2003. **39**(6): p. 615-621.

64.   Velichenko, A., T. Luk'yanenko, N. Nikolenko, R. Amadelli, and F. Danilov, *Nafion effect on the lead dioxide electrodeposition kinetics.* Russian Journal of Electrochemistry, 2007. **43**(1): p. 118-120.

65.   Velichenko, A.B., D.V. Girenko, and F.I. Danilov, *Mechanism of lead dioxide electrodeposition.* Journal of Electroanalytical Chemistry, 1996. **405**(1-2): p. 127-132.

66.   Velichenko, A.B. and D. Devilliers, *Electrodeposition of fluorine-doped lead dioxide.* Journal of Fluorine Chemistry, 2007. **128**(4): p. 269-276.

67.   Amadelli, R., L. Armelao, A.B. Velichenko, N.V. Nikolenko, D.V. Girenko, S.V. Kovalyov, and F.I. Danilov, *Oxygen and ozone evolution at fluoride modified lead dioxide electrodes.* Electrochimica Acta, 1999. **45**(4-5): p. 713-720.

68.   Mohd, Y. and D. Pletcher, *The fabrication of lead dioxide layers on a titanium substrate.* Electrochimica Acta, 2006. **52**(3): p. 786-793.

69.   Iniesta, J., J. González-García, E. Expósito, V. Montiel, and A. Aldaz, *Influence of chloride ion on electrochemical degradation of phenol in alkaline medium using bismuth doped and pure PbO2 anodes.* Water Research, 2001. **35**(14): p. 3291-3300.

70.   Johnson, D.C., J. Feng, and L.L. Houk, *Direct electrochemical degradation of organic wastes in aqueous media.* Electrochimica Acta, 2000. **46**(2-3): p. 323-330.

71.   Andrade, L.S., L.A.M. Ruotolo, R.C. Rocha-Filho, N. Bocchi, S.R. Biaggio, J. Iniesta, V. García-Garcia, and V. Montiel, *On the performance of Fe and Fe,F doped Ti-Pt/PbO2 electrodes in the electrooxidation of the Blue Reactive 19 dye in simulated textile wastewater.* Chemosphere, 2007. **66**(11): p. 2035-2043.

72.   Zhou, M., Q. Dai, L. Lei, C.a. Ma, and D. Wang, *Long Life Modified Lead Dioxide Anode for Organic Wastewater Treatment: Electrochemical Characteristics and Degradation Mechanism.* Environmental Science & Technology, 2004. **39**(1): p. 363-370.

73.   Ghaemi, M., E. Ghafouri, and J. Neshati, *Influence of the nonionic surfactant Triton X-100 on electrocrystallization and electrochemical performance of lead dioxide electrode.* Journal of Power Sources, 2006. **157**(1): p. 550-562.

74.   Velichenko, A., D. Girenko, N. Nikolenko, R. Amadelli, E. Baranova, and F. Danilov, *Oxygen evolution on lead dioxide modified with fluorine and iron.* Russian Journal of Electrochemistry, 2000. **36**(11): p. 1216-1220.

75.   He, L., J.R. Anderson, H.F. Franzen, and D.C. Johnson, *Electrocatalysis of Anodic Oxygen-Transfer Reactions: Bi3Ru3O11 Electrodes in Acidic Media.* Chemistry of Materials, 1997. **9**(3): p. 715-722.

76.   Popović, N.D. and D.C. Johnson, *A Ring Disk Study of the Competition between Anodic Oxygen-Transfer and Dioxygen-Evolution Reactions.* Analytical Chemistry, 1998. **70**(3): p. 468-472.

77.   Fenton, H.J.H., *LXXIII.-Oxidation of tartaric acid in presence of iron.* Journal of the Chemical Society, Transactions, 1894. **65**: p. 899-910.

78.   Haber, F. and J. Weiss, *The Catalytic Decomposition of Hydrogen Peroxide by Iron Salts.* Proceedings of the Royal Society of London. Series A, Mathematical and Physical Sciences, 1934. **147**(861): p. 332-351.

79.   George, P., W.G. Barb, K.R. Hargrave, and J.H. Baxendale, *Reactions of Ferrous and Ferric Ions with Hydrogen Peroxide.* Nature (London), 1949. **163**(4148): p. 692-694.

80.   Wang, H.-Y., Y.-N. Hu, G.-P. Cao, and W.-K. Yuan, *Degradation of propylene glycol wastewater by Fenton's reagent in a semi-continuous reactor.* Chemical Engineering Journal, 2011. **170**(1): p. 75-81.

81.   Zazo, J.A., J.A. Casas, A.F. Mohedano, M.A. Gilarranz, and J.J. Rodríguez, *Chemical Pathway and Kinetics of Phenol Oxidation by Fenton's Reagent.* Environmental Science & Technology, 2005. **39**(23): p. 9295-9302.

82.   Méndez-Arriaga, F., S. Esplugas, and J. Giménez, *Degradation of the emerging contaminant ibuprofen in water by photo-Fenton.* Water Research, 2010. **44**(2): p. 589-595.

83.   Chen, R. and J.J. Pignatello, *Role of Quinone Intermediates as Electron Shuttles in Fenton and Photoassisted Fenton Oxidations of Aromatic Compounds.* Environmental Science & Technology, 1997. **31**(8): p. 2399-2406.

84. Boye, B., M.M. Dieng, and E. Brillas, *Degradation of Herbicide 4-Chlorophenoxyacetic Acid by Advanced Electrochemical Oxidation Methods.* Environmental Science & Technology, 2002. **36**(13): p. 3030-3035.

85. Anotai, J., C.-C. Su, Y.-C. Tsai, and M.-C. Lu, *Effect of hydrogen peroxide on aniline oxidation by electro-Fenton and fluidized-bed Fenton processes.* Journal of Hazardous Materials, 2010. **183**(1-3): p. 888-893.

86. Ozcan, A., Y. Sahin, A. Savas Koparal, and M.A. Oturan, *Carbon sponge as a new cathode material for the electro-Fenton process: Comparison with carbon felt cathode and application to degradation of synthetic dye basic blue 3 in aqueous medium.* Journal of Electroanalytical Chemistry, 2008. **616**(1-2): p. 71-78.

87. Daneshvar, N., S. Aber, V. Vatanpour, and M.H. Rasoulifard, *Electro-Fenton treatment of dye solution containing Orange II: Influence of operational parameters.* Journal of Electroanalytical Chemistry, 2008. **615**(2): p. 165-174.

88. Wells, C.F. and M.A. Salam, *The effect of pH on the kinetics of the reaction of iron(II) with hydrogen peroxide in perchlorate media.* Journal of the Chemical Society A: Inorganic, Physical, Theoretical, 1968: p. 24-29.

89. Chen, L., J. Ma, X. Li, J. Zhang, J. Fang, Y. Guan, and P. Xie, *Strong Enhancement on Fenton Oxidation by Addition of Hydroxylamine to Accelerate the Ferric and Ferrous Iron Cycles.* Environmental Science & Technology, 2011. **45**(9): p. 3925-3930.

90. Flynn, C.M., *Hydrolysis of inorganic iron(III) salts.* Chemical Reviews, 1984. **84**(1): p. 31-41.

91. Gallard, H., J. De Laat, and B. Legube, *Spectrophotometric study of the formation of iron(III)-hydroperoxy complexes in homogeneous aqueous solutions.* Water Research, 1999. **33**(13): p. 2929-2936.

92. Sun, Y. and J.J. Pignatello, *Chemical treatment of pesticide wastes. Evaluation of iron(III) chelates for catalytic hydrogen peroxide oxidation of 2,4-D at circumneutral pH.* Journal of Agricultural and Food Chemistry, 1992. **40**(2): p. 322-327.

93. Pignatello, J.J. and K. Baehr, *Ferric Complexes as Catalysts for "Fenton" Degradation of 2,4-D and Metolachlor in Soil.* Journal of Environmental Quality, 1994. **23**(2): p. 365-370.

94. Wang, X. and M.L. Brusseau, *Effect of pyrophosphate on the dechlorination of tetrachloroethene by the Fenton reaction.* Environmental Toxicology and Chemistry, 1998. **17**(9): p. 1689-1694.

95. Oturan, M.A., I. Sirés, N. Oturan, S. Pérocheau, J.-L. Laborde, and S. Trévin, *Sonoelectro-Fenton process: A novel hybrid technique for the destruction of organic pollutants in water.* Journal of Electroanalytical Chemistry, 2008. **624**(1-2): p. 329-332.

96. Panizza, M. and M.A. Oturan, *Degradation of Alizarin Red by electro-Fenton process using a graphite-felt cathode.* Electrochimica Acta, 2011. **56**(20): p. 7084-7087.

97. Zhang, H., D. Zhang, and J. Zhou, *Removal of COD from landfill leachate by electro-Fenton method.* Journal of Hazardous Materials, 2006. **135**(1-3): p. 106-111.

98. Zhang, H., C. Fei, D. Zhang, and F. Tang, *Degradation of 4-nitrophenol in aqueous medium by electro-Fenton method.* Journal of Hazardous Materials, 2007. **145**(1-2): p. 227-232.

99.   Panizza, M. and G. Cerisola, *Removal of organic pollutants from industrial wastewater by electrogenerated Fenton's reagent.* Water Research, 2001. **35**(16): p. 3987-3992.

100.   Brillas, E. and J. Casado, *Aniline degradation by Electro-Fenton and peroxi-coagulation processes using a flow reactor for wastewater treatment.* Chemosphere, 2002. **47**(3): p. 241-248.

101.   Boye, B., E. Brillas, A. Buso, G. Farnia, C. Flox, M. Giomo, and G. Sandonà, *Electrochemical removal of gallic acid from aqueous solutions.* Electrochimica Acta, 2006. **52**(1): p. 256-262.

102.   Chou, S., Y.-H. Huang, S.-N. Lee, G.-H. Huang, and C. Huang, *Treatment of high strength hexamine-containing wastewater by electro-Fenton method.* Water Research, 1999. **33**(3): p. 751-759.

103.   Ting, W.-P., M.-C. Lu, and Y.-H. Huang, *The reactor design and comparison of Fenton, electro-Fenton and photoelectro-Fenton processes for mineralization of benzene sulfonic acid (BSA).* Journal of Hazardous Materials, 2008. **156**(1-3): p. 421-427.

104.   Panizza, M. and G. Cerisola, *Electrochemical generation of H2O2 in low ionic strength media on gas diffusion cathode fed with air.* Electrochimica Acta, 2008. **54**(2): p. 876-878.

105.   Saha, M.S., A. Denggerile, Y. Nishiki, T. Furuta, and T. Ohsaka, *Synthesis of peroxyacetic acid using in situ electrogenerated hydrogen peroxide on gas diffusion electrode.* Electrochemistry Communications, 2003. **5**(6): p. 445-448.

106.   Drogui, P., S. Elmaleh, M. Rumeau, C. Bernard, and A. Rambaud, *Oxidising and disinfecting by hydrogen peroxide produced in a two-electrode cell.* Water Research, 2001. **35**(13): p. 3235-3241.

107.   Da Pozzo, A., L. Di Palma, C. Merli, and E. Petrucci, *An experimental comparison of a graphite electrode and a gas diffusion electrode for the cathodic production of hydrogen peroxide.* Journal of Applied Electrochemistry, 2005. **35**(4): p. 413-419.

108.   Agladze, G.R., G.S. Tsurtsumia, B.I. Jung, J.S. Kim, and G. Gorelishvili, *Comparative study of hydrogen peroxide electro-generation on gas-diffusion electrodes in undivided and membrane cells.* Journal of Applied Electrochemistry, 2007. **37**(3): p. 375-383.

Chapter 2. Experimental

2.1. Instrumentation

2.1.1. Potentiostats

Cyclic voltammetry and electrochemical impedance spectroscopy (EIS) measurements were performed using a computer-controlled Eco Chemie Autolab PGSTAT 302 potentiostat running GPES v.4.09 software. Bulk electrolysis and deposition of PbO_2 coatings were undertaken with a computer controlled EG&G PAR 273A potentiostat. Unless otherwise stated, electrochemical measurements were made at room temperature in solutions that were purged with N_2 to significantly reduce the oxygen content.

Electrochemical impedance spectroscopy (EIS) data were collected at 60 frequencies in the range 10^4 to 0.1 Hz using an ac amplitude of 10 mV that was added to the dc potential of the working electrode. The dc potential corresponded to $E_{1/2}$ of the redox couple $Fe(CN)_6^{3-/4-}$. The working electrode was preconditioned for 2 min at the same potential. The in-phase and out-of-phase impedance data were extracted from the experimental data using the software associated with the potentiostat. Equivalent circuit modeling based on the Randles circuit was used to calculate resistance and capacitance values.

2.1.2. Scanning Electron Microscope (SEM) imaging

SEM imaging was carried out using a JEOL JSM 7000F field emission, high-resolution scanning electron microscope using an accelerating voltage of 8 kV. The stigmation and aperture were adjusted prior to image capture to improve image quality.

2.1.3. Mass spectrometry

Mass spectrometry analysis was carried out using a Bruker maXis 3G ultra high resolution time of flight mass spectrometer. Analysis was performed by Dr. Marie Squire of the Chemistry Department at the University of Canterbury.

2.1.4. UV-Visible spectroscopy

UV-Visible spectroscopy was carried out using a Varian Cary 50 UV-Vis Spectrometer. A 1 cm path length quartz cell was used for all data collection and subsequent analysis.

2.2. Electrodes and electrochemical cells

2.2.1. Glassy carbon (GC)

GC plates (figure 2.1a) (15 mm × 15 mm × 3 mm) and GC disks (diameter 3 mm) were used as the working electrodes. GC disk electrodes were fabricated into rod electrodes (figure 2.1b) in the mechanical workshop in the Department of Chemistry, University of Canterbury, by sealing a small piece of 3 mm diameter GC in a Teflon sleeve. Electrical contact to the GC was made with a brass rod.

Initially, electrodes were polished by using graded sandpaper followed by polishing with 9, 6 and 3 μm diamond paste. Finally, 1 and 0.05 μm alumina-water slurries on LECO Lecloth were used to bring the electrodes to a mirror finish. Polished electrodes were rinsed and sonicated in water for 10 minutes to remove any residual alumina from the electrode. Between experiments, electrodes were hand polished with 1 and 0.05 μm alumina slurries followed by rinsing and sonication, as described above. Cyclic voltammetry of potassium ferricyanide was used to probe electron transfer at electrode surfaces. The cell contained 5 mM $K_3Fe(CN)_6$, 0.1 M KCl, a working electrode, auxiliary electrode and an SCE reference electrode. Cyclic voltammograms were obtained between the range of 0.6 V and -0.2 V at a scan rate of 100 mVs^{-1}. The peak separation (ΔE_p) obtained during a cyclic voltammetry scan in ferricyanide probe solution was used to check whether an electrode surface was clean. A high ΔE_p means that electron transfer is being restricted and the surface is blocked; a low ΔE_p indicates a clean surface.

(a)   (b)
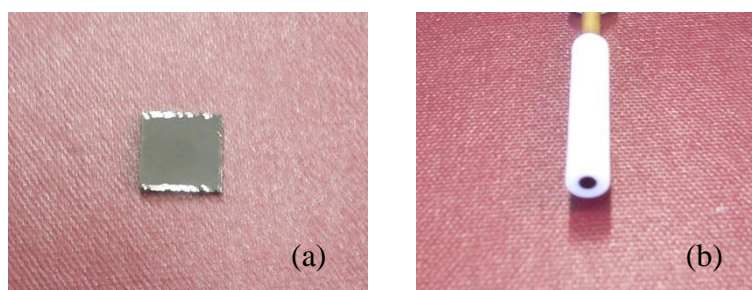
Figure 2.1: (a): GC plate. (b): GC rod.

2.2.2. Graphite rod electrodes

Graphite rod electrodes (figure 2.2) were immersed to a specific depth in solution to give an area of 4 cm^2 in contact with the electrolyte. The electrodes were lightly sanded using

fine grade sandpaper and ultrasonicated in water to give a fresh clean surface for each experiment.

Figure 2.2. Graphite rod electrode

2.2.3. PbO$_2$ electrodes

PbO$_2$ electrodes (figure 2.3) were prepared by electroplating lead dioxide onto platinum and carbon substrates from a solution of 0.5 M Pb(NO$_3$)$_2$ + 0.1 M HNO$_3$ with varied concentrations of NaF from 0 - 0.04 M. A large area copper counter electrode and a Ag/AgCl reference electrode were used to complete the standard 3-electrode cell configuration. A constant current of 60 mA/cm^2 was used for all depositions except when stated otherwise. A temperature of 60° C, controlled by a thermostatically controlled water bath, was used for all depositions. Depositions onto platinum mesh were made from 30 mL of 0.5 M Pb(NO$_3$)$_2$ + 0.1 M HNO$_3$ with varied concentrations of NaF from 0 - 0.04 M. A cylindrical copper counter electrode with an area of 15 cm^2 was used to surround the platinum mesh working electrode to help provide an even coating to the electrode. The physical dimensions of the platinum mesh were 1 cm × 0.5 cm. This area was used to calculate current density for the deposition. After the deposition the holes in the mesh were covered by PbO$_2$ giving PbO$_2$ electrodes of 1 cm^2 based on the dimensions alone.

Figure 2.3. Left side: PbO$_2$ coated platinum mesh electrode. Right side: Platinum Mesh electrode.

PbO$_2$ coatings were removed from platinum mesh electrodes by immersing the electrode in a 1:1 solution of glacial acetic acid and hydrogen peroxide until all of the PbO$_2$ coating had dissolved (~2 minutes).

2.2.4. Woven carbon fibre electrodes

Woven carbon fibre fabric was obtained from a local boat builder. Electrodes (figure 2.4) were prepared by cutting a 4 cm × 8 cm rectangle of carbon fibre fabric. The edges were then sealed with silicone sealant and the two short ends of the rectangle were fixed together to give a cylinder with a surface area of 64 cm^2. Several bundles of fibres were not cut at the top of the cylinder and these provided electrical contact to the electrode. Ultrasonicating in acetone, ethanol and water for 10 minutes each was used to clean the electrodes before first use.
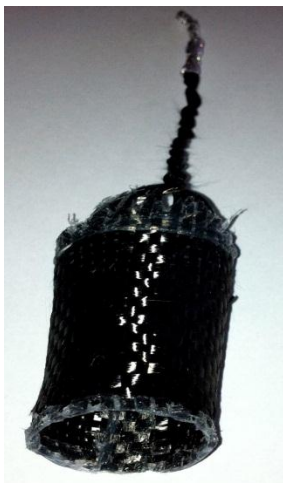
Figure 2.4. Cylindrical woven carbon fibre electrode.

2.3. Cell set-up

2.3.1. Undivided cell experiments

Electrochemical measurements involving rod type electrodes were carried out in a pear shaped glass cell (figure 2.5) with fittings that allowed for a standard 3-electrode setup. Electrochemical measurements involving plate electrodes were carried out in a pear shaped cell with a hole in the bottom (figure 2.3). Viton O-rings were used to form a seal between the electrode surface and the cell. Four springs were used to stabilize the cell and maintain pressure on the O-ring to give a good seal. A strip of copper was placed under the GC plate to provide electrochemical contact. A high surface area platinum electrode was used as a counter electrode and a Ag/AgCl electrode was used as a reference electrode in aqueous solutions. In non-aqueous conditions a silver/silver nitrate reference was used (Ag/10^{-2}M Ag$^+$) (10^{-2}M AgNO$_3$ in acetonitrile/ 0.1 M tetrabutylammonium

tetrafluoroborate ($[Bu_4N]BF_4$)). Electrochemical cells were stored in a 10 % HNO_3 acid

bath. Cells were washed with acetone and water and dried at 50° C in an oven before use.
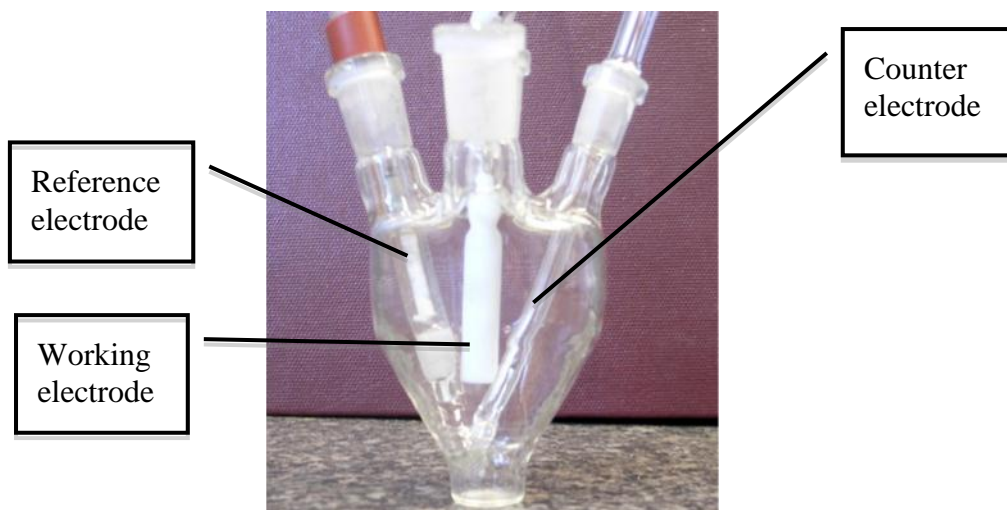
Figure 2.5. Cell setup for rod type electrodes.
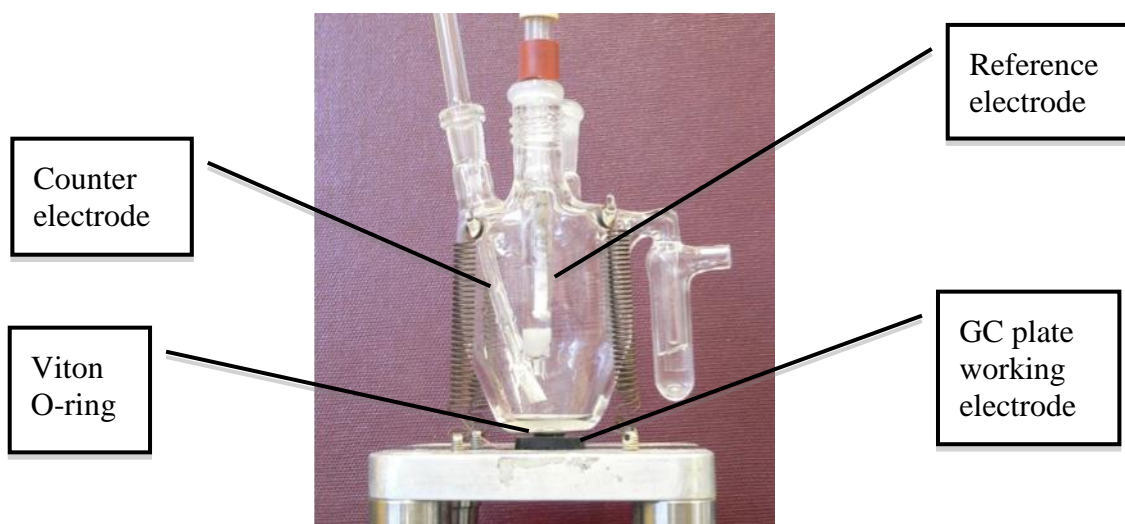
Figure 2.6. Cell setup for GC plate type electrodes.

2.3.2. Divided cell experiments

For divided cell experiments in the generation of H_2O_2 with a woven carbon fibre working electrode, the inner compartment contained the woven carbon fibre and reference electrodes and the outer compartment contained a cylindrical platinum counter electrode. The compartments were separated by a porous glass frit (figure 2.7) which separated the anodic and cathodic solutions but allowed current to flow between the electrodes. A 50 ml volume of electrolyte (0.1M Na_2SO_4) was added to the inner compartment and 40 ml of electrolyte was added to the outer compartment. Oxygen was sparged into the central compartment. A magnetic flea at the bottom of the inner compartment was used to stir the solution.

Figure 2.7. Divided cell used for woven carbon fibre electrode experiments.

2.4. Synthesis and solutions

2.4.1. Aqueous and non-aqueous solutions

Analytical grade reagents were used for all synthesis and solutions. Milli-Q with a resistivity of >18 MΩ.cm was used for all aqueous solutions.

Acetonitrile (HPLC grade) was dried over CaH_2 for 2 days and refluxed under N_2 for 2 hours prior to distilling in a N_2 atmosphere. Tetrabutylammonium tetrafluoroborate ($[Bu_4N]BF_4$) was prepared by neutralisation of the corresponding acid and base and dried under a vacuum at 80 °C for 2 days.

2.4.2. Buffer solutions

Phosphate buffer solutions (0.1 M) of pH 6-8 were prepared by mixing specific volumes of 0.1 M NaH_2PO_4 and 0.1 M Na_2HPO_4 stock solutions until the desired pH was reached. Phosphate buffers from pH 2-3 or pH 11-13 were made by dissolving either NaH_2PO_4 or Na_2HPO_4 in order to give a 0.1 M concentration in 80 % of the required volume of water. The solution was then adjusted to the desired pH with 1 M HCl or 1 M NaOH while monitoring with a pH meter. The solution was then made up to the final volume with water.

Tris (2-Amino-2-hydroxymethyl-propane-1,3-diol), glycine, potassium hydrogen phthalate, MES (2-(*N*-morpholino)ethanesulfonic acid) and HEPES buffers were all prepared by dissolving a known amount of each reagent to give a 0.05 M or 0.1 M concentration in 80 % of the required volume of water. The solution was then adjusted to the desired pH with 1 M HCl or 1 M NaOH while monitoring with a pH meter. The solution was then made up to the final volume with water.

2.4.3. Protein solutions

BSA, β-lactoglobulin and β-casein were obtained from Sigma-Aldrich and technical grade whey and casein were provided by AgResearch Ltd, Lincoln, New Zealand. A concentration of 1 mg/mL was used for all protein electrochemistry and solution chemistry. The solutions were prepared by dissolving lyophilised protein powder in water. Protein solutions were prepared fresh for each experiment. Heating to 65° C and maintaining the pH below 3 or above 9 was required in order to dissolve β-casein and casein proteins in water. The pH of casein solutions was then able to be adjusted to some extent without the protein precipitating out after cooling the solution.

When desalting of protein solutions was necessary it was carried out using GE Healthcare PD10 Desalting Columns. These were used according to the manufacturer's instructions and stored containing a solution of 20 % ethanol in water.

2.4.4. Diazonium salt preparation

Diazonium salts were prepared using literature methods[1, 2] using the following procedure: fluoroboric acid solution (40 %, 2 ml) was added to 2 ml of water and the solution was added slowly to 5 mmol of arylamine and cooled to 0° C with constant stirring. Sodium nitrite (5 mmol), dissolved in a small amount of water (~1 ml), was added slowly to the arylamine and fluoroboric acid solution with continued cooling and stirring. This mixture formed a precipitate with time (~30 min). The aryldiazonium salt product was then collected over a sintered frit under vacuum and washed with cold 5 % fluoroboric acid, methanol and ether. The product was air dried in a fumehood overnight. Purification of the aryldiazonium was by recrystalisation. The aryldiazonium salt was dissolved in a minimum volume of cold acetonitrile (2-4 ml). Cold diethyl ether (200 ml) was slowly added and the diazonium salt re-crystallized, collected over a porous frit and dried under vacuum. Diazonium salts were stored in the dark; particular care was taken not to expose the salts to ultraviolet light.

2.5. Modification of electrode surfaces

2.5.1. Diazonium salt modification

The electrode surface was modified by reduction of the aryldiazonium ion.[3] A solution containing 1 mM diazonium salt and 0.1 M [Bu$_4$N]BF$_4$ in dry acetonitrile was degassed with nitrogen for 15 min prior to electrode modification. The working electrode was cycled through the aryldiazonium reduction potential region between 1 and 5 cycles at a

rate of 100 mVs^{-1}. In general, the film thickness is controlled by the length of time the working electrode potential was in the aryldiazonium reduction potential region.

2.5.2. Electrochemical oxidation of amines for surface modification

Electrochemical oxidation of amine containing polyethylene glycol (PEG) solutions was used to graft PEG films to the electrode surface. The reaction proceeds via the oxidation of the amine to an amine radical that then covalently attaches to the electrode surface.[4, 5] Electrode modification was undertaken in a cell containing 5 mM amine-PEG in anhydrous acetonitrile (prepared as described in section 2.4.), 0.1 M [Bu$_4$N]BF$_4$, a GC working electrode, platinum counter and silver/silver nitrate reference electrode.

2.6. Analytical methods

2.6.1. Error reporting

Experiments were carried out in duplicate. The average value is reported and the associated uncertainty indicates the range of values obtained.

2.6.2. Procedure for determination of Fe(II) and Fe(III) concentrations

Fe(II) concentration was determined by UV-Visible spectroscopy at 510 nm after complexing Fe(II) with 1,10 phenanthroline in pH 3.5 M acetate buffer and measuring against prepared standard solutions. The standard solutions also contained hydroxylamine to maintain iron species as Fe(II). To avoid interference from Fe(III), ammonium

fluoride was used as a masking agent.[6] The Fe(III) ion affinity for fluoride is very high, and mono, di, and trifluoride complexes are formed.[7] Catalase was used to scavenge H_2O_2 when it was present in the Fe(II) containing solution. Catalase was also included in the concentration standards for these experiments.

2.6.3. Hydrogen peroxide determination

Hydrogen peroxide concentrations were determined with UV-Visible spectroscopy by the iodide method.[8, 9] 20 μL aliquots were taken during production of H_2O_2 and diluted to 1500 μL with water. This solution was then mixed with 0.75 ml of 0.1 M potassium hydrogen phthalate and 0.75 ml of iodide reagent (0.4 M potassium iodide, 0.06 M NaOH, 1×10^{-4} M ammonium molybdate). The mixture was then transferred to a 1 cm quartz cuvette. Finally, the absorbance of the generated I_3^- was measured with a UV–Visible spectrophotometer at 352 nm ($\varepsilon(I_3^-) = 26\ 400\ M^{-1}cm^{-1}$).

2.6.4. Gel Electrophoresis

10 μL of 4 × concentrate lithium dodecyl sulfate (LDS) and 1 μL of stabilized 0.5 M DTT were added to 29 μL of each protein sample. This mixture was heated for 10 min in a water bath at > 90° C. Aliquots (20 μL) of the freshly prepared samples were then loaded into the wells of Life Technologies™ NuPAGE® Bis-Tris polyacrylamide gels and run at 200 V for 35 min with MES (2-(N-morpholino)ethanesulfonic acid) running buffer. After removal from the casing, the gel was transferred to a staining container and 100 ml of staining solution containing 0.1 % Coomassie R-250 in 40 % ethanol and 10 % acetic acid was added. The solution was then loosely covered and the solution and gel were

microwaved until the solution was almost boiling. The staining container was then removed from the microwave and gently shaken on an orbital shaker for 1 hour. The staining solution was then decanted off and the gel was rinsed with water. Destain solution (100 ml) containing 10 % ethanol and 7.5 % acetic acid was then added to the container with the gel. The container was loosely covered and microwaved until almost boiling. The container was then placed on the orbital shaker until the desired background was achieved. This usually occurred after 4 or more hours. Often the gel was left to destain overnight; in this situation the destain solution was diluted with water. The gel was then removed from the destaining solution, rinsed with water and imaged on a light box. Densitometric analysis of gels was conducted with ImageJ version 1.45 software.

2.6.5. Accelerated PbO_2 lifetime testing

The stability of PbO_2 electrodes was assessed by applying a current density of 100 mA/cm^2 with a platinum counter electrode in a solution of 1 M H_2SO_4. The rate of deterioration of the electrodes is accelerated and can be measured by weighing the electrode periodically to give the percentage mass loss over time. This data was then used to compare the stability of the electrodes produced under different conditions.

References

1. DuVall, S.H. and R.L. McCreery, *Self-catalysis by Catechols and Quinones during Heterogeneous Electron Transfer at Carbon Electrodes.* Journal of the American Chemical Society, 2000. **122**(28): p. 6759-6764.
2. Saunders, K.H. and R.L.M. Allen, *Aromatic diazo compounds.* 1985, London; Baltimore, Md.: E. Arnold.
3. Pinson, J. and F. Podvorica, *Attachment of organic layers to conductive or semiconductive surfaces by reduction of diazonium salts.* Chemical Society Reviews, 2005. **34**(5): p. 429-439.
4. Barbier, B., J. Pinson, G. Desarmot, and M. Sanchez, *Electrochemical bonding of amines to carbon fiber surfaces toward improved carbon-epoxy composites.* Journal of The Electrochemical Society, 1990. **137**(6): p. 1757-1764.
5. Liu, J. and S. Dong, *Grafting of diaminoalkane on glassy carbon surface and its functionalization.* Electrochemistry Communications, 2000. **2**(10): p. 707-712.
6. Tamura, H., K. Goto, T. Yotsuyanagi, and M. Nagayama, *Spectrophotometric determination of iron(II) with 1,10-phenanthroline in the presence of large amounts of iron(III).* Talanta, 1974. **21**(4): p. 314-318.
7. SillÈn, L.G., A.E. Martell, and J. Bjerrum, *Stability constants of metal-ion complexes.* 1964, London: Chemical Society.
8. Ovenston, T.C.J. and W.T. Rees, *The spectrophotometric determination of small amounts of hydrogen peroxide in aqueous solutions.* analyst, 1950. **75**(889).
9. Ozcan, A., Y. Sahin, A. Savas Koparal, and M.A. Oturan, *Carbon sponge as a new cathode material for the electro-Fenton process: Comparison with carbon felt cathode and application to degradation of synthetic dye basic blue 3 in aqueous medium.* Journal of Electroanalytical Chemistry, 2008. **616**(1-2): p. 71-78.

Chapter 3. Direct electrochemical cleavage of proteins

3.1. Introduction

As outlined in section 1.4, electrochemical oxidation of peptides and proteins on platinum[1, 2] and graphite[3, 4] electrodes has been shown to lead to main chain cleavage next to tyrosine and tryptophan residues. However, once tryptophan or tyrosine are electrochemically oxidized, there are a number of competitive processes, giving multiple reaction pathways and products, which means that not all oxidized tryptophan or tyrosine residues will lead to backbone cleavage in the protein. Some of the reaction pathways will lead to backbone cleavage and some will result in a mass change of the starting material as a result of nucleophilic attack by water or formation of a new double bond.

Permentier et al investigated oxidation of a range of proteins in solutions of acetonitrile, water and formic acid using a porous flow through graphite electrode, connected directly to a mass spectrometer.[5] Their results demonstrated that the outcome of electrolysis depends on the particular protein; in some cases proteins were fully fragmented and in others, non-cleavage products dominated.

The initial work in this chapter focuses on bulk electrolysis with unmodified graphite electrodes. Electrode fouling by protein adsorption was found to be a problem during bulk electrolysis with graphite electrodes and hence the second part of the chapter

investigates the effects of electrode fouling during electrolysis. Modification of the GC electrode surfaces was undertaken in order to gain insight into the protein adsorption process and to attempt to reduce this problem.

3.2. Experimental

Bulk electrolysis was conducted using a graphite rod working electrode, a platinum mesh counter electrode and a Ag/AgCl reference electrode. 4 cm^2 of the graphite electrode was immersed in a 10 ml volume of protein containing electrolyte in a single compartment three electrode cell with stirring. Theoretical peptide masses were calculated with the Swiss Institute of Bioinformatics Peptide Mass Calculator.

GC rod electrodes were used for the studies of protein adsorption and surface modification. Conditions used for surface modification are outlined in section 2.5.

3.3. Results and discussion

3.3.1. Bulk electrolysis of proteins

Graphite was chosen as the electrode material for the study of direct bulk electrochemical cleavage of proteins as it has been used with some success in other laboratories.[3, 4] The electrode was a solid graphite rod, which was immersed in solution to give a geometric surface area (based on the dimensions of the electrode) of 4 cm^2. The potential window

for carbon based electrodes is typically in the in the range of -1 V to 1.5 V vs SCE in an aqueous environment and is shifted by solution pH.[6] Using potentials outside the electrochemical window yields significant current that result from reactions of both the electrolyte and electrode itself. At high positive potentials oxidation of the graphite surface to graphitic oxide will occur reducing the conductivity of the electrode and the electrolysis of water will produce oxygen and hydrogen gas on the anode and cathode respectively. A potential of 1.5 V, which is at the edge of the potential window for graphite was selected initially for the oxidation of whey proteins in phosphate buffer, as it was assumed that a high oxidation potential would be most likely to produce detectable results in a short time frame.

3.3.1.1. Electrolysis of Whey and β-lactoglobulin

Whey was electrolysed at 1.5 V for 8 hours and aliquots of the electrolysis solution were taken for analysis every 2 hours. Electrophoresis was undertaken on the aliquots to give a visual representation of the effects of electrolysis on the whey proteins (figure 3.1). Over 8 hours there was a loss of intensity in the main protein bands of β-lactoglobulin and α-lactalbumin at ~18.3 kDa and ~14.1 kDa, respectively. Densitometric analysis showed only 35% of the α-lactalbumin band remained after 8 hours of electrolysis. There is some broad staining under the β-lactoglobulin band but no evidence of specific fragments can be seen on the gel. The same experiment was also run at 2 V for 4 hours. This increased the rate of protein degradation (lanes 6 and 7, figure 3.1), however this potential is outside the potential window for carbon based electrodes as mentioned earlier and some damage to the electrode was evident with black particles visible in the electrolysis cell. Due to electrode instability, this potential is not suitable for further use.

(b)

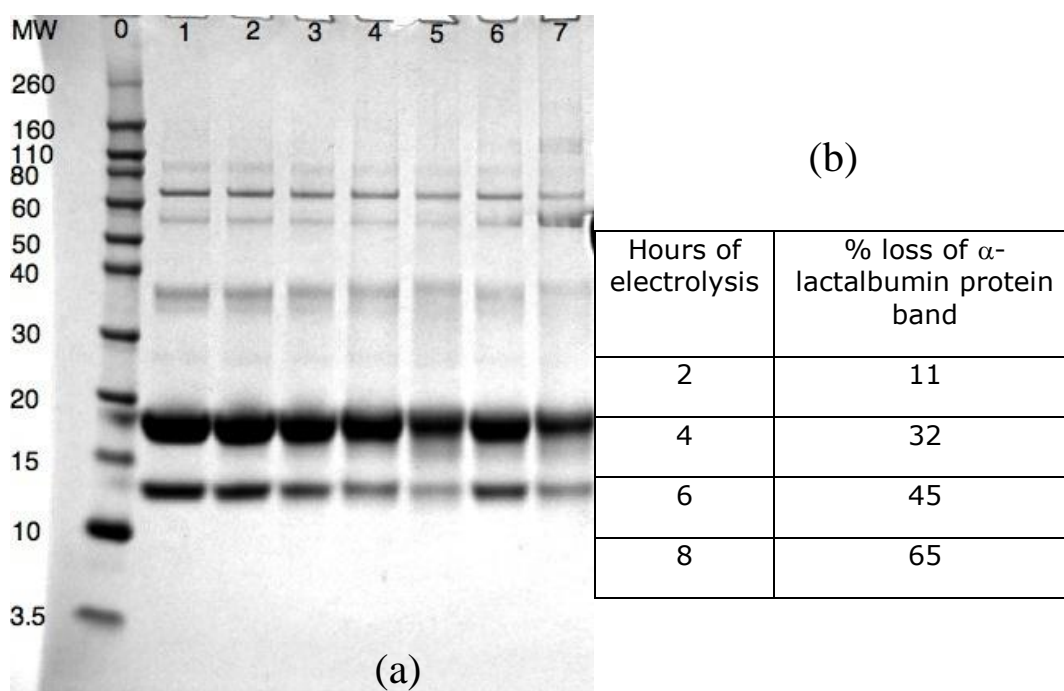| Hours of electrolysis	% loss of α-lactalbumin protein band
2	11
4	32
6	45
8	65

(a)

Figure 3.1. (a) Gel image showing effect of electrolysis with a graphite electrode on whey proteins in a supporting electrolyte of 0.1 M phosphate buffer at pH 7.2. Lane 0: Molecular weight markers. Lane 1: Whey control. Lane 2-5: 2, 4, 6, 8 hours of electrolysis respectively at 1.5 V. Lane 6-7: 2 and 4 hours of electrolysis respectively at 2 V. (b) Table showing the percentage loss of the α-lactalbumin band during electrolysis at 1.5 V over time determined by densitometric analysis.

As mentioned above, no specific fragments could be observed using gel electrophoresis, however some specific fragmentation may be occurring in low concentration not visible on the gel image. Permentier et al showed specific fragments generated by electrochemistry using mass spectroscopy.[5] They generated fragments in a 47.5/47.5/5 (vol/vol/vol) water/acetonitrile/formic acid electrolyte solution using a porous graphite flow through cell. This electrolyte composition is suitable for using mass spectroscopy to study the products and has the added advantage that it will solubilise a variety of proteins. Although a different cell setup was used in the present study, this electrolyte composition was chosen for use with the graphite rod electrode and cell described earlier. Using acetonitrile in an industrial setting is not desirable, but its use was explored because the known fragmentation might give a starting point when developing a more appropriate (aqueous-based) protocol for industry.

β-lactoglobulin was electrolysed with stirring using a graphite electrode in 47.5/47.5/5 (vol/vol/vol) water/acetonitrile/formic acid electrolyte at 1 V for 2 hours. Figure 3.2 shows the mass spectra for (a) β-lactoglobulin without electrolysis, (b) β-lactoglobulin after 1 hour electrolysis and (c) β-lactoglobulin after 2 hours electrolysis. Figure 3.2 (d) shows the mass spectrum after 1 hour electrolysis, reconstructed using MaxEnt deconvolution software. New peaks appearing in the lower mass range between m/z 300 and 800 are more prominent after 2 hours of electrolysis than 1 hour (figure 3.2 (b) and (c)), showing that more contact time with the electrode increases the concentration of the cleavage products. The deconvoluted spectrum (figure 3.2 (d)) shows that the new peaks appearing in the lower m/z range of figure 3.2 (b) and (c) are the result of smaller protein fragments created by the electrolysis. In the spectra representing 1 and 2 hours electrolysis time, the multiply charged protein peaks above m/z 1000 became increasingly broader and shifted to higher m/z. The reconstructed spectrum of the broader multiply charged protein peaks above m/z 1000, show an increase in molecular weight of the starting protein material. Increased molecular weight is assumed to result from oxidation of the protein without fragmentation.[4] The reconstructed mass spectrum of figure 3.2(a) (not shown) showed that the starting β-lactogloblin material mainly consisted of genetic variants A (18363 Da) and B (18276 Da) with other genetic variants in much lower abundance. Hence the increase in mass after electrolysis to 18457.8 Da, shown in figure 3.2(d), is most likely the result of non-cleavage oxidation of tyrosine and tryptophan which usually occurs through nucleophilic attack by water on the positively charged tyrosine or tryptophan intermediates (see section 1.4.1 for a proposed mechanism). Oxidation of methionine and cysteine to sulfoxides and sulfones will also lead to a mass increase of the starting protein material.
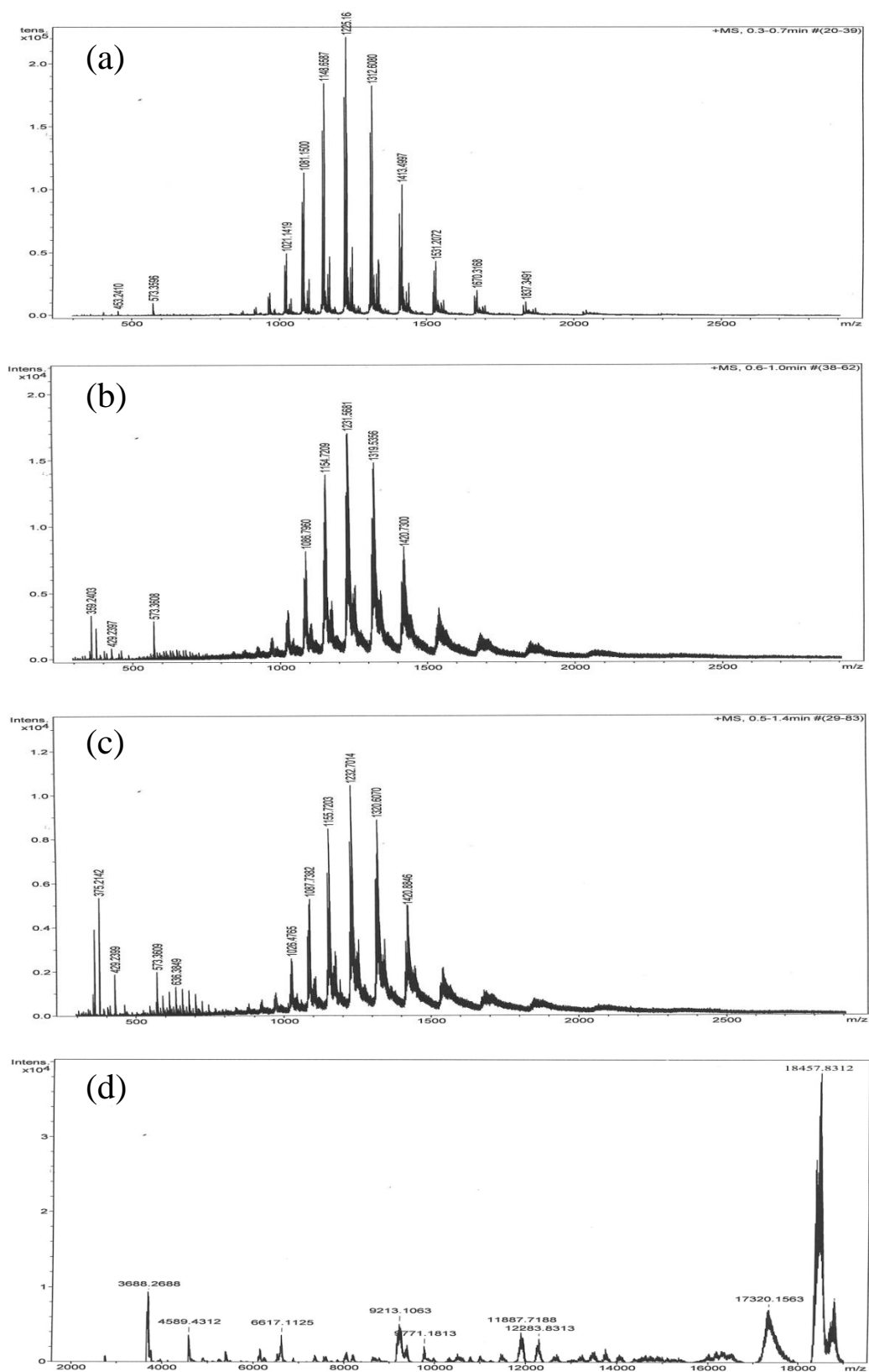
Figure 3.2. Mass spectra of β-lactoglobulin showing the effect of electrochemical oxidation with a graphite electrode at 1 V in a 47.5/47.5/5 (vol/vol/vol) acetonitrile/water/formic acid electrolyte. (a) No electrolysis. (b) 1 hour electrolysis. (c) 2 hours electrolysis. (d) Reconstructed mass spectrum for 1 hour electrolysis.

Figure 3.3 is an amino acid sequence diagram for β-lactoglobulin variant A showing possible electrochemical cleavage points at tyrosine and tryptophan residues. Tryptophan and tyrosine residues are displayed in blue boldface. Cysteine residues are shown in red and the double-headed arrows represent disulfide bridges between them. Disulfide bridges are expected to be able to hold some fragments together. Fragment number 6 is shown in red because cleavage needs to occur on both sides before it will be separated from fragment 5 (due to disulfide bridges holding the remaining fragment 5 together). The masses of the possible fragments and some combinations of fragments are shown on the right side of figure 3.3. It is difficult to assign the mass spectrum (figure 3.2(d)) to the expected fragments as the fragments themselves can also be oxidized changing their mass. This is evident in the data shown in figure 3.2, for example, the peak at 4589 Da after 1 hour electrolysis on the reconstructed mass spectrum in figure 3.2(d) is shifted to 4614 Da on the reconstructed spectrum after 2 hours electrolysis (not shown). However some combinations of the calculated molecular weights of the fragments shown in figure 3.3 are in the vicinity of the experimental values, especially in the ~4000 Da and ~11000 Da regions. This means that it is likely that some of the expected electrochemical cleavages are occurring, but further investigation is necessary to confirm these results. Tandem mass spectroscopy is required to determine the amino acid composition and actual cleavage points of the fragments obtained, however this was not undertaken due to the time constraints of this project. It cannot be excluded that some additional electrochemical cleavage is occurring at residues other than tyrosine and tryptophan as some of the prominent fragments cannot be attributed to cleavage at these locations.

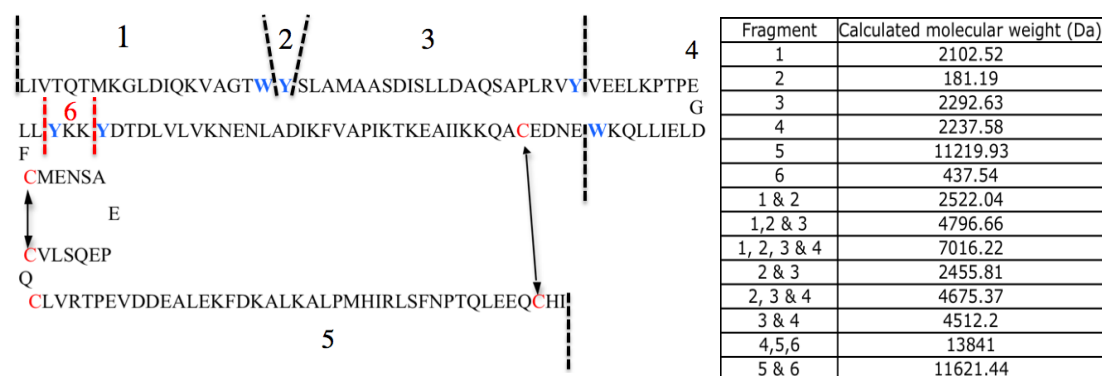| Fragment	Calculated molecular weight (Da)
1	2102.52
2	181.19
3	2292.63
4	2237.58
5	11219.93
6	437.54
1 & 2	2522.04
1,2 & 3	4796.66
1, 2, 3 & 4	7016.22
2 & 3	2455.81
2, 3 & 4	4675.37
3 & 4	4512.2
4,5,6	13841
5 & 6	11621.44

Figure 3.3. (Left side) Amino acid sequence of β-lactoglobulin variant A, showing predicted cleavage points based on cleavage at tyrosine and tryptophan (black and red dashed lines). (Right side) Table showing the calculated mass of the fragments and some combinations of the fragments shown on the amino acid sequence diagram.

Further examination of the electrolysis products of β-lactoglobulin in 47.5/47.5/5 (vol/vol/vol) acetonitrile/water/formic acid electrolyte was undertaken by gel electrophoresis on an aliquot of solution after 1 hour electrolysis. Prior to running the gel, the protein was exchanged from electrolyte solution into milliQ water using GE Heathcare PD 10 desalting columns. This step was necessary because the high formic acid concentration caused broad staining of the protein band when the sample was run directly from the electrolysis solution. The gel image (figure 3.4) shows no evidence of specific fragmentation below the β-lactoglobulin band at 18.3 kDa. This confirms that any fragmentation during the electrolysis of the protein is occurring in low concentration.
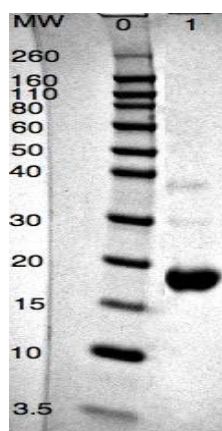

Figure 3.4. Gel image of β-lactoglobulin after 1 hour electrolysis with a graphite electrode at 1 V in a 47.5/47.5/5 (vol/vol/vol) acetonitrile/water/formic acid electrolyte. Lane 0: molecular weight markers. Lane 1: β-lactoglobulin after 1 hour electrolysis.

3.3.1.2. Effect of applied potential

Variations on the applied electrolysis potential were trialed with the effectiveness of each potential judged by the appearance of m/z values in the 300-800 range in the mass spectra. Peaks in this range represent the smaller fragments generated by electrolysis of the protein. Potentials of 0.8 V, 1.0 V, 1.2 V and 1.5 V were tested (results not shown) and the best results for production of cleavage products were obtained at 1 V. There was less fragmentation at 0.8 V. Potentials of 1.2 V and 1.5 V also led to fragmentation, but less than at 1 V, suggesting that at these higher potentials, oxidation pathways that do not result in specific fragmentation become more favourable. For this reason 1 V was used to carry out the remaining experiments described in this chapter.

3.3.1.3. Effect of solution composition

The solution composition was altered in an attempt to try and increase the amount of fragmentation during electrolysis. Further, from an industrial perspective having a lower concentration of reagents gives cost reductions. The concentrations of acetonitrile and formic acid were lowered in separate experiments to see if this would have an impact on the fragmentation of β-lactoglobulin. Figure 3.5(a) shows the mass spectrum of β-lactoglobulin after 1 hour electrolysis at 1 V in a solution containing 25/70/5 (vol/vol/vol) acetonitrile/water/formic acid. Some fragmentation is apparent at the lower acetonitrile concentration, but it is significantly less than that shown in figure 3.2(b) for the higher acetonitrile concentration. The reason for this remains unclear, but it could be a result of a change in conformation of the protein in the two different solution compositions bringing different amino acid residues into contact with the electrode surface. There was also a decrease in fragmentation when the formic acid concentration was lowered to 48.75/48.75/2.5 (vol/vol/vol) water/acetonitrile/formic acid (figure 3.5(b)). The

conductivity of the solution is expected to decrease as the concentration of formic acid decreases, and smaller currents (and hence electrolysis rate) would result. This effect would account for at least part of the decrease in protein fragmentation. Roeser et al also obtained a higher percentage of cleavage products in strongly acidic conditions than in weak acidic conditions when electrochemically fragmenting tyrosine and tryptophan containing tripeptides.[3]
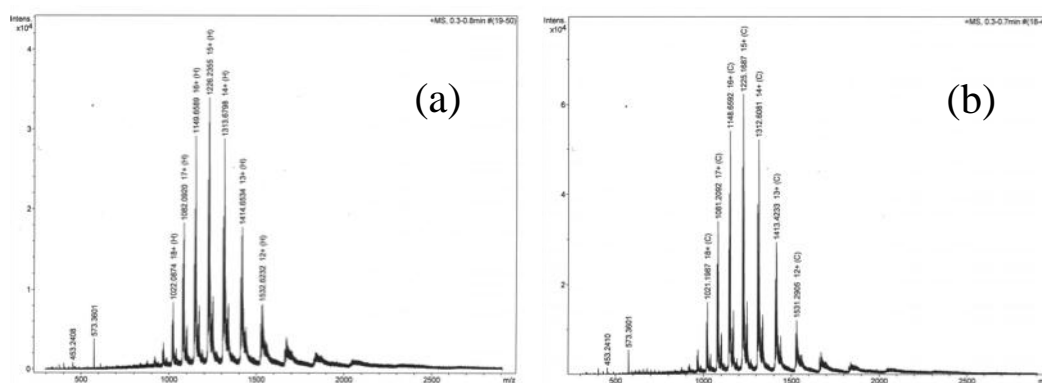
Figure 3.5. Mass spectra of β-lactoglobulin after 1 hour of electrolysis with a graphite electrode at 1 V showing the influence of electrolyte composition. (a) Decreased acetonitrile concentration, 25/70/5 (vol/vol/vol) acetonitrile/water/formic acid. (b) Decreased formic acid concentration, 48.75/48.75/2.5 (vol/vol/vol) acetonitrile/water/formic acid.

3.3.1.4. Electrolysis of beta-casein and BSA

The utility of the system was assessed by electrolysing β-casein and BSA under the conditions that were most successful in generating fragments for β-lactoglobulin. The appearance of peaks in the low m/z range in mass spectra obtained after electrolysis (figure 3.6) suggests some fragmentation occurs. However reconstruction of the mass spectra did not show any distinguishable peaks above the background noise.

A potential problem for BSA fragmentation is that the many internal disulfide bonds could provide enough internal structure to hold the protein fragments together. To examine this possibility, prior to electrolysis, the disulfide bonds were reduced with DTT

and capped with iodoacetic acid, thereby removing the internal disulfide bond structure of the BSA. The resulting mass spectrum (not shown) obtained after 1 hour electrolysis at 1 V had significant background noise, probably a result of incompatibility of residual iodoacetic acid with the ionization source of the mass spectrometer. This problem could not be significantly improved by desalting the solution. No specific fragments were observed in the reconstructed mass spectrum of this BSA electrolysis sample and no further investigations of the system were undertaken.
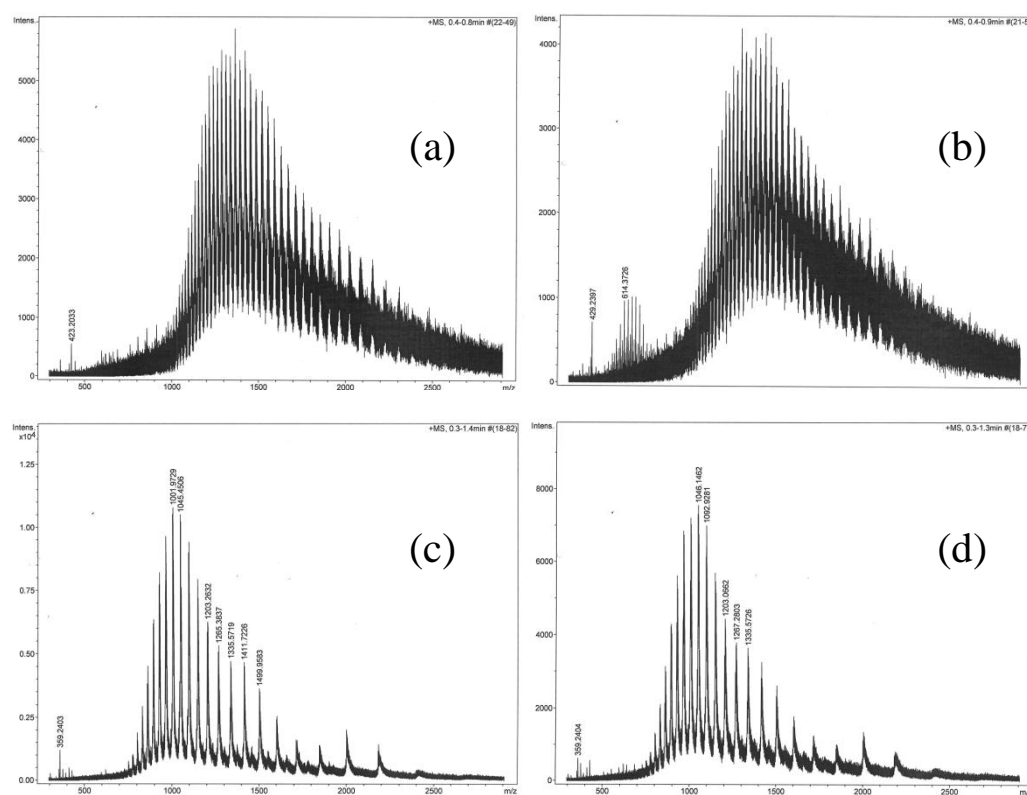
Figure 3.6. Mass spectra of BSA and β-casein before and after 1 hour electrolysis with a graphite electrode at 1 V in 47.5/47.5/5 (vol/vol/vol) acetonitrile/water/formic acid electrolyte. (a) BSA, no electrolysis. (b) BSA, after 1 hour electrolysis. (c) β-casein, no electrolysis. (d) β-casein, after 1 hour of electrolysis.

It is likely that the low level of protein fragmentation observed in the electrolysis experiments thus far is a result of electrode fouling by protein adsorption. The adsorbed protein may be blocking or hindering electron transfer from the electrode to the remaining protein in solution. The next section focuses on investigating the extent of this problem and exploring options to overcome it.

3.3.2. Investigation of protein adsorption on GC electrodes.

GC electrodes were chosen for the study of protein adsorption because they are a carbon based material suitable for protein fragmentation and their electrochemistry and surface modification is well understood.

Direct electrochemical oxidation of proteins could be observed at a GC electrode in a solution of whey protein in 0.1 M phosphate buffer at pH 7.2 using cyclic voltammetry. Figure 3.7 shows a broad oxidation peak in the cyclic voltammogram (first scan), however on subsequent scans the signal diminished very rapidly, which suggested protein was adsorbing to the electrode surface and blocking electron transfer between the electrode surface and the protein. Electrochemical impedance spectroscopy was used to measure the rate of electron-transfer to ferricyanide/ferrocyanide solution species across the working electrode interface at a bare GC electrode and at the same surface following 3 scans in protein solution (same conditions as in figure 3.7). The charge transfer resistance was found to be greatly increased after scanning in protein solution; this is indicative of a blocked or fouled electrode surface due to protein adsorption.
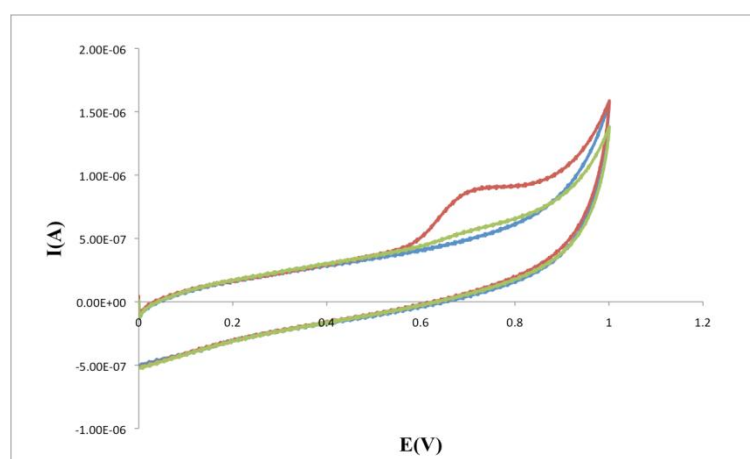

Figure 3.7. CVs showing direct oxidation of whey protein in 0.1 M phosphate buffer, pH 7.2. with a GC electrode. Red line: First scan in whey. Green line: Second scan in whey. Blue line: Blank, phosphate buffer.

The oxidation peak observed for whey protein is in the same potential region as that of some of the 5 electrochemically oxidisable amino acids contained in the protein. These are tyrosine, tryptophan, histidine, cysteine and methionine. The oxidation of the tyrosine ring OH group to a ketone (same initial reaction of tyrosine as shown in chapter 1 figure 1.2) at a GC electrode is shown in figure 3.8 for comparison to the oxidation of whey in figure 3.7. Tryptophan also gives a peak at a similar potential (not shown).[7] Hence it is likely that the oxidation peak for whey in figure 3.7 is made up at least in part by the oxidation of tyrosine and tryptophan residues in the proteins.
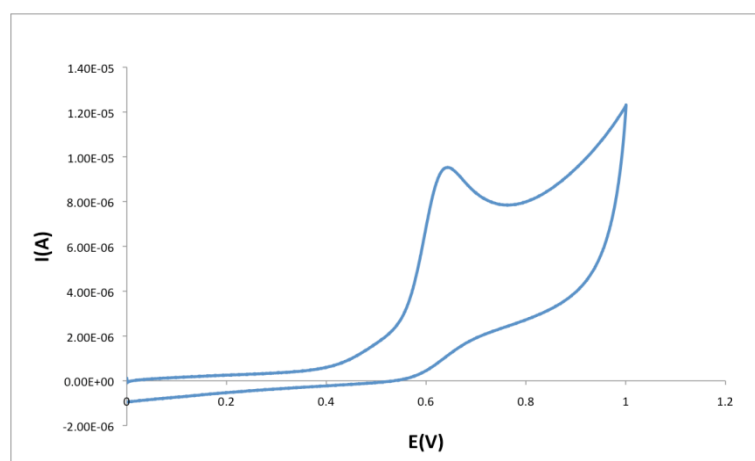
Figure 3.8. CV showing the oxidation of 0.1 mg/ml tyrosine in 0.1 M phosphate buffer, pH 7.2 on a GC electrode.

Mechanisms initiated by the oxidation of tyrosine and tryptophan residues in a protein have been shown to lead to cleavage of the protein backbone.[5] Hence observation of an oxidation process for whey proteins which is likely to involve oxidation of tyrosine residues, indicates that oxidative cleavage of the whey protein backbone is also a possibility.

3.3.2.1. Modification of the GC electrode with a tolyl film

The main challenge with this strategy for cleaving proteins with carbon electrodes is adsorption of the protein to the electrode surface (electrode fouling). Fouling significantly

limits the amount of protein oxidation that can be achieved. One strategy investigated to counter this was to covalently attach a film to the electrode surface that would be resistant to protein fouling, but still allow electron transfer to the protein. A tolyl film was covalently attached to the electrode surface via electrochemical reduction of the corresponding diazonium salt (figure 3.9).[8] This film was chosen as it was thought that oxygen containing functional groups natively present on the GC surface might be influencing adsorption of the protein molecules. Other factors will also influence the adsorption of proteins to the electrode surface, such as the hydrophobic nature of the GC surface interacting with hydrophobic areas of the protein molecule. However, the tolyl film should provide a more uniform, oxygen-free electrode surface and establish whether oxygen functionalities on the GC surface play a major role in protein adsorption.
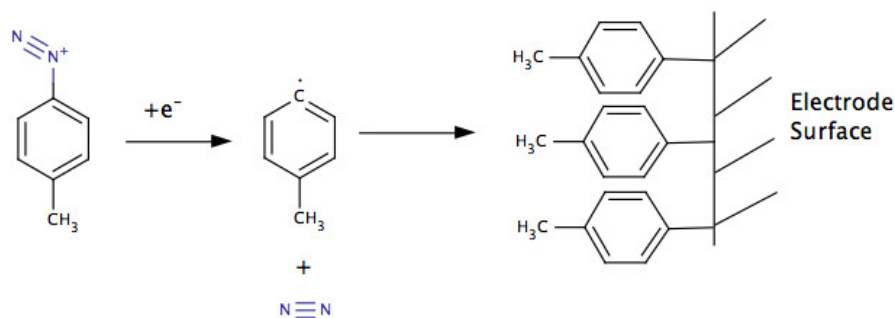
Figure 3.9. Proposed mechanism for electrochemical covalent attachment of a tolyl film to a GC electrode surface.

A thin layer of the tolyl film was covalently attached to the electrode surface using a single cyclic voltammetric scan from 0.1 V to -0.5 V (figure 3.10). A single scan was performed as the film will form a multilayer if a reducing potential is applied for too long and will quickly passivate the electrode surface. Evidence of modification was obtained from cyclic voltammograms of ferricyanide at the modified electrode. A substantial increase in ΔE_p was observed at the modified electrode (results not shown) indicating that the electron transfer rate is decreased by the film.
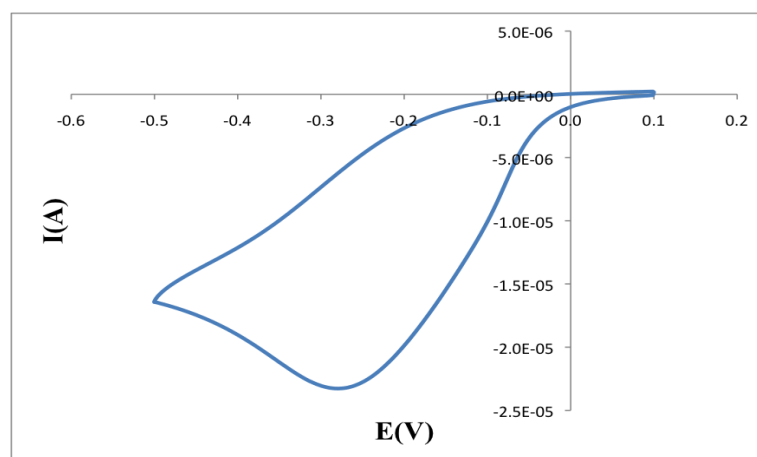
Figure 3.10. CV scan (Blue line) in a solution of 1 mM methyl benzene salt, and 0.1 M [Bu$_4$N]BF$_4$ in acetonitrile on a GC electrode. Potential vs Ag/AgNO$_3$ reference electrode.

Electron transfer through the thin tolyl film was sufficiently rapid to give a visible oxidation peak for whey protein in the same conditions as in figure 3.8 (results not shown). However, on repeat scans the electrode was also fouled in the same manner as the bare electrode, suggesting that it is not primarily oxygen functionalities on the electrode surface that are responsible for adsorption of protein to the electrode surface.

As a further strategy to counter electrode fouling problems, a second electrochemical step was introduced to try and remove the adsorbed protein from the tolyl modified electrode. Figure 3.11 shows the electrochemical response of ferricyanide at a bare GC electrode, a tolyl modified electrode, a tolyl modified electrode after 2 scans in whey protein from 0-1 V and after -2 V was applied to the protein-fouled tolyl modified GC electrode. After application of -2 V for 30 seconds, the electrode is more active towards ferricyanide reduction than is the initial tolyl modified electrode. This indicates that the tolyl film is being removed, to some extent, under these conditions. A further study was conducted to see if the protein could be removed under milder conditions, but it was found that the

conditions required for removal of the adsorbed protein were also sufficient to remove the attached tolyl film.
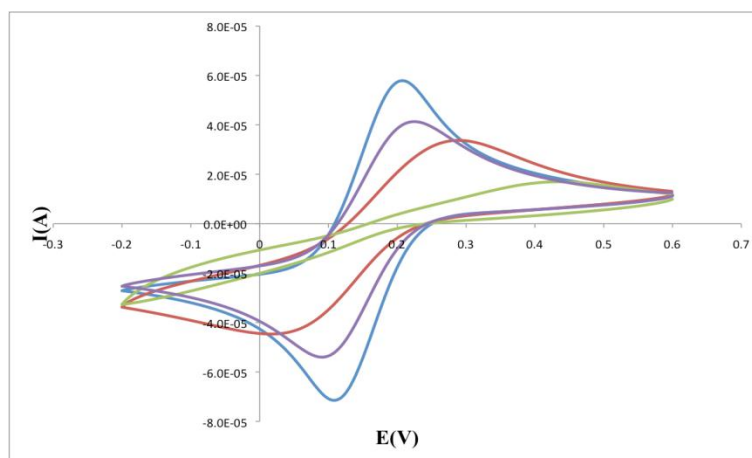
Figure 3.11. CVs at a GC electrode in 5 mM ferricyanide and 0.1 M KCl solution at various stages of modification. Blue line: Polished GC electrode. Red line: After tolyl grafting. Green line: After tolyl grafting and 2 scans in whey protein. Purple line: After tolyl grafting, 2 scans in whey protein and -2 V for 30 seconds in 0.1 M pH 7.2 phosphate buffer.

3.3.2.2. Modification of the GC electrode with a PEG film

The second film chosen to be trialed as an anti-fouling layer was an amine containing polyethylene glycol (PEG) film. PEG is very well known for reducing protein adsorption[9] and this strategy has previously been used with some success for reducing electrode fouling by BSA, lysozyme and RNase.[10] The PEG film was attached via electrochemical oxidation of the amine functionality giving a radical species which attacks and grafts to the GC surface. There are 3 proposed mechanisms for this reaction; all of them involve generation of a radical intermediate.[11, 12]Figure 3.12 shows one of the proposed mechanisms as it applies to the grafting of the amine containing PEG film to a GC surface.
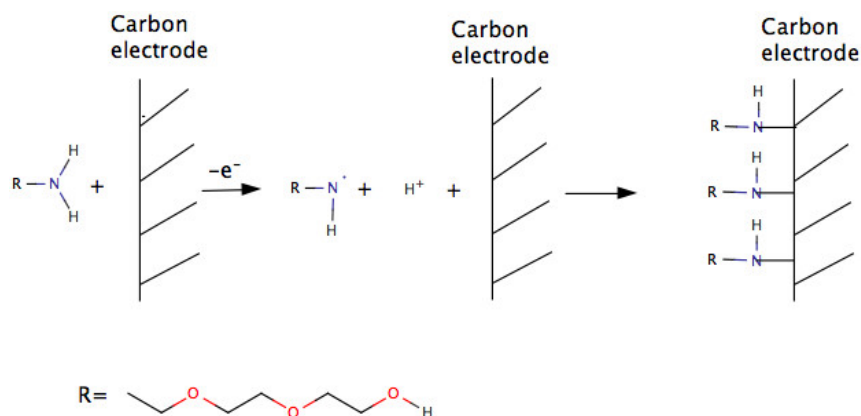
Figure 3.12. A proposed reaction mechanism for electrode modification by electrochemical amine oxidation.

A single potential cycle starting at 0 V and going to 1.4 V was used to graft a thin film as shown in figure 3.13. Cyclic voltammograms were also obtained in ferricyanide solution for the PEG modified surface; an increase in ΔE_p compared to the bare surface was observed and is evidence for successful PEG modification.
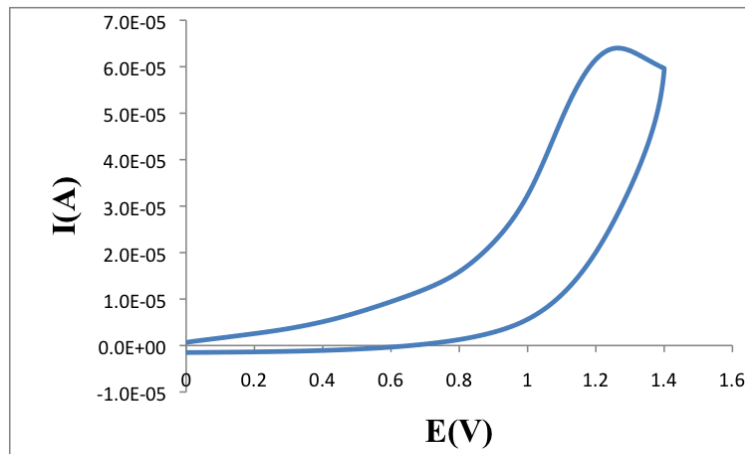
Figure 3.13. CV scan (blue line) in a solution of 5 mM amine terminated PEG and 0.1 M [Bu$_4$N]BF$_4$ in acetonitrile at a GC electrode vs Ag/AgNO$_3$ reference electrode.

Oxidation of proteins through the PEG film was not observed with cyclic voltammetry. It is possible that the film was too thick to allow a significant electron transfer rate from the electrode to the protein in solution or alternatively that the current from protein oxidation was unable to be detected above the background current. Probing the surface with

66

ferricyanide voltammetry after 3 CV scans in whey protein solution showed very little change compared to the CV of ferricyanide obtained at the modified electrode before use in whey solution (figure 3.14). The origins of the distorted voltammogram shown in figure 3.14 were not investigated; the important aspect for this study is there is very little change after use of the electrode in protein solution.
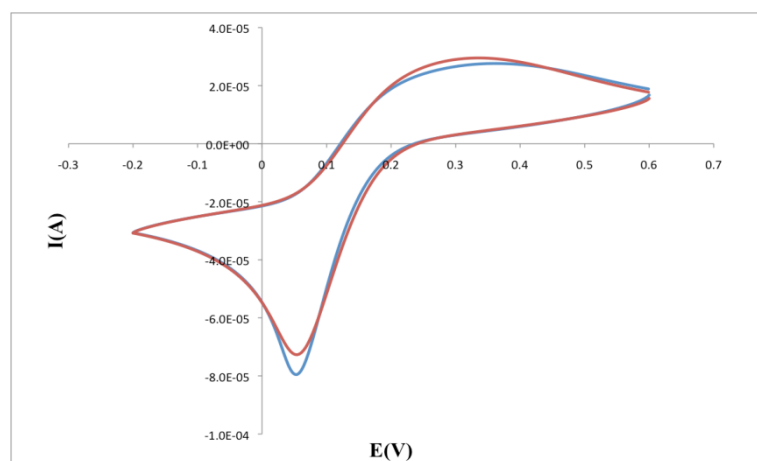
Figure 3.14. CVs of a PEG modified GC rod in ferricyanide solution. Blue line: Before 3 scans in whey protein solution. Red line: After scans in whey protein solution.

This is a promising result as it suggests that there is very little protein adsorption on the PEG modified electrode. Further studies were conducted using electrochemical impedance spectroscopy to monitor surface fouling. These experiments showed little change in charge transfer resistance after 3 scans from 0 to 1 V in whey protein solution confirming that the electrode surface was not becoming fouled by protein adsorption. Another study was conducted by immersing the electrode in the protein solution for 24 hours. Once again, there was very little change in charge transfer resistance for the PEG coated electrode. In contrast, bare GC electrodes and tolyl coated electrodes exhibited a large increase in charge transfer resistance under the same conditions. Hence the PEG modified electrode displays antifouling properties that bare GC and tolyl grafted electrodes do not. Due to time constraints it was not possible to investigate whether a

PEG film could be prepared which both prevented adsorption and allowed a satisfactory rate of protein oxidation.

3.4. Conclusion

Bulk electrolysis of the target proteins was carried out with a graphite rod electrode in a solution containing 47.5/47.5/5 (vol/vol/vol) acetonitrile/water/formic acid. β-lactoglobulin fragmentation was detected by mass spectroscopy, but fragmentation did not occur to an extent where fragments were observable by gel electrophoresis. Hence it appears that the fragmentation products are present in low concentrations. Most of the electrolysis products appear to arise from non-cleavage oxidation reactions. These results are consistent with previous reports of electrolysis experiments on similar proteins. Attempts made to increase fragmentation by changing the electrolysis solution composition resulted in reduced protein fragmentation, possibly due to protein conformation effects and reduction in solution conductivity. Some evidence for fragmentation of BSA and β-casein was apparent in mass spectra of the electrolysis experiments. However the fragments were not able to be observed in the reconstructed spectra. Attempts were made to improve fragmentation by reducing and capping the disulphide bonds in BSA, however this did not improve fragmentation.

Electrode fouling by protein material adsorbing to the electrode surface was thought to be the main reason why protein fragmentation was occurring in low yield. For this reason a study of electrode fouling was conducted with GC electrodes. Whey protein oxidation

was observed by cyclic voltammetry but it was apparent that the protein adsorbs to the electrode surface during the electrochemical experiment. Some progress was made towards modifying the properties of the GC electrode to make the electrode surface more resistant to fouling. A tolyl film was grafted to the electrode surface in an attempt to remove the interaction between oxygen functionalities present on the electrode surface and the protein in solution. This appeared to have no effect on protein adsorption. A PEG film was also grafted to the electrode. Initial results are promising with evidence of decreased protein adsorption at PEG modified GC electrodes, however this process requires further testing. In particular, it is not yet known whether a PEG film can be prepared that prevents protein adsorption and at the same time allows a significant rate of protein oxidation.

Direct electrochemical fragmentation was demonstrated with β-lactoglobulin, but at this stage with the current experimental conditions and knowledge about the process, it is not appropriate for scaling up for use in bulk fragmentation of proteins. This is because the necessity for complex solutions and electrode antifouling films makes the method unlikely to be of industrial importance. An indirect electrochemical method appears to be preferable, that is, electrochemically generating active agents that cleave proteins, thus avoiding the need for proteins to be in contact with the electrode surface and so reducing the effects of electrode fouling. The electrochemical generation of strong oxidants such as hydroxyl radicals is potentially well suited to this purpose. For this reason, a specialised electrode material based on lead dioxide will be investigated in the next chapter for direct electrochemical generation of hydroxyl radicals. In the following chapter, generation of hydrogen peroxide for use with catalytic additives for generating hydroxyl radicals via the Fenton reaction will be explored.

References

1.   Iwasaki, H. and B. Witkop, *New Methods for Nonenzymatic Peptide Cleavage. Electrolytic, Differential, and Solvolytic Cleabage of the Antibiotic Cyclopeptide Rufomycin.* Journal of the American Chemical Society, 1964. **86**(21): p. 4698-4708.

2.   Cohen, L.A. and L. Farber, *Cleavage of tyrosyl-peptide bonds by electrolytic oxidation.* Methods Enzymol., 1967. **11**: p. 299-308.

3.   Roeser, J., H.P. Permentier, A.P. Bruins, and R. Bischoff, *Electrochemical Oxidation and Cleavage of Tyrosine- and Tryptophan-Containing Tripeptides.* Analytical Chemistry, 2010. **82**(18): p. 7556-7565.

4.   Permentier, H.P., U. Jurva, B. Barroso, and A.P. Bruins, *Electrochemical oxidation and cleavage of peptides analyzed with on-line mass spectrometric detection.* Rapid Commun Mass Spectrom, 2003. **17**(0951-4198).

5.   Permentier, H.P. and A.P. Bruins, *Electrochemical oxidation and cleavage of proteins with on-line mass spectrometric detection: Development of an instrumental alternative to enzymatic protein digestion.* Journal of the American Society for Mass Spectrometry, 2004. **15**(12): p. 1707-1716.

6.   McCreery, R.L., *Advanced Carbon Electrode Materials for Molecular Electrochemistry.* Chemical Reviews, 2008. **108**(7): p. 2646-2687.

7.   Jin, G.-P. and X.-Q. Lin, *The electrochemical behavior and amperometric determination of tyrosine and tryptophan at a glassy carbon electrode modified with butyrylcholine.* Electrochemistry Communications, 2004. **6**(5): p. 454-460.

8.   Pinson, J. and F. Podvorica, *Attachment of organic layers to conductive or semiconductive surfaces by reduction of diazonium salts.* Chemical Society Reviews, 2005. **34**(5): p. 429-439.

9.   Zalipsky, S. and J.M. Harris, *Introduction to Chemistry and Biological Applications of Poly(ethylene glycol)*, in *Poly(ethylene glycol).* 1997, American Chemical Society. p. 1-13.

10.   Downard, A.J. and A. bin Mohamed, *Suppression of Protein Adsorption at Glassy Carbon Electrodes Covalently Modified with Tetraethylene Glycol Diamine.* Electroanalysis, 1999. **11**(6): p. 418-423.

11.   Barbier, B., J. Pinson, G. Desarmot, and M. Sanchez, *Electrochemical Bonding of Amines to Carbon Fiber Surfaces Toward Improved Carbon-Epoxy Composites.* Journal of The Electrochemical Society, 1990. **137**(6): p. 1757-1764.

12.   Deinhammer, R.S., M. Ho, J.W. Anderegg, and M.D. Porter, *Electrochemical oxidation of amine-containing compounds: A route to the surface modification of glassy carbon electrodes.* Langmuir, 1994. **10**(4): p. 1306-1313.

Chapter 4. Hydroxyl radical production at lead dioxide electrodes to fragment proteins

4.1 Introduction

4.1.1. Hydroxyl radical initiated cleavage of the protein backbone

As outlined in section 1.5, hydroxyl radicals are capable of fragmenting proteins. The mechanism of fragmentation is a result of the hydroxyl radical's ability to abstract a proton from a saturated carbon site or add to unsaturated carbon atoms or aromatic rings.[1-3] This gives rise to a radical species that can undergo further reactions. Some of these reaction pathways can lead to cleavage of the protein backbone.

4.1.2. Electrochemical generation of hydroxyl radicals

The current interest in producing hydroxyl radicals electrochemically is to achieve complete mineralization or oxidation of organic pollutants and therefore reduce their toxicity or persistence in the environment.[4-6] Hydroxyl radicals are one of the strongest oxidants known (E° = 2.73 V) so they are excellent at the task of breaking down and oxidizing organic material. The aim of this work is to fabricate electrodes capable of producing hydroxyl radicals and then to try and control the way the radicals interact with proteins to give specific protein fragments.

4.1.3. Common electrodes for production of hydroxyl radicals

Two of the most common anodes for oxidation of organic species are lead dioxide and boron doped diamond (BDD).[7-12] These two electrodes have high oxidation power because they generate hydroxyl radicals that are physisorbed to the electrode surface.[13, 14] Once generated, the radicals are able to react with organic molecules that are in the vicinity of the electrode. It is expected that organic molecules have to come close to the electrode surface in order to react with the physisorbed hydroxyl radicals. The average lifetime and estimated diffusion distances of hydroxyl radicals are 8.7×10^{-9} sec and 92 Å respectively,[15] therefore if the radicals were able to leave the electrode surface they are not expected to travel far before reacting. BDD electrodes are capable of a higher mineralisation rate of organics than PbO_2 electrodes, however PbO_2 electrodes are much cheaper and easier to produce making them more suitable for a commercial setting.

4.1.4. Lead dioxide electrodes

PbO_2 is a material that is often used when high oxidising potentials are required as it is a relatively stable low cost material with good electrocatalytic activity. Important properties, such as: mechanical strength,[6] surface area[16] and oxygen evolution potential[17] can be influenced by inclusion of dopants in the deposition bath. Dopants such as fluorine,[18, 19]bismuth[20, 21] and iron[22, 23] have been incorporated into the deposited PbO_2 films.

The detailed mechanism by which PbO_2 electrodes generate hydroxyl radicals is not well understood and could be quite complex. Johnson and co-workers propose that there are

surface sites on PbO_2 capable of adsorbing hydroxyl radicals produced during the hydrolysis of water (mechanism outlined in section 1.5.7).[24, 25]

As outlined in section 1.5, PbO_2 films can be electrochemically deposited on many different substrates; variable deposition conditions can be used to control the quality and characteristics of the resulting films. There are a large number of conditions that can be varied including pH, substrate, Pb^{2+} concentration, current density, potential and mass transport in the plating bath. There are many studies on PbO_2 deposition in the literature but in many cases not all variables are controlled or reported, and hence it is difficult to determine the optimum film deposition conditions.

A preliminary study on deposition conditions was undertaken to produce PbO_2 films that are capable of producing hydroxyl radicals and have a high level of stability under the conditions required for fragmenting proteins. When using PbO_2 electrodes for fragmenting proteins it was considered to be important to minimise contamination from lead leaching into solution, as the toxic nature of lead would limit the potential applications for this process. Due to the large number of variables in the deposition process, a starting point for deposition was established from earlier studies and several variables were adjusted to try and improve the PbO_2 coatings obtained.

4.2. Experimental

PbO_2 electrodes were prepared according to the deposition conditions outlined in section 2.2.3. All protein solution concentration used in this chapter were 1 mg/ml. Electrolysis of protein solutions with PbO_2 electrodes in an undivided cell was undertaken in a standard 3-electrode electrochemical cell shown in figure 2.5. Divided cell electrolysis of protein solutions was undertaken in a 2-compartment cell separated by a Nafion 115 membrane, magnetic fleas in both the anodic and cathodic compartments stirred the electrolysis solutions.

Electrolysis of methyl orange solutions with PbO_2 electrodes was performed in a 3-electrode undivided cell with constant stirring for the purpose of testing the oxidation power of PbO_2 electrodes. The electrolysis solution contained 0.25 mM methyl orange and 0.05 M Na_2SO_4 as supporting electrolyte at pH 3. Aliquots of the methyl solution were analysed by UV-Vis spectroscopy at 503 nm.

Undivided cell electrolysis of N,N-dimethyl-4-nitrosoaniline (RNO) solutions was performed in a standard 3-electrode cell for the purpose of determining hydroxyl radical production of PbO_2 electrodes. The electrolysis solution contained 2×10^{-5} M RNO in 0.1 M pH 7.2 phosphate buffer. UV-Vis spectroscopy was used to monitor RNO adsorption at 440 nm. For divided cell experiments, two standard cells were used with a connecting KNO_3 salt bridge.

4.3. Results and Discussion

4.3.1. Fabrication of lead dioxide electrodes

A survey of the literature suggests that doping PbO_2 with fluorine by adding NaF to the deposition bath may provide benefits such as enhanced hydroxyl radical production and stability.[6, 26] The initial films for the effect of deposition rate study were deposited from a bath of 0.5 M PbO_2, 0.1 M HNO_3 and 0.04 M NaF at 60 °C. PbO_2 films were deposited on a platinum mesh substrate as the chemical inertness of platinum allowed the lead coating to be completely removed and the platinum mesh reused multiple times, thus controlling variables that might be associated with using different sized and structured substrates for the depositions.

To test the effect of changing deposition variables on the quality of the films produced, a method of accelerated lifetime testing was used to monitor the rate of deterioration of the PbO_2 films and follows previously reported methods.[6, 27] The method involved using the prepared electrodes at a current density of 100 mA/cm^2 with a platinum counter electrode in a solution of 1 M H_2SO_4. The current density is 10 × that used to effect protein fragmentation and the strong acid conditions are much harsher on the PbO_2 electrode than conditions in normal use. The accelerated deterioration of the electrodes occurs at a rate that can be measured by weighing the electrode periodically to give the percentage mass loss over time. This data was then used to compare the stability of the electrodes produced under different conditions.

Scanning electron microscopy (SEM) imaging was used to observe the effect of changing variables in the deposition process on the surface morphology of the PbO_2 films. PbO_2 films were deposited on glassy carbon chips for SEM analysis because the flat surface of the glassy carbon gave uniform films that allowed for easy comparison between different depositions. It was assumed the carbon substrate used for imaging would produce similarly structured films as those produced in Pt, but this assumption requires further investigation and was not considered further in this study.

4.3.2. Stability of films produced at different deposition rates

PbO_2 films were deposited at different rates by varying the deposition current density. Constant current densities of 20, 40, 60 and 80 mA/cm^2 were applied for 30 min to study the effect of deposition rate on film stability (figure 4.1). Deposition at 40 and 60 mA/cm^2 gave the most stable films with a 19 % and 15 % loss in mass of the original coating respectively after 4 days of accelerated lifetime testing. The coatings applied at 20 and 80 mA/cm^2 quickly failed during accelerated lifetime testing with almost complete loss of coating after 1 day.

The deposition of PbO_2 is always in competition with the evolution of oxygen from the substrate. At 80 mA/cm^2, a high deposition rate, deposition of PbO_2 may be interrupted at to a great extent by the evolution of oxygen from the platinum substrate during deposition, leading to a disordered film with low stability. All of the coatings were applied for 30 min so at 20 mA/cm^2 the initial mass of the coating was 25 % less than the coating from the 60 mA/cm^2 deposition. The thin coating obtained at 20 mA/cm^2 may have cracks in the structure exposing the platinum substrate producing a significant

evolution of oxygen, as PbO_2 has a higher overpotential for oxygen evolution than platinum, this would be very damaging to the surrounding PbO_2 coating.
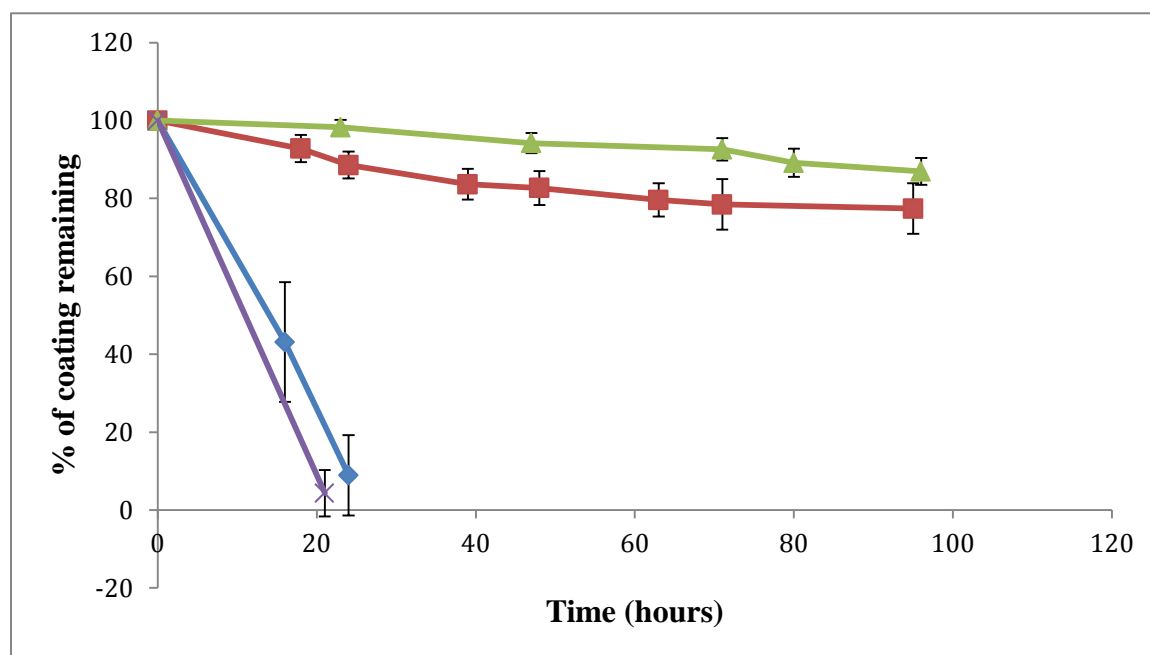

Figure 4.1. Percentage loss of PbO_2 films over time during accelerated lifetime testing at 100 mA/cm^2 in 1M H_2SO_4. Films were initially deposited at 20 mA/cm^2 (blue line), 40 mA/cm^2 (red line), 60 mA/cm^2 (green line) and 80 mA/cm^2 (purple line) from a bath containing 0.5 M $PbNO_3$, 0.1 M HNO_3 and 0.04 M NaF at 60 °C onto a platinum substrate with a copper counter electrode.

Evidence from the SEM analysis showed that very different film morphologies were produced by varying the deposition current in the bath containing 0.5 M $PbNO_3$, 0.1 M HNO_3 and 0.04 M NaF (figure 4.2). Films deposited at 20 mA/cm^2 comprised of crystals with a spherical appearance. Films deposited at 40 mA/cm^2 showed a mixture of large and small elongated crystals and films deposited at 60 mA/cm^2 had small elongated crystals that appeared more uniform in nature. The size of the PbO_2 crystals appears to reduce as the current is increased producing a different surface morphology at each different rate of deposition.
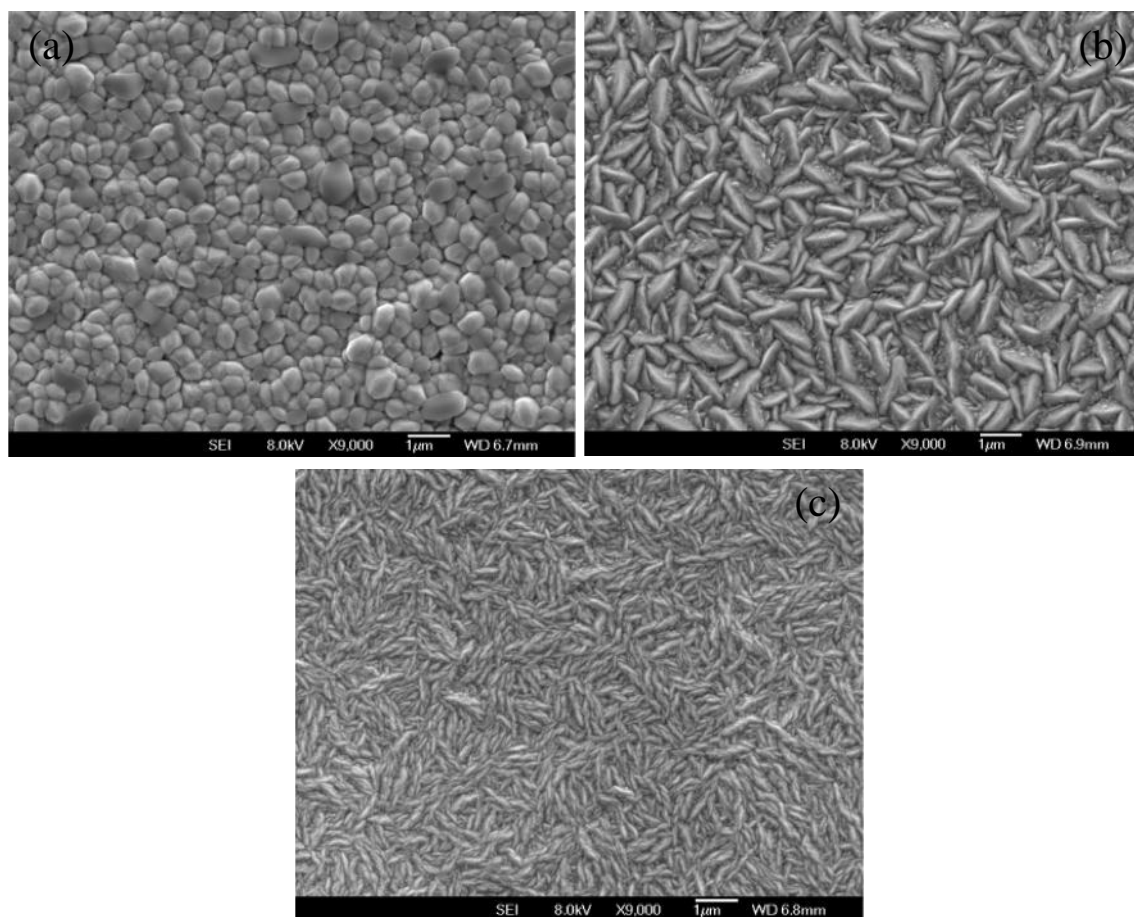
Fig 4.2. PbO$_2$ layer formed on glassy carbon from a solution of 0.5M PbNO$_3$, 0.1M HNO$_3$ and 0.04M NaF at varying current densities. (a) 20 mA/cm^2. (b) 40 mA/cm^2. (c) 60 mA/cm^2.

PbO$_2$ films were also deposited in the absence of fluorine (figure 4.3). The size of the crystals also decreased as the current was increased in a similar way to the films produced with fluorine. Energy dispersive spectroscopy was used to demonstrate that fluorine was being incorporated into the film structure at 0.6 to 0.8 %, when it was present in the deposition bath. Negatively charged fluorine adsorbs to the positively charged film surface and is incorporated into the film structure.[28] It is also likely that fluorine can substitute for oxygen in the PbO$_2$ crystal structure.[18] This change in crystal structure could explain the difference in film morphologies between the films produced with and without fluorine being present in the deposition bath.
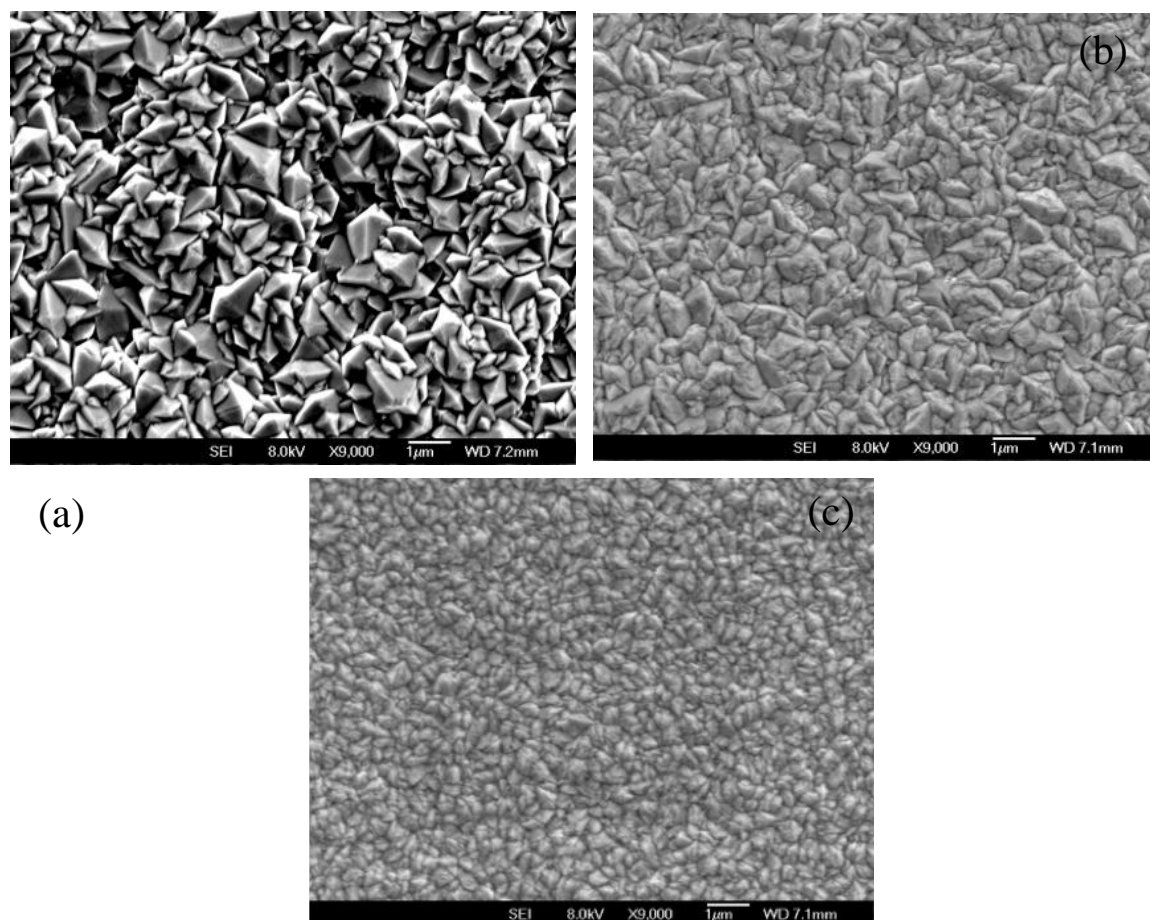
Figure 4.3. PbO$_2$ layer formed on glassy carbon from a solution of 0.5 M PbO$_2$ and 0.1 M HNO$_3$ at varying current densities. (a) 20 mA/cm^2. (b) 40 mA/cm^2. (c) 60 mA/cm^2.

4.3.3. Effect on stability of cycling PbO$_2$ films in H$_2$SO$_4$

Based on the stability data, PbO$_2$ films deposited with a constant current of 60 mA/cm^2 were used for further studies. Cycling the freshly prepared PbO$_2$ electrode in H$_2$SO$_4$ before use could lead to an increase in film stability. Cycling is thought to reorder the film structure and has been shown to reduce the amount of α-PbO$_2$ while increasing the β phase.[29] The cycling of the electrode causes dissolution of the film during reduction, and re-deposition as the oxidation potential is reached. Cycling was undertaken by placing the freshly deposited electrode in 0.5 M H$_2$SO$_4$ and cycling from 0 to 1.8 V until a stable

cyclic voltammogram was obtained. The accelerated lifetime testing results (figure 4.4) show that cycling in H_2SO_4 does not increase film stability within experimental error.
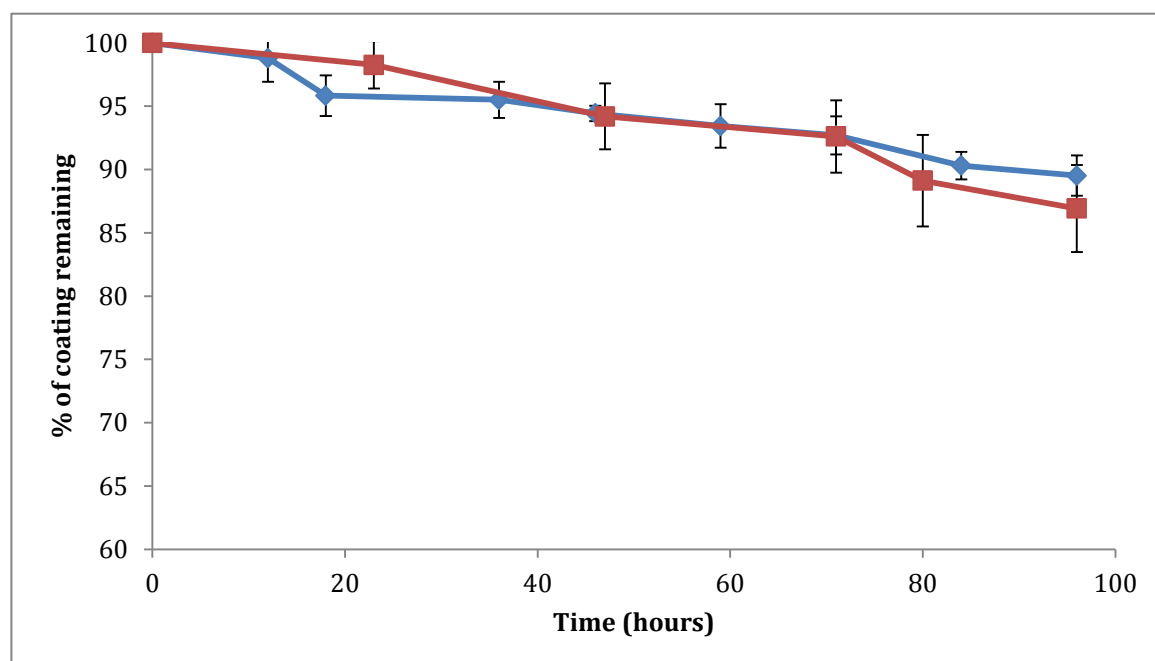
Figure 4.4. Effect of cycling PbO_2 film in H_2SO_4 on lifetime of the film. Blue line: Deposited film was cycled in H_2SO_4 prior to accelerated lifetime testing. Red line: No cycling in H_2SO_4.

Cycling the film in H_2SO_4 may create a more porous structure as shown in figure 4.5. The re-deposition appears to be occurring in an outwards manner growing the crystals taller rather than in an even spread across the entire film. The cycled film has larger features than the original film. No further testing of the cycled films was conducted as cycling did not give an increase in film stability. However cycling could be an effective method for creating more porous films and exposing a greater electrode surface area.

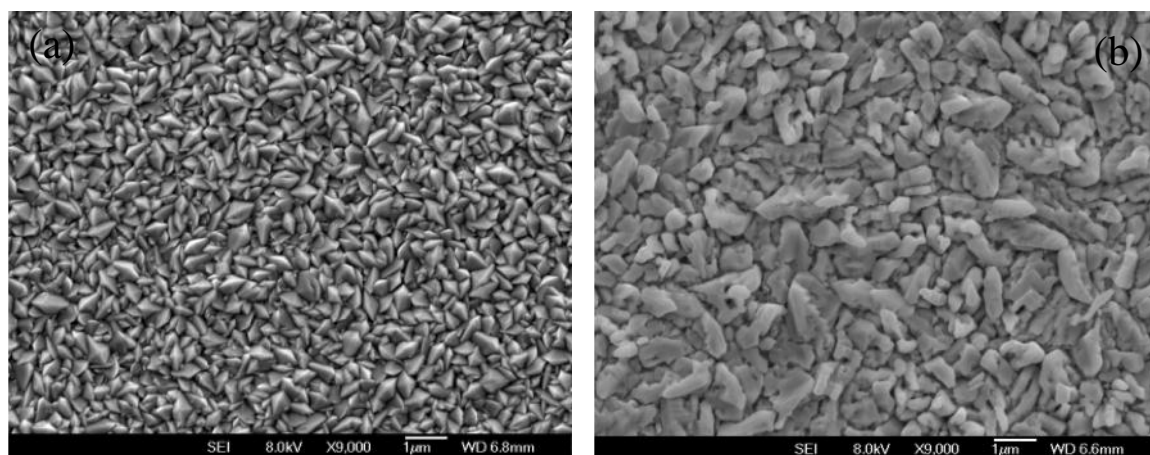Figure 4.5. Effect of cycling PbO$_2$ films in 0.5 M H$_2$SO$_4$. Both surfaces were prepared from a deposition bath containing 0.5 M PbNO$_3$, 0.1 M HNO$_3$ and 0.04 M NaF at a current density of 60 mA/cm^2 at 60 °C. (a) No cycling in H$_2$SO$_4$. (b) Potential cycling in 0.5 M H$_2$SO$_4$ from 0-1.8 V for 30 scans.

4.3.4. Influence of the surfactant Triton X-100 on film stability

The surfactant, Triton X-100 has also been shown to be an effective additive in the PbO$_2$ deposition bath, to improve film stability. It is suggested to form a self-assembled network of surfactant molecules on the electrode surface, which has been shown to increase the overpotential for oxygen evolution from the platinum substrate during electro-deposition of PbO$_2$ films.[16] Decreased oxygen evolution during deposition is desirable for producing films with greater integrity and stability.

Addition of 0.005 M Triton X-100 to the deposition bath containing 0.05 M PbNO$_3$, 0.1 M HNO$_3$, 0.04 M NaF at 60 °C produced a film that had very poor stability as shown in figure 4.6. An unfavourable interaction between Triton X-100 and the negatively charged fluorine ion at the positive electrode surface may disrupt the self assembled network of surfactant molecules during deposition. In order to investigate this possibility, the deposition was repeated under the same conditions but without NaF. This produced a film

with excellent stability; it was the most stable film produced in this study. After 175 hours of accelerated lifetime testing, the film had only lost 0.2 % of its initial mass.

As a comparison, another film was deposited in the absence of Triton X-100 and NaF. This produced a more stable film than that produced with NaF and no Triton X-100, but not as stable as that produced with Triton X-100 and no NaF. After 98 hours of accelerated lifetime testing 2.1 % of the initial mass of the film had been lost. This shows that NaF does not play a part in improving film stability on a platinum substrate. Several reports suggest that NaF has a positive effect on the stability of films produced on a titanium substrate,[26, 30] but it appears to have the opposite effect for films deposited on platinum.
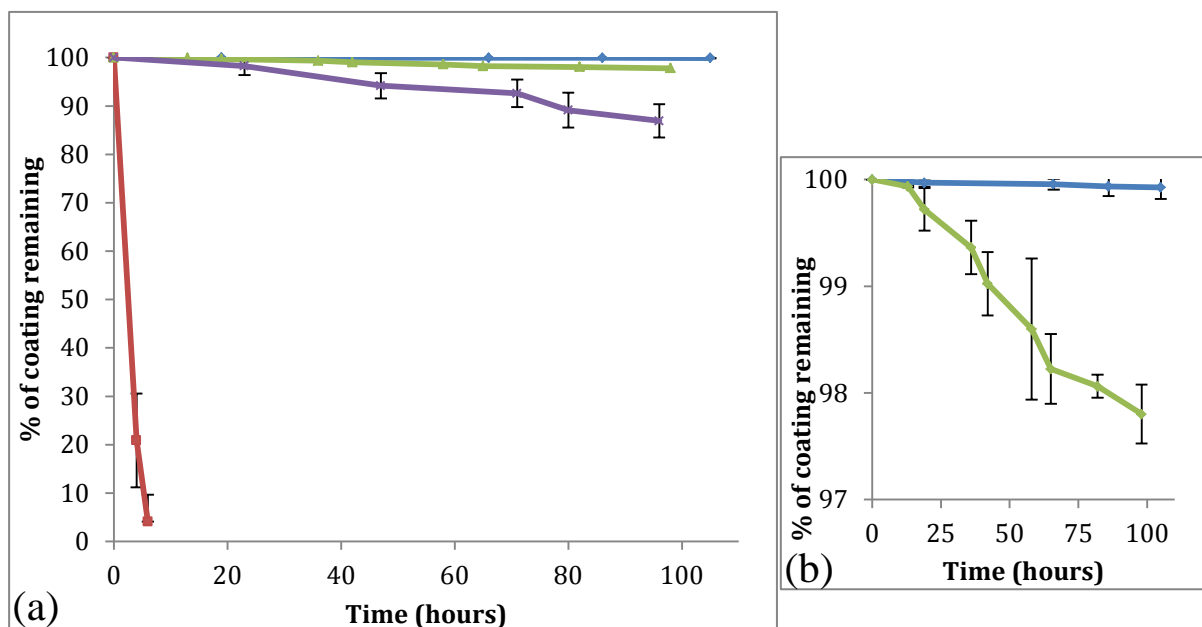
Figure 4.6. Accelerated lifetime testing of PbO_2 films produced with Triton X-100. All deposition baths contained 0.5 M PbO_2 and 0.1 M HNO_3 at a temperature of 60 °C and current density of 60 mA/cm². (a) Green line: No additives. Purple line: 0.04 M NaF added to the bath. Blue line: 0.005 M Triton X-100 added to the bath. Red lane: 0.04 M NaF and 0.005 M Triton X-100 added to the bath. (b) Enlarged view of blue and green lines from part (a).

Although stability of the films produced without NaF was better than those produced with NaF, the effectiveness of hydroxyl radical production at each film is also important. Methyl orange was used to compare the effectiveness of the two films. Cleavage of the methyl orange chromophore group occurs upon reaction of methyl orange with hydroxyl radicals.[31] Observing the intensity changes for the absorption band at 503nm is a convenient way to monitor this reaction over time during electrolysis. Please refer to section 4.2 for experimental conditions used for the electrolysis of methyl orange with PbO_2 electrodes.

Figure 4.7 shows that decomposition of methyl orange occurred more rapidly using the PbO_2 film prepared without NaF than with NaF. Hence hydroxyl radical production is more efficient in the former film. This shows that there is no advantage to incorporating NaF from the deposition bath under the conditions used to prepare the films in this work and was therefore removed for future studies.
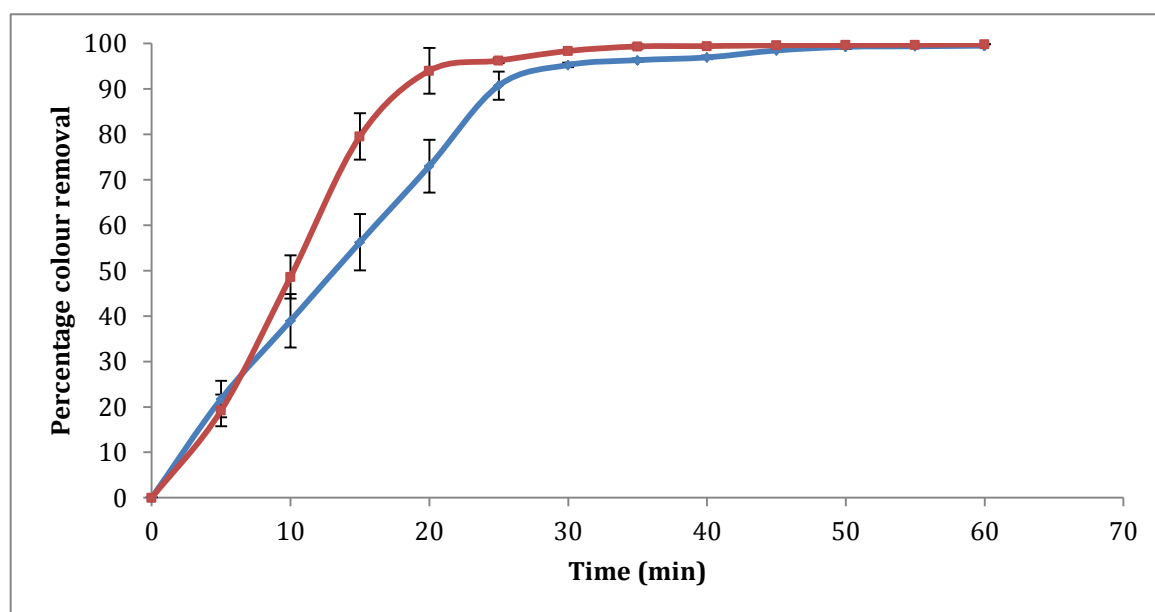

Figure 4.7. Comparison of the degradation of 0.25 mM methyl orange by PbO_2 electrodes at a current density of 10 mA/cm^2 over time produced with 0.04 M NaF (blue line) and without NaF (red line) in the deposition bath.

4.3.5. Testing hydroxyl radical production of fabricated PbO$_2$ electrodes

To provide further evidence that the PbO$_2$ electrodes were generating hydroxyl radicals as oxidants, a method using N,N-dimethyl-4-nitrosoaniline (RNO) was chosen to test the manufactured electrodes. RNO acts as a hydroxyl radical scavenger and its degradation by hydroxyl radicals can be easily detected by UV-Vis absorbance at 440 nm. RNO is a good candidate for detection of hydroxyl radicals because it has the following properties:[13]

1. It is very selective for the reaction with hydroxyl radicals, neither singlet oxygen nor other "peroxo" compounds interfere with the chromophoric group of RNO.

2. It has high rate of reaction with OH radicals ($1.2 \times 10^{10} \, M^{-1}s^{-1}$).

3. It gives very clear results by simply monitoring the change in the sensitive absorption band at 440 nm.

4. RNO is electrochemically inactive at Pt, IrO$_2$,, SnO$_2$ and PbO$_2$ anodes when examined with cyclic voltammetry.[13]

RNO reacts with hydroxyl radicals according to figure 4.8, This reaction causes a bleaching of the yellow coloured solution which can be monitored by UV-Vis Spectroscopy.
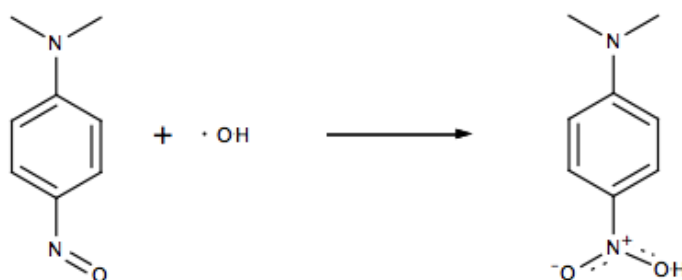

Figure 4.8. Reaction of RNO with hydroxyl radicals.

The PbO_2 electrolysis cell decolourised a RNO solution over time as shown in figure 4.9(a). These results show that the PbO_2 electrodes are effectively producing hydroxyl radicals at a current density of 10 mA/cm^2 as the characteristic RNO absorbance at 440 nm decreases as a result of increasing electrolysis time. The rate of degradation is strongly affected by the current density of the working electrode as shown in figure 4.9(b). Increased current density leads to an increased rate of RNO degradation after 10 minutes of electrolysis.
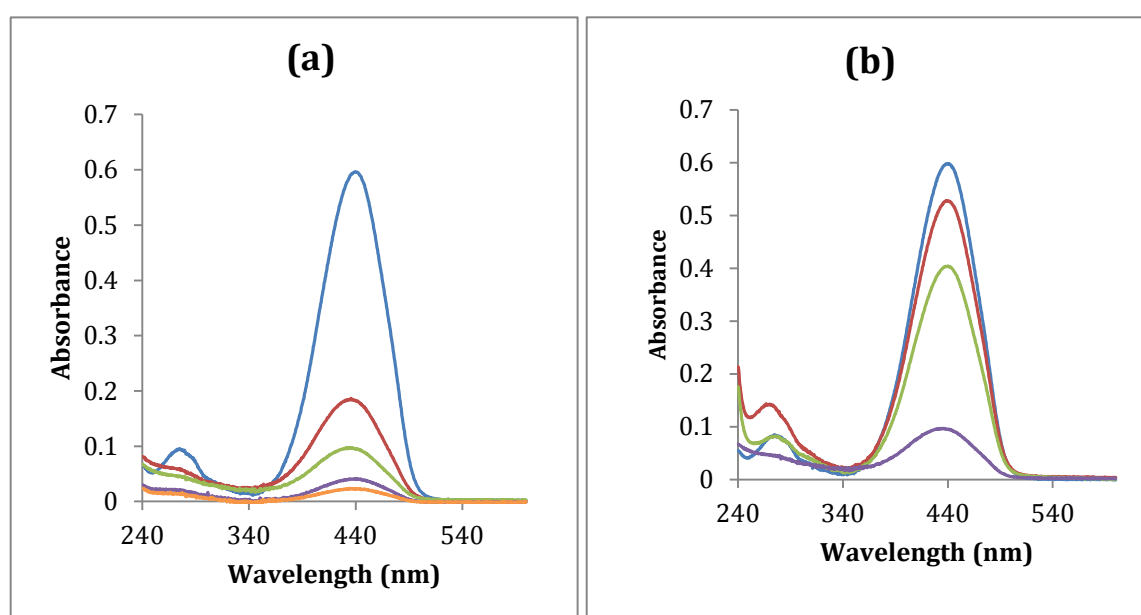
Figure 4.9. UV-Vis spectra of RNO in 0.1 M pH 7.2 phosphate buffer. (a) Degradation of RNO over time at 10 mA/cm^2 using a PbO_2 electrode. Before electrolysis (blue line), after 5 min (red line), after 10 min (green line), after 20 min (purple line), after 30 min (orange line). (b) Degradation of RNO in 0.1 M pH 7.2 phosphate buffer after 10 min using a PbO_2 electrode at different current densities. Before electrolysis (blue line), 1 mA/cm^2 (red line), 3 mA/cm^2 (green line), 10 mA/cm^2 (purple line).

RNO has been used to detect hydroxyl radicals in several studies,[32],[33] but its use is not widespread, hence some further experiments were undertaken to provide more evidence that this method of hydroxyl radical detection is a reliable one.

4.3.6. Influence of counter electrode on RNO degradation

A divided cell separated by a salt bridge was used to ensure that the counter electrode (cathode) did not influence the degradation of RNO. Figure 4.10 shows that RNO is stable in the cathodic compartment of the divided cell, so does not cause, or add to, the degradation rate of RNO.
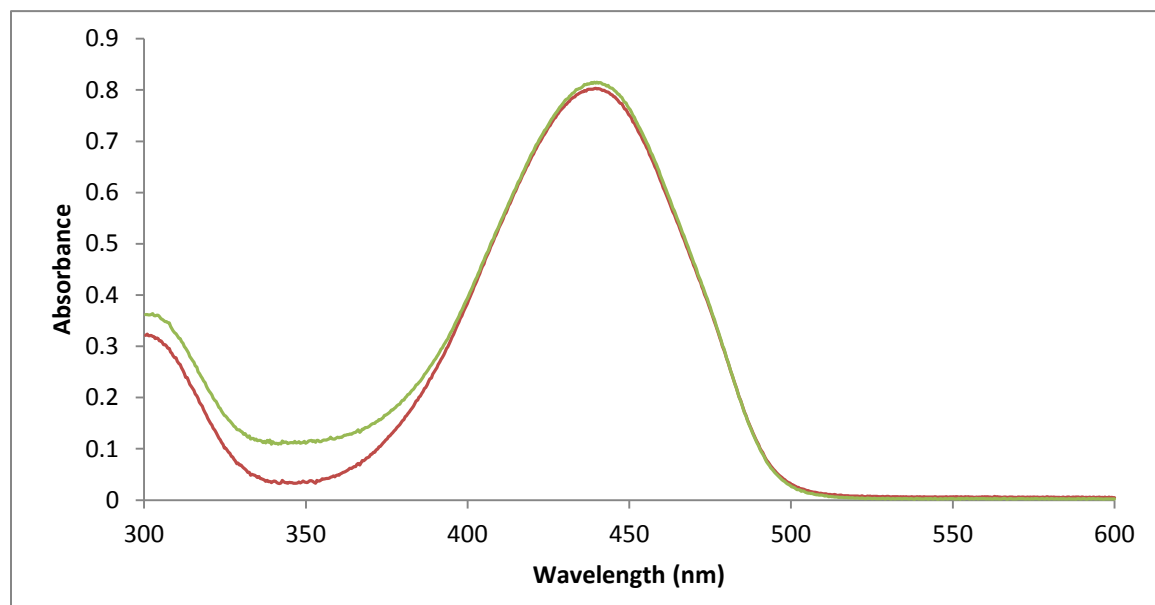
Figure 4.10. UV Vis spectra of RNO after 30 min in a divided cell. PbO_2 anode (Red line), Platinum counter cathode (Green line) and Blank RNO solution (Purple line).

The next step was to provide further evidence that it is hydroxyl radicals and not direct anodic oxidation causing the bleaching of RNO. This was achieved by adding increasing concentrations of tert-butanol to the electrolysis cell. Tert-butanol is a well-known hydroxyl radical scavenger,[34],[35] and will compete with RNO to react with the hydroxyl radicals. The rate constant for the reaction of tert-butanol with hydroxyl radicals is $5 \times 10^8 \ M^{-1} \ s^{-1}$,[36] so it will not react as quickly as RNO ($1.2 \times 10^{10} \ M^{-1} s^{-1}$) but should react sufficiently fast to give a visual indication of competition for hydroxyl radicals. Figure 4.11 shows that this is indeed the case; as the concentration of tert-butanol is increased, the amount of RNO bleaching is reduced.

This initial testing of the electrodes with RNO is good evidence that the electrodes are functioning well and are producing hydroxyl radicals as expected. In the following section the PbO$_2$ electrodes are tested for their ability to fragment proteins.
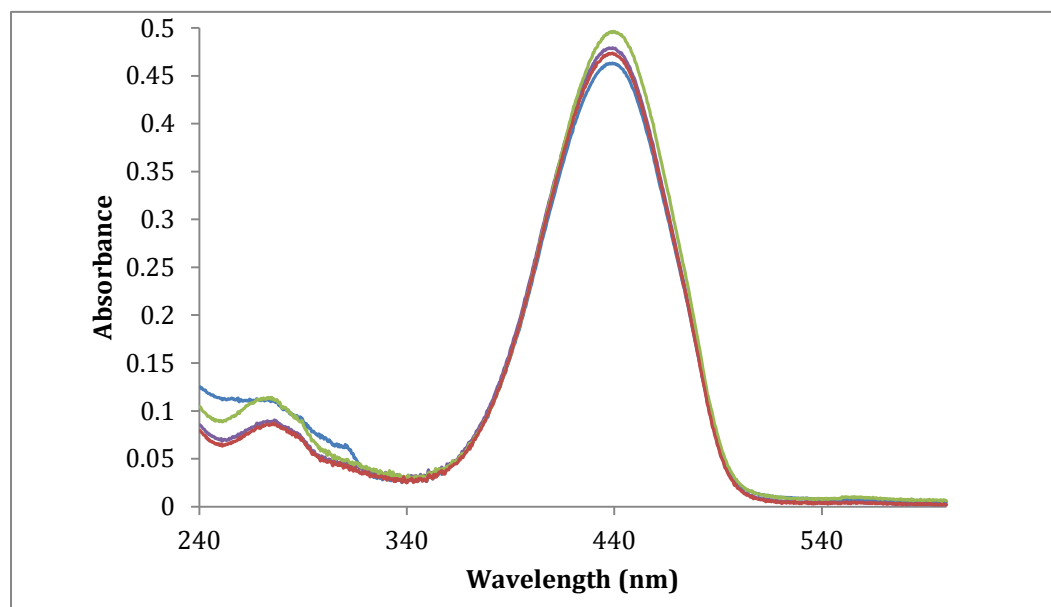
Figure 4.11. UV Vis spectra of RNO after 5 min of electrolysis with a PbO$_2$ electrode at 10 mA/cm^2 in an undivided cell using various concentrations of tert-butanol as a radical scavenger. No tert-butanol (blue line), 50 mM tert-butanol (red line), 200 mM tert-butanol (purple line), 1 M tert-butanol (green line).

4.3.7. Protein degradation by electrochemically generated hydroxyl radicals

Initial testing of protein fragmentation with PbO$_2$ electrodes was conducted with the model protein, BSA in phosphate buffer as it one of the most commonly used buffers for biological systems with the added benefit of having 3 useful pKa values which allows a broad pH range to be used.

Aliquots of protein solution were removed from the electrolysis cell in 1 hour intervals to monitor protein fragmentation by gel electrophoresis. Figure 4.12(a) shows the image of the electrophoresis gel after the electrolysis of BSA in pH 7.2 phosphate buffer over time

up to 5 hours. The major band of BSA at ~66 kDa in the gel decreases over time due to destruction by hydroxyl radicals produced at the electrode. However, no smaller fractions are evident in the lanes below the main band. Increasing the electrolysis current density from 10 mA/cm^2 to 20 mA/cm^2 increases the speed of the disappearance of the main BSA band (~66 kDa) as shown in lane 6 of figure 4.12(a). Similar results can be seen for the main fractions of whey, β-lactoglobulin (~18.4 kDa) and α-lactalbumin (~14 kDa) in figure 4.12(b). The bands for these two proteins are almost completely gone after 3 hours of electrolysis at 10 mA/cm^2, but once again no smaller fractions become evident during the loss of the main bands. It also appears that some cross linking of the proteins is occurring under these conditions as high molecular weight aggregates are apparent at the top of the bands in lanes 2, 3 and 4, of figure 4.12(a). However, these protein aggregates are also gone in lane 5 after 5 hours. It has been suggested previously that covalent linkages between proteins can be formed after exposure to hydroxyl radicals.[37] The stability of these aggregates during the denaturing conditions of electrophoresis support this theory. It has also been suggested that one pathway for aggregation may result from hydroxyl radical initiated formation of inter molecular dityrosine linkages.[38]
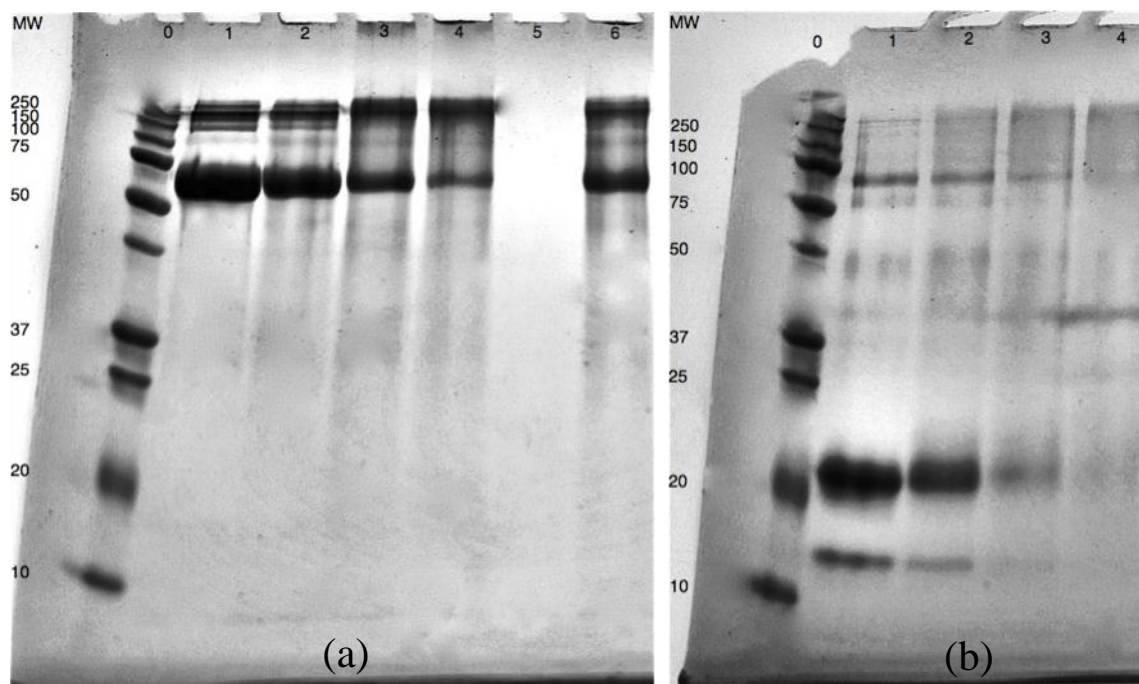
Figure 4.12 (a) Image of an electrophoresis gel showing effect of electrolysis on BSA with a PbO_2 electrode in pH 7.2, 0.1 M phosphate buffer. Lane 0: Molecular weight markers. Lane 1: BSA control. Lane 2: 1 hour electrolysis at 10 mA/cm^2. Lane 3: 2 hours electrolysis at 10 mA/cm^2. Lane 4: 3 hours electrolysis at 10 mA/cm^2. Lane 5: 5 hours electrolysis at 10 mA/cm^2. Lane 6: 1 hour electrolysis at 20 mA/cm^2. (b) Electrophoresis gel image showing effect of electrolysis of whey proteins using a PbO_2 electrode in pH 7.2, 0.1 M phosphate buffer. Lane 0: Molecular weight markers. Lane 1: Whey control. Lane 2: 1 hour electrolysis at 10 mA/cm ^{2}. Lane 3: 2 hours electrolysis at 10 mA/cm^2. Lane 4: 3 hours electrolysis at 10 mA/cm^2.

4.3.8. pH study in phosphate buffer

BSA degradation by PbO_2 electrodes was tested at 3 different pH values in phosphate buffer to see if pH has any influence on cleavage patterns or the speed of degradation. Electrophoresis gels run from aliquots of the electrolysis solution are shown in figure 4.13(a). The pH values tested were pH 2.8 (lane 2), pH 7 (lane 4) and pH 11.2 (lane 6). The earlier studies in phosphate buffer suggested a 20 minute electrolysis time with a constant current of 10 mA/cm^2 would give sufficient protein fragmentation for comparison of the different pH value phosphate buffers.

When BSA was electrolysed for 20 minutes at a constant current of 10 mA/cm^2, 18.3 % of the main band of BSA was lost at pH 2.8 compared to 1.7 % and 0.8 % respectively for the neutral and basic pH experiments. Some evidence of smearing beneath the major band of BSA in lane 2 is apparent, but no well-defined bands have formed. Lanes 1 and 2 have been enlarged (figure 4.13(b)) and the densitometric intensity graphed alongside shows a reduction in all of the BSA bands. These results show that the destruction of proteins by hydroxyl radicals occurs much more readily in phosphate buffer at an acidic pH than at neutral pH or basic pH. The reason for the increased fragmentation in acid is not well understood and will be investigated further below.

PH	% loss of 66kDa band
2.8	18.3
7	1.7
11.2	0.83
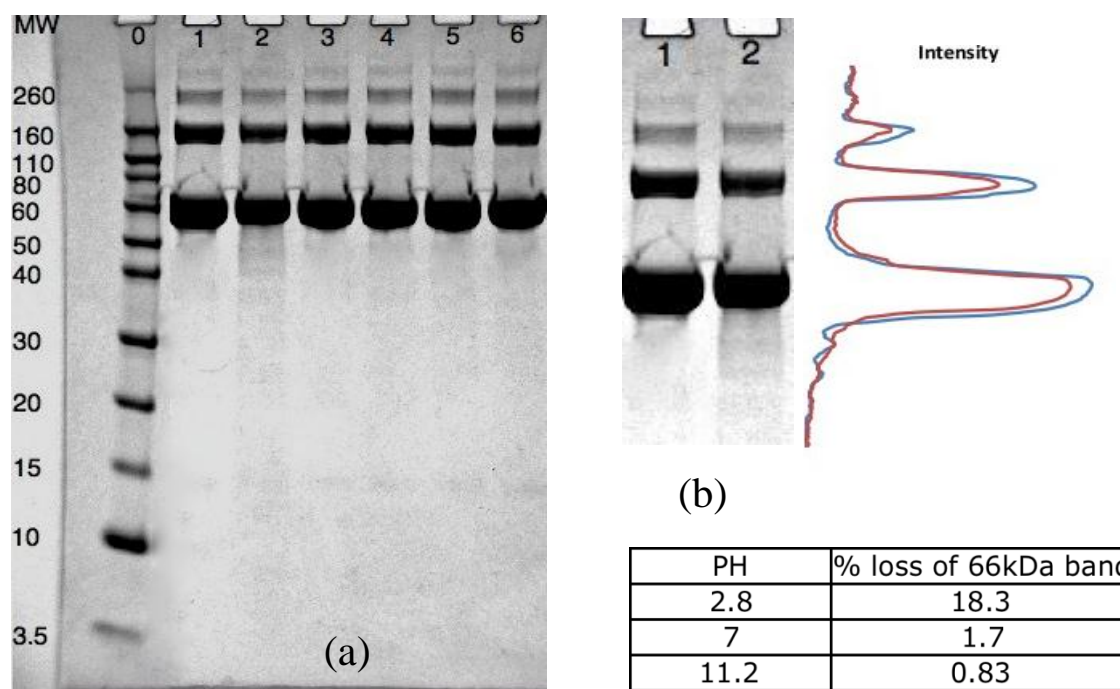
Figure 4.13(a) Electrophoresis gel image showing the effect of pH on BSA electrolysis with a PbO$_2$ electrode in 0.1 M phosphate buffer. Lane 0: molecular weight markers. Lane 1: pH 2.8 control. Lane 2: pH 2.8, 10 mA/cm^2 for 20 min. Lane 3: pH 7 control. Lane 4: pH 7, 10 mA/cm^2 for 20 min. Lane 5: pH 11.2 control. Lane 6: pH 11.2, 10 mA/cm^2 for 10 min. (b) Enlargement of lane 1 and 2 with densitometric intensity graphed alongside. Blue line: Lane 1 intensity. Red line: Lane 2 intensity

Using the PbO$_2$ electrodes in phosphate buffer showed that the system was capable of fragmenting all of the target proteins, but the process was indiscriminate. Instead of

fragmenting the proteins at specific points and producing useful fragments, it appeared that proteins were randomly chopped and did not produce fragments of any one size. This is why no well-defined bands could be seen below the main bands of each protein in the gel lanes.

4.3.9. Significance of the solution composition

The importance of the chemical environment in this system was investigated by testing the PbO$_2$ electrode's ability to fragment proteins in a range of different buffers. Tris/HCl buffer (pH 7) was tested initially with BSA as tris has been shown to scavenge hydroxyl radicals, the rate constant for reaction with hydroxyl radicals is $1.1x10^9$ L·mol^{-1}·s^{-1}.[39] The hydroxyl radical scavenging ability of the buffer is thought to be crucial in protecting certain parts of the protein from attack by hydroxyl radicals, leading to defined cleavage sites.[40] It is possible that hydroxyl radicals can access certain parts of a protein such as hydrophobic areas or size restricted areas that could be inaccessible to hydroxyl radical scavengers. If this is indeed possible then this strategy may lead to specific fragmentation of protein molecules.

Tris has a pKa of 8.06 and an effective buffering range of pH 7-9. A pH of 7 was chosen for this work because earlier results showed that more degradation of the protein occurs at lowered pH. The loss of the intact BSA occurred much quicker in tris/HCl than in phosphate buffer and more importantly some evidence of specific cleavage was visible with light protein bands appearing in the 40 to 50 kDa range (figure 4.14a). This is an important result as specific protein fragmentation as a result of electrochemically generated hydroxyl radicals has not been demonstrated before.

The strength of the buffer was also tested to examine whether higher concentration would lead to more defined cleavage products (Figure 4.14b). An increase in concentration of the tris/HCl buffer from 0.05 to 0.1 M did reduce the loss of protein after 1 hour of electrolysis and visually there appeared to be more cleavage products between 40 and 50kDa. Densitometric analysis showed that the loss of the major BSA band at 66kDa was 63.8% in the 0.05M tris/HCl buffer compared to 40.2% in the 0.1M tris/HCl buffer. This suggests that the increase in concentration of the tris/HCl buffer increased the protection of the protein to non-specific attack by hydroxyl radicals.
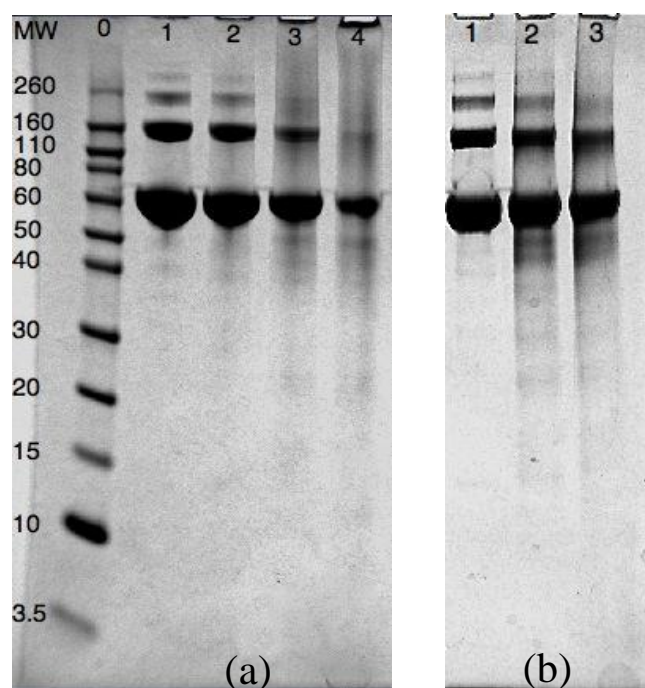
Figure 4.14. Electrophoresis gel images showing effect tris/HCl concentration on BSA fragmentation as a result of electrolysis with a PbO$_2$ electrode at a current density of 10 mA/cm^2. (a) 0.05 M pH 7 tris/HCl buffer. Lane 0: molecular weight markers. Lane 1: BSA control. Lanes 2-4: Electrolysis time of 5 min, 30 min and 60 min respectively. (b) 0.1 M pH 7 tris/HCl buffer. Lane 1: BSA control. Lane 2-3: 30 min and 60 min electrolysis time respectively.

4.3.10. Investigation of buffer systems

The results from the tris/HCl experiment gave a strong indication that the chemical environment is a crucial factor in determining whether or not specific cleavage products could be formed in this system. A way of directing the radicals to specific parts of the

proteins appears to be required, and hence as electrolysis media. Tris/HCl buffer has alcohol groups and abstractable hydrogens, which make it an excellent hydroxyl radical scavenger as hydroxyl radicals react very readily with available hydrogens. Phosphate buffer has no abstractable hydrogens or alcohol groups, so it is unable to scavenge hydroxyl radicals. This explains why no visible cleavage products were produced in phosphate buffer.

The tris/HCl buffer system showed promising results, hence several buffers were chosen that contained similar features to further examine the influence of solution species on protein fragmentation by hydroxyl radicals produced at PbO_2 electrodes. The buffers chosen were 2-(*N*-morpholino)ethanesulfonic acid (MES), glycine and 4-(2-hydroxyethyl)-1-piperazineethanesulfonic acid (HEPES). These buffers including tris and phosphate are shown in figure 4.15.
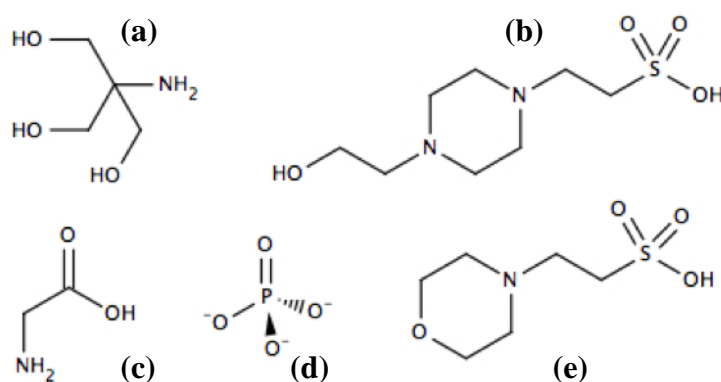

Figure 4.15. Chemical structure of the buffers trialed for their ability to produce specific cleavage of proteins in the PbO_2 electrode system. (a) Tris. (b) HEPES. (c) Glycine. (d) Phosphate. (e) MES.

All of the buffers were adjusted to their working pH by addition of either 1 M HCl or 1 M NaOH. MES and HEPES have a pKa of 6.15 and 7.5 respectively and were adjusted to

pH 7. Glycine has a useful pKa at 2.3 (carboxyl) and 9.6 (amino), and was adjusted to pH 2.8 and pH 10.6. The results of these experiments are shown in figure 4.16(a-d) with the crucial result shown in part (a). The PbO_2 electrode in pH 2.8 Glycine/HCl buffer gives specific fragmentation of BSA producing a range of different sized fragments. 12 fragments are clearly visible on the electrophoresis gel and it also appears to reduce the formation of larger molecular weight aggregates seen in earlier experiments. MES/NaOH, HEPES/NaOH and glycine/NaOH buffer systems did not produce any noticeable fragments under the same conditions. This led to the observation that in the two systems, glycine/HCl and tris/HCl, that produced fragmentation, HCl was used to adjust the pH. This could mean that the chloride ion is playing some part in the process. The systems that used NaOH to adjust the pH including the glycine/NaOH system failed to produce specific fragmentation. This along with the results in phosphate buffer that showed that the loss of protein occurred much faster in acidic conditions suggests that there is some dependence on pH and the process is more efficient at a lower pH. The tris/HCl system at pH 7 gave some specific fragmentation, but to a lesser extent than the glycine/HCl system at pH 2.8. A further common characteristic is that both tris and glycine both contain a primary amine.
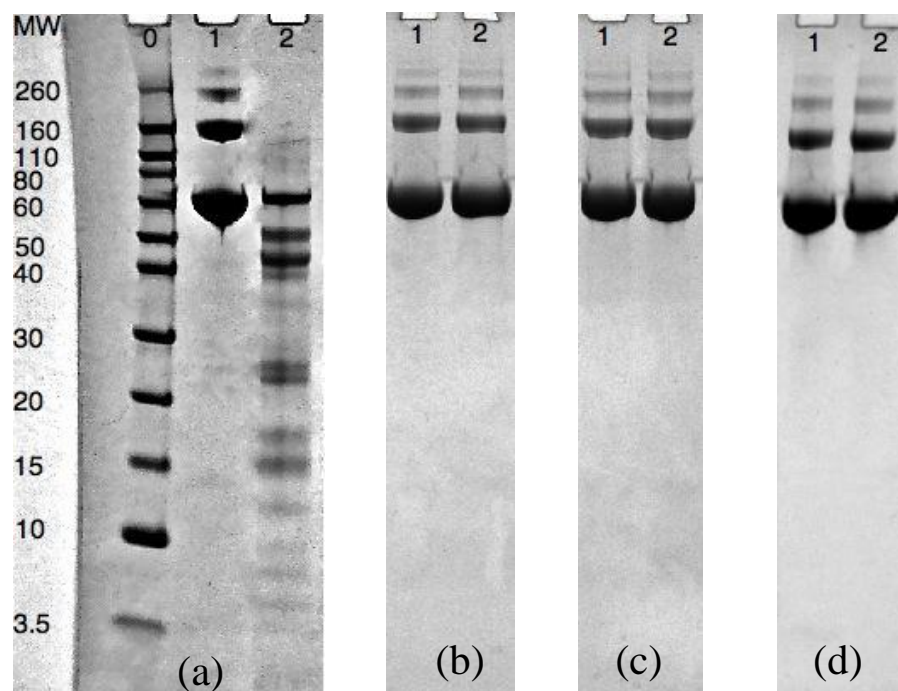
Figure 4.16. Electrophoresis gel images showing the effect of different buffer combinations on the fragmentation of BSA with a PbO$_2$ electrode at 10 mA/cm^2. Lane 0: Molecular weight markers. For all experiments: Lane 1: control. Lane 2: 10 min at 10 mA/cm^2 with a PbO$_2$ electrode. All buffers were 0.05 MolL^{-1} (a) pH 2.8 glycine/HCl buffer. (b) pH 7 MES/NaOH buffer. (c) pH 7 HEPES/NaOH buffer. (d) pH 10.6 glycine/NaOH buffer)

To check whether MES and HEPES were ineffective simply as a result of their neutral pH, they were also used at pH 2.8 adjusted with HCl (Figure 4.17(a),(b)). Even though this pH is beyond their effective buffering range, the pH did not change significantly during the experiment. There was no specific fragmentation with either MES or HEPES at pH 2.8 indicating that these two buffer systems are not effective for the selective cleavage of proteins even though they have useful radical scavenging ability.
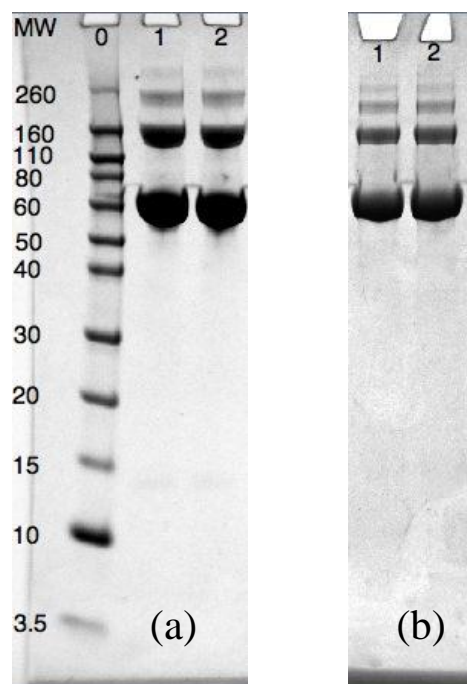
Figure 4.17. Electrophoresis gel images showing the effect of adjusting the pH to 2.8 with HCl in the MES and HEPES buffer systems on electrolysis of BSA with a PbO$_2$ electrode at 10mA/cm^2 Lane 0: Molecular weight markers. Lane 1: HEPES control. Lane 2: HEPES, 10 min electrolysis time. (b) Lane 1: MES control. Lane 2: MES, 10 min electrolysis time.

4.3.11. Influence of HCl on the system

Even though HCl did not improve the MES and HEPES systems, it may play a role in the effective tris and glycine buffer systems. A number of experiments were conducted to try and elucidate the role of HCl. In the first set, the concentration of HCl in the tris system was increased by adjusting the pH to 2.8. This is outside the buffering range of tris, but as in earlier experiments the pH did not change significantly throughout the duration of the electrolysis experiment. The results shown in figure 4.18(a) show a significant improvement in the amount of fragmentation of BSA at pH 2.8 compared to earlier experiments at pH 7. The fragmentation pattern on the electrophoresis gel is very similar to that obtained in glycine buffer at pH 2.8, which suggests that both systems are functioning in the same way. However, the increase in fragmentation could be a result of

the change in pH and does not give a definite indication of the importance of HCl in the system.

A second experiment was conducted at pH 2.8 with potassium hydrogen phthalate/HCl as the buffer system. This buffer system has a range of 2.2 to 4.0 and hence pH 2.8 is within the buffering range. As can be seen in figure 4.18(b), this system did not produce a fragmentation pattern similar to glycine and tris in combination with HCl. This experiment shows that HCl alone does not produce fragmentation in the PbO_2 system and is strong evidence against the possibility that an active chlorine species may be being generated and causing protein fragmentation.
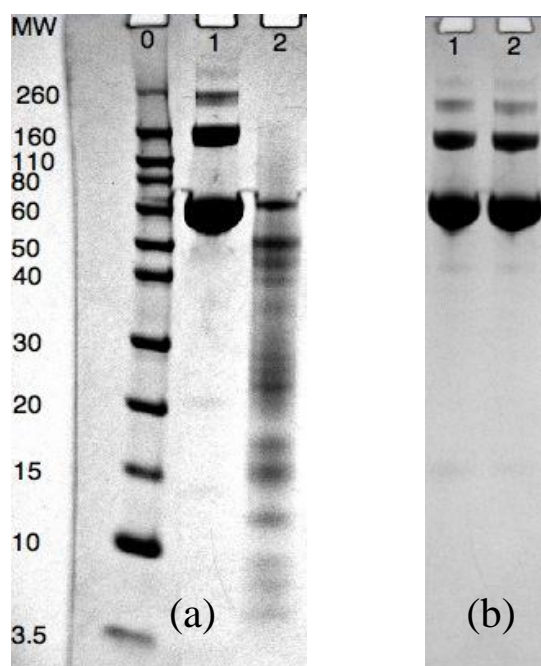
Figure 4.18 (a) Electrophoresis gel image showing the influence of HCl on the tris system for the fragmentation of BSA with a PbO_2 electrode at 10 mA/cm^2. 0.05 M tris was pH adjusted to pH 2.8 with HCl. Lane 0: Molecular weight markers. Lane 1: pH 2.8 tris control. Lane 2: 10 min electrolysis time. (b) Gel image showing the effect of using potassium hydrogen phthalate/HCl buffering system at pH 2.8 on BSA fragmentation with a PbO_2 electrode at 10 mA/cm^2. Lane 1: Control. Lane 2: 10 min electrolysis time.

A third series of experiments was performed in order to evaluate the importance of HCl on the glycine buffer system by adjusting the pH to 2.8 with a range of different acids, including perchloric, sulfuric, nitric and fluoroboric. The results are shown in figure 4.19. The fragmentation pattern produced when HCl is used as the acid is not apparent when sulfuric, perchloric, nitric and fluroboric acids are used to adjust the pH. The results suggest that HCl is playing a crucial role in the fragmentation process in the presence of glycine and tris. However the nature of this role remains unclear.
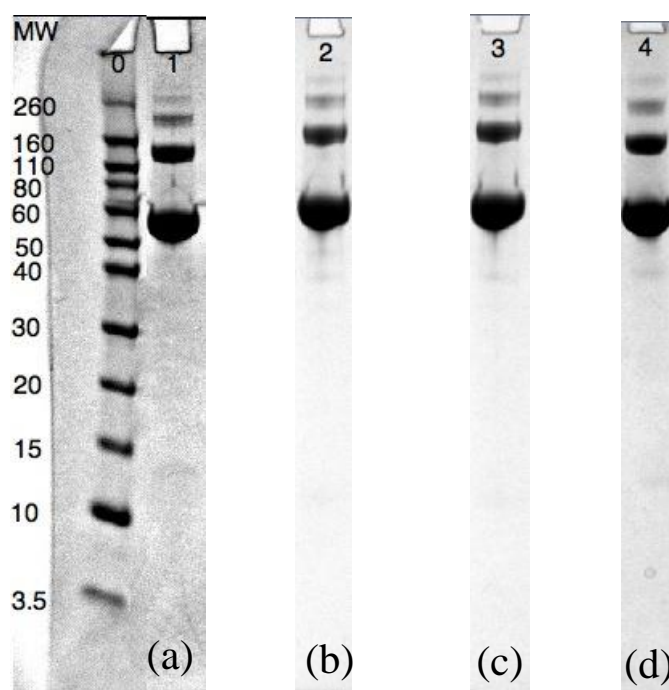
Figure 4.19. Electrophoresis gel images showing the effect of changing the acid used to adjust the pH to 2.8 in the Glycine buffer system on the fragmentation of BSA with a PbO$_2$ electrode at 10 mA/cm^2. Lane 0: molecular weight markers. Lane 1-4: After 10 min electrolysis. (a) Fluoroboric acid (b) Sulfuric acid (c) Nitric acid (d) Perchloric acid.

4.3.12. Importance of the primary amine functionality in the buffer system

Both of the successful systems (tris and glycine) contained a primary amine. In order to confirm that this functionality was playing a role in producing specific fragmentation of the proteins, further experiments were conducted. N-butylamine (figure 4.20(b)) was selected as it is a simple compound with one amine functionality attached to butane and it

does not contain any other complicating functional groups. When 0.05 M N-butylamine was added to the electrolysis medium and acidified to pH 2.8 with HCl, there was some specific cleavage and a noticeable reduction in size of the main BSA band at ~66kDa (figure 4.20(a)). This suggests the amine functionality is playing an important role in the fragmentation process. N-butylamine is not as effective as glycine or tris at fragmenting proteins at pH 2.8, but it lacks other functional groups (alcohols or organic acids) of tris and glycine. This suggests that the additional functional groups on glycine and tris add to their effectiveness, possibly by improving the scavenging ability of hydroxyl radicals, providing more protection to the areas of the protein that do not undergo cleavage as readily.

Bicine figure (4.20c) was selected to test the importance of a primary amine group. Bicine contains two alcohols and a carboxylic acid, so it has many similarities to tris and glycine except that the amine is tertiary and not primary. Figure 4.20(b) shows that there were no fragmentation products visible on the electrophoresis gel after 10 min of electrolysis with a PbO_2 electrode at pH 2.8 and very little visible loss of the main BSA protein band intensity. The three systems that give specific protein cleavage all include a primary amine in their structure. Therefore the evidence strongly suggests that the primary amine is crucial for obtaining specific protein cleavage using a PbO_2 electrode.

These results suggest that a combination of factors influence the specific fragmentation of proteins with PbO_2 electrodes. In order to achieve specific fragmentation of proteins, these factors have been found to improve the fragmentation or be required to make specific fragmentation possible:

- An acidic pH - lower pH leads to faster protein cleavage.

- A buffer system or other hydroxyl radical scavenger that contains a primary amine.

- HCl - other acids used to adjust the pH do not give specific fragmentation.
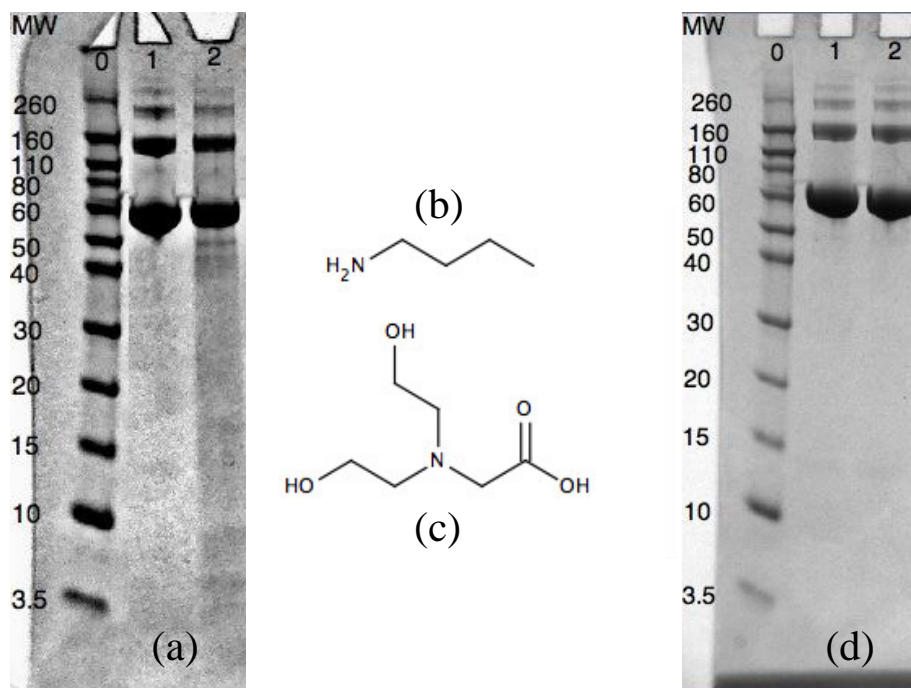
Figure 4.20. Testing the importance of the primary amine functionality of the buffer in the process of fragmenting BSA with a PbO$_2$ electrode. (a) Gel image showing fragmentation of BSA in 0.05 M N-butylamine/HCl (pH 2.8) at 10 mA/cm^2. Lane 0: molecular weight markers. Lane 1: control. Lane 2: 10 min electrolysis time. (b) Structure of n-butylamine. (c) Structure of bicine. (d) Gel image showing fragmentation of BSA in 0.05 M Bicine/HCl (pH 2.8) at 10 mA/cm^2. Lane 0: molecular weight markers. Lane 1: control. Lane 2: 10 min electrolysis time.

It appears that all of the factors outlined above work together to produce specific fragmentation of proteins. A primary amine containing hydroxyl radical scavenging molecule does not produce specific fragmentation of the protein unless HCl is present in the solution even if the pH is acidic. HCl without the presence of a primary amine containing hydroxyl radical scavenger in the system does not lead to specific

fragmentation. Further, HCl in the system but at pH 7, as in the tris buffer system, does not give good fragmentation until the pH is lowered.

4.3.13. Investigation of glycine buffer system

The glycine/HCl buffer system gave the best results of all the buffer systems tested. It is superior to tris as it is able to buffer the system at an acidic pH. Further work was undertaken towards optimizing conditions and providing a greater understanding of the mechanism involved.

In order to establish the timeframe of the reaction, the reaction progress was monitored by sampling the solution during electrolysis at selected time intervals and analyzing by gel electrophoresis. In figure 4.21(a), it can be seen that the bands at 40 and 50kDa after 5 minutes are more intense than after 10 minutes, showing that these bands are further broken down over time to give smaller products. This shows that when targeting a specific fraction that results from cleavage of the starting protein, electrolysis time will be a very important factor. Figure 4.21(b) shows the change in concentration of the fragments from 1 to 5 minutes.
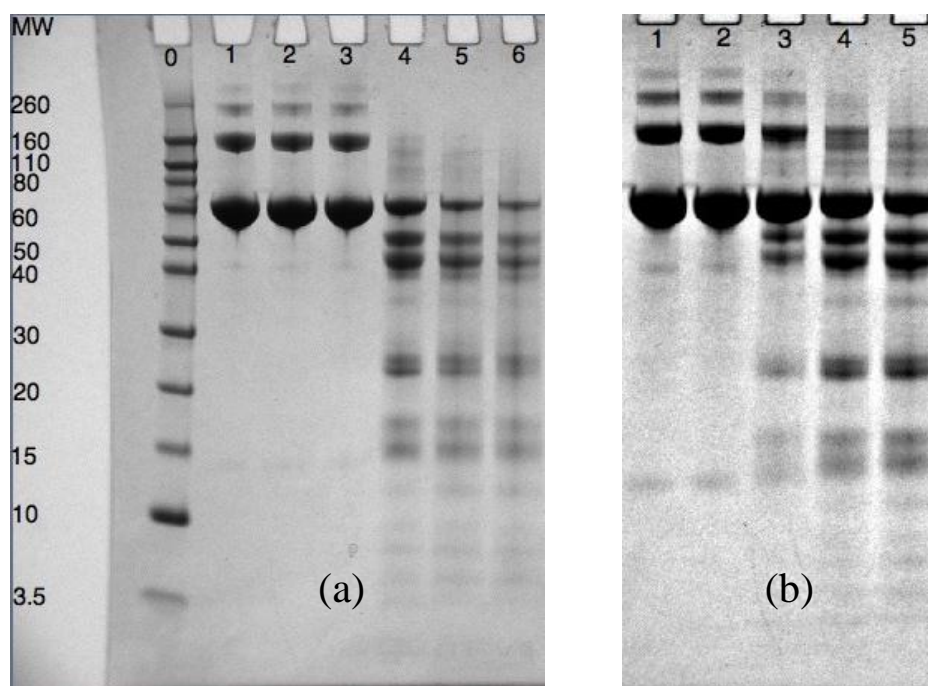
Figure 4.21. Electrophoresis gels showing fragmentation of BSA by a PbO_2 electrode as a result of electrolysis time at a current density of 10 mA/cm^2. (a) Lane 0: molecular weight markers. Lane 1: 0 min. Lane 2: 30 sec. Lane 3: 1 min. Lane 4: 5 min. Lane 5: 10 min. Lane 6: 20 min. (b) Lane 1: 1 min. Lane 2: 2 min. Lane 3: 3 min. Lane 4: 4 min. Lane 5: 5 min

4.3.14. Effect of pH on glycine buffer system

To demonstrate the effect that pH has on the glycine buffer system, pH values of 2.2, 2.9 and 3.6 were used for electrolysis. The three pH values were chosen as they are spread within the effective buffering range of glycine/HCl buffer. The experiments were run at a constant current density of 10 mA/cm^2 for 10 min using a PbO_2 electrode to fragment BSA; the results are shown in figure 4.22(a). The rate of protein cleavage increases significantly as pH decreases. At pH 2.2 there is no starting material remaining after 10 minutes electrolysis. It should be noted that the ionic strength of the solution will become higher as pH is lowered, because additional HCl is added. However a constant current was used, and hence the same amount of charge is passed in each experiment. The voltage varied between the 3 experiments with the pH 2.2 experiment at ~2 V and the pH 2.9 experiment at ~ 2.8 V and the pH 3.6 experiment at ~5.4 V. To avoid ionic strength

effects, the experiment was repeated with 0.05 M NaCl as added supporting electrolyte to provide a similar ionic strength to all of the experiments (results not shown). This resulted in all experiments having a potential of ~2 V. The pattern of fragmentation was the same as in Figure 4.22(a) showing that the fragmentation depends on H^+ activity and not on ionic strength or Cl^- concentration.

4.3.15. Effect of divided cell on fragmentation of proteins

In addition to the PbO_2 electrode at a positive potential in the cell, there is also a platinum counter electrode at a strong negative potential. In order to make sure that the PbO_2 electrode was solely responsible for protein fragmentation, an experiment was run in a cell with a Nafion membrane separating the anodic and cathodic compartments. The electrophoresis gel image from this experiment is shown in figure 4.22(b). The protein was specifically fragmented into visible fragments in the anodic compartment (PbO_2 electrode), but there was no fragmentation in the cathodic compartment (Pt electrode). This experiment shows that the key process is occurring at the PbO_2 electrode and does not require any interaction with the counter electrode to give fragmentation.
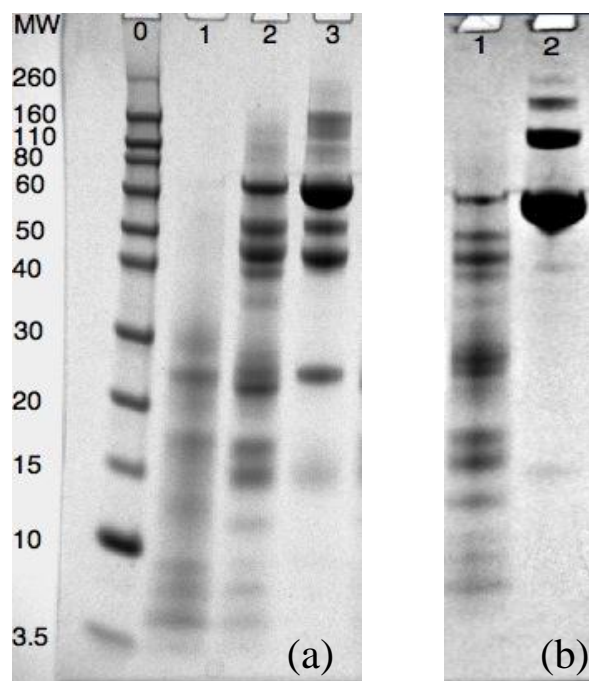
Figure 4.22. (a) Gel image showing effect of pH on fragmentation of BSA with a PbO$_2$ electrode in glycine/HCl buffer at a current density of 10 mA/cm^2 and 10 min electrolysis time. Lane 0: Molecular weight markers. Lane 1: pH 2.2. Lane 2: pH 2.9. Lane 3: pH 3.6. (b) Gel image showing BSA fragmentation results from a cell divided into an anodic and a cathodic compartment with a Nafion membrane. BSA was present in both the anodic (PbO$_2$ electrode) and cathodic (Pt electrode) compartments in pH 2.8, 0.05 M glycine/HCl buffer. A current density of 10 mA/cm^2 and a time of 10 min was used for the electrolysis experiment. Lane 1: Anodic compartment (PbO$_2$ electrode). Lane 2: Cathodic compartment (Pt electrode).

4.3.16. Fragmentation of target proteins in glycine buffer

The target proteins were investigated using the glycine/HCl buffer systems to ascertain if they would also undergo fragmentation similar to that of BSA under the same conditions. The results of these experiments were again observed visually by gel electrophoresis of the electrolysed protein solutions and also by mass spectrometry. Casein and whey are both groups of proteins that contain several similar proteins each. The results of the fragmentation of whey are shown in figure 4.23(a). Some fragmentation of β-lactoglobulin (the main protein band at ~18.3 kDa) is evident by the staining beneath the band. The fragmentation of casein is shown in figure 4.23(b) Four new protein bands are visible beneath the casein bands after electrolysis.

Figure 4.23. Electrophoresis gels showing fragmentation of proteins over time with electrolysis by a PbO_2 electrode at 10 mA/cm^2. (a) Whey proteins. Lane 0: Molecular weight markers. Lane 1: Control. Lane 2: 30 min electrolysis. Lane 3: 60 min electrolysis. (b): Casein proteins. Lane 0: Molecular weight markers. Lane 1: Control. Lane 2: 30 min electrolysis. Lane 3: 60 min electrolysis.

In further experiments, one protein from the casein group of proteins and one from the whey group were selected to reduce the number of possible products from cleavage experiments, and therefore make it easier to deconvolute the results. The aim was to elucidate cleavage sites on the protein molecules. β-lactoglobulin was selected, as it is the most abundant protein in whey and β-casein was chosen to be representative of the casein proteins. β-lactoglobulin produces 5 new clearly visible fragments (figure 4.24(a)) and fragmentation is quite extensive, although there is still some starting material remaining after 1 hour of electrolysis. The process is not as efficient as that of BSA as a similar amount of the starting BSA protein is removed in only 20 minutes under the same conditions. β-lactoglobulin fragmentation appears to occur more readily when it is separated from the other whey proteins, suggesting that a cleaner solution matrix is an

important factor in the process. β-casein produces one clearly visible fragment at ~18kDa

and several other smaller fragments that are less clearly visible (figure 4.24(b)). After one

hour of electrolysis a large proportion of the original protein is still visible, however the

major cleavage product is stable also. Higher molecular weight products also appear over

time with electrolysis at ~60kDa.
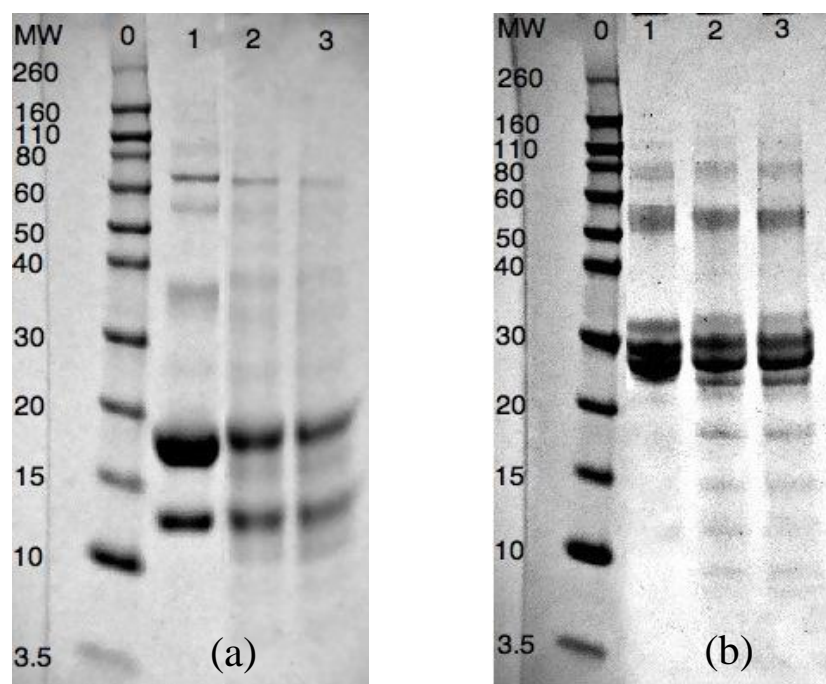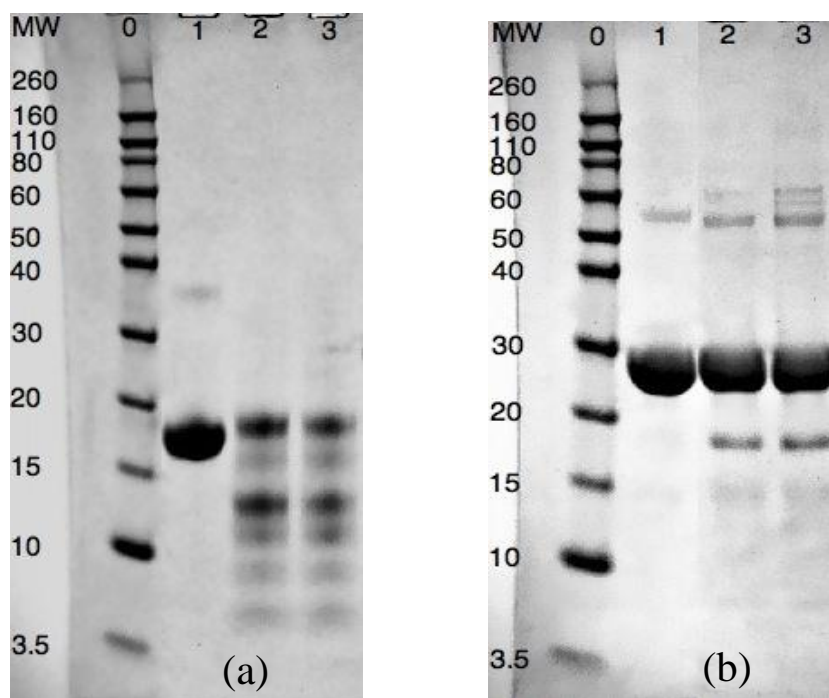

Figure 4.24. Electrophoresis gels showing fragmentation of proteins over time with electrolysis by a PbO$_2$ electrode at 10 mA/cm^2. (a) β-lactoglobulin. Lane 0: Molecular weight markers. Lane 1: Control. Lane 2: 30 min electrolysis. Lane 3: 60 min electrolysis. (b) β-casein. Lane 0: Molecular weight markers. Lane 1: Control. Lane 2: 30 min electrolysis. Lane 3: 60 min electrolysis.

4.3.17. Mass spectrometry of fragmented β-lactoglobulin and β-casein

Mass spectrometry was used to obtain a more accurate view of the size of the protein

fragments. The mass spectrum of β-lactoglobulin after 60 minutes of electrolysis with a

PbO$_2$ electrode in glycine/HCl buffer is shown in figure 4.25. Deconvolution of the

spectra reveals major fragments at 2166 Da, 4602 Da, 5005 Da, 6448 Da, 6886 Da and

7281 Da. Some of the fragments above 10000 Da that are visible on the electrophoresis

gels were not able to be resolved during deconvolution of the spectrum.

Figure 4.25. Mass spectrum of β-lactoglobulin (a) before and (b) after 60 minutes of electrolysis with a PbO_2 electrode in pH 2.8 glycine/HCl buffer at a current density of 10 mA/cm^2.

New peaks appearing as a result of the electrolysis with a PbO_2 electrode in glycine/HCl

buffer on the mass spectrum of β-casein after 60 minutes are marked on figure 4.26.

Deconvolution of the spectra was difficult with so much of the original protein material

remaining, however major fragments could be seen at 8125 Da, 10041 Da, 13320 Da,

15835 Da and 18644 Da on the deconvoluted spectra.
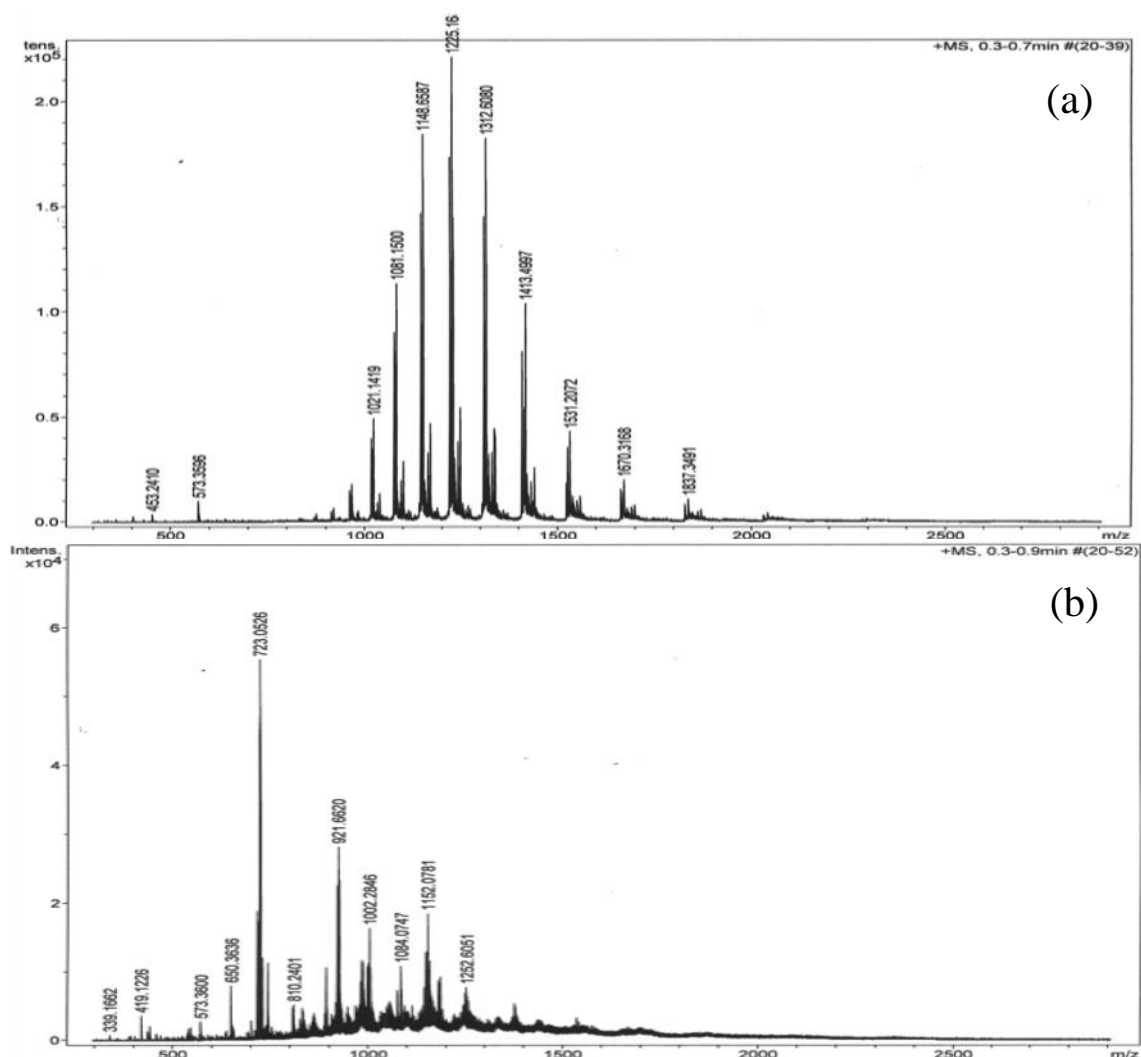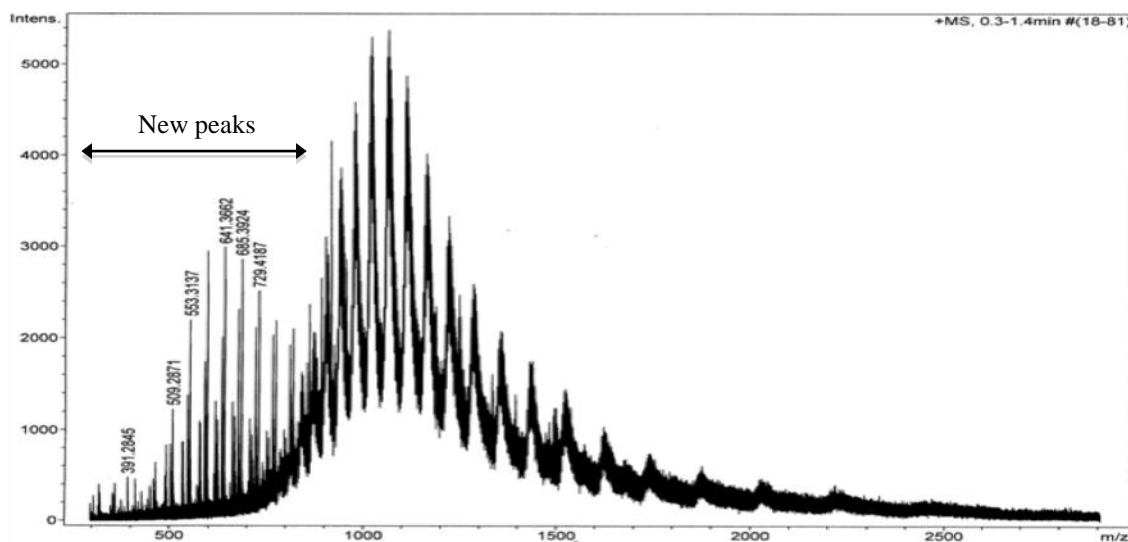
Figure 4.26. Mass spectrum of β-casein after 60 minutes of electrolysis with a PbO$_2$ electrode in pH 2.8 glycine/HCl buffer at a current density of 10 mA/cm^2.

A more rigorous mass spectrometry analysis such as tandem MS is required to give the kind of sequence information and accuracy required to be able to elucidate cleavage points in the two proteins studied. Time constraints prevented such an analysis.

4.4. Conclusion

The most stable PbO$_2$ films on a platinum substrate were produced with Triton X-100 in the deposition bath and were not doped with fluorine. The films were tested for suitability using methyl orange and RNO. These films were shown to have excellent hydroxyl radical production and were suitable for fragmenting proteins. Thus, PbO$_2$ working electrodes used for protein fragmentation were deposited onto a platinum substrate from a deposition bath containing 0.005 M Triton X-100, 0.05 M PbNO$_3$, 0.1 M HNO$_3$ at 60 °C for 30 minutes at 60 mA/cm^2.

Non-specific fragmentation was demonstrated using phosphate buffer as the supporting electrolyte. Lowering the pH of the phosphate buffer increased the speed of the protein fragmentation. The importance of the pH and chemical environment was examined by using a range of different buffers and additives at varied pH.

For the first time, specific fragmentation of proteins has been achieved by electrochemical generation of hydroxyl radicals. In order to achieve specific protein fragmentation, three factors were found to be crucial. These were low pH, a medium that contained a primary amine containing radical scavenger and HCl. Glycine/HCl buffer was found to give the best results for fragmentation. Specific fragmentation was achieved with a PbO_2 electrode in 0.05 M pH 2.8 glycine/HCl buffer at a current density of 10 mA/cm^2.

The target groups of proteins, whey and casein were able to be specifically fragmented using a PbO_2 electrode in glycine/HCl buffer. Individual proteins from whey and casein were however able to be fragmented more effectively without the other whey or casein proteins being present. Of the individual proteins that were examined, BSA fragmentation occurred to the greatest extent and the most rapidly. β-lactoglobulin fragmentation was also extensive but occurred over a longer time frame under the same conditions as BSA. Some fragmetation of β-casein was able to be achieved, but not to the same extent as BSA and β-lactoglobulin.

The results in this chapter have shown that specific electrochemical fragmentation of proteins using PbO_2 electrodes could be a viable alternative to other chemical or enzymic fragmentation techniques and may produce a different fragmentation pattern that could provide access to fragments that were previously difficult to produce.

In order to ascertain whether the PbO_2 system has advantages or unique effects due to the way the hydroxyl radicals are produced, the following chapter will investigate the electro-Fenton system, a different method of producing hydroxyl radicals electrochemically for protein fragmentation.

References

1. Pignatello, J.J., E. Oliveros, and A. MacKay, *Advanced Oxidation Processes for Organic Contaminant Destruction Based on the Fenton Reaction and Related Chemistry.* Critical Reviews in Environmental Science and Technology, 2006. **36**(1): p. 1-84.
2. Headlam, H.A. and M.J. Davies, *Beta-scission of side-chain alkoxyl radicals on peptides and proteins results in the loss of side-chains as aldehydes and ketones.* Free Radical Biology and Medicine, 2002. **32**(11): p. 1171-1184.
3. Schuessler, H. and K. Schilling, *Oxygen Effect in the Radiolysis of Proteins -- Part 2 Bovine Serum Albumin.* International Journal of Radiation Biology, 1984. **45**(3): p. 267-281.
4. Boonrattanakij, N., M.-C. Lu, and J. Anotai, *Kinetics and mechanism of 2,6-dimethyl-aniline degradation by hydroxyl radicals.* Journal of Hazardous Materials, 2009. **172**(2-3): p. 952-957.
5. Oturan, N., M. Hamza, S. Ammar, R. Abdelhédi, and M.A. Oturan, *Oxidation/mineralization of 2-nitrophenol in aqueous medium by electrochemical advanced oxidation processes using Pt/carbon-felt and BDD/carbon-felt cells.* Journal of Electroanalytical Chemistry, 2011. **661**(1): p. 66-71.
6. Zhou, M., Q. Dai, L. Lei, C.a. Ma, and D. Wang, *Long Life Modified Lead Dioxide Anode for Organic Wastewater Treatment: Electrochemical Characteristics and Degradation Mechanism.* Environmental Science & Technology, 2004. **39**(1): p. 363-370.
7. Luong, J.H.T., K.B. Male, and J.D. Glennon, *Boron-doped diamond electrode: synthesis, characterization, functionalization and analytical applications.* analyst, 2009. **134**(10): p. 1965-1979.
8. Karolina, P., J. Musilova, and J. Barek, *Boron-Doped Diamond Film Electrodes - New Tool for Voltammetric Determination of Organic Substances.* Critical Reviews in Analytical Chemistry, 2009. **39**(3): p. 148-172.
9. Kapalka, A., G. Foti, and C. Comninellis, *The importance of electrode material in environmental electrochemistry: Formation and reactivity of free hydroxyl radicals on boron-doped diamond electrodes.* Electrochimica Acta, 2009. **54**(7): p. 2018-2023.
10. Liu, Y. and H. Liu, *Comparative studies on the electrocatalytic properties of modified PbO2 anodes.* Electrochimica Acta, 2008. **53**(16): p. 5077-5083.
11. Cong, Y. and Z. Wu, *Electrocatalytic Generation of Radical Intermediates over Lead Dioxide Electrode Doped with Fluoride.* The Journal of Physical Chemistry C, 2007. **111**(8): p. 3442-3446.
12. Velichenko, A.B., R. Amadelli, G.L. Zucchini, D.V. Girenko, and F.I. Danilov, *Electrosynthesis and physicochemical properties of Fe-doped lead dioxide electrocatalysts.* Electrochimica Acta, 2000. **45**(25-26): p. 4341-4350.
13. Comninellis, C., *Electrocatalysis in the electrochemical conversion/combustion of organic pollutants for waste water treatment.* Electrochimica Acta, 1994. **39**(11-12): p. 1857-1862.
14. Panizza, M., I. Sirés, and G. Cerisola, *Anodic oxidation of mecoprop herbicide at lead dioxide.* Journal of Applied Electrochemistry, 2008. **38**(7): p. 923-929.

15.   Roots, R. and S. Okada, *Estimation of Life Times and Diffusion Distances of Radicals Involved in X-Ray-Induced DNA Strand Breaks or Killing of Mammalian Cells.* Radiation Research, 1975. **64**(2): p. 306-320.

16.   Ghaemi, M., E. Ghafouri, and J. Neshati, *Influence of the nonionic surfactant Triton X-100 on electrocrystallization and electrochemical performance of lead dioxide electrode.* Journal of Power Sources, 2006. **157**(1): p. 550-562.

17.   Velichenko, A., D. Girenko, N. Nikolenko, R. Amadelli, E. Baranova, and F. Danilov, *Oxygen evolution on lead dioxide modified with fluorine and iron.* Russian Journal of Electrochemistry, 2000. **36**(11): p. 1216-1220.

18.   Amadelli, R., L. Armelao, A.B. Velichenko, N.V. Nikolenko, D.V. Girenko, S.V. Kovalyov, and F.I. Danilov, *Oxygen and ozone evolution at fluoride modified lead dioxide electrodes.* Electrochimica Acta, 1999. **45**(4-5): p. 713-720.

19.   Mohd, Y. and D. Pletcher, *The fabrication of lead dioxide layers on a titanium substrate.* Electrochimica Acta, 2006. **52**(3): p. 786-793.

20.   Iniesta, J., J. González-García, E. Expósito, V. Montiel, and A. Aldaz, *Influence of chloride ion on electrochemical degradation of phenol in alkaline medium using bismuth doped and pure PbO2 anodes.* Water Research, 2001. **35**(14): p. 3291-3300.

21.   Johnson, D.C., J. Feng, and L.L. Houk, *Direct electrochemical degradation of organic wastes in aqueous media.* Electrochimica Acta, 2000. **46**(2-3): p. 323-330.

22.   Andrade, L.S., L.A.M. Ruotolo, R.C. Rocha-Filho, N. Bocchi, S.R. Biaggio, J. Iniesta, V. García-Garcia, and V. Montiel, *On the performance of Fe and Fe,F doped Ti-Pt/PbO2 electrodes in the electrooxidation of the Blue Reactive 19 dye in simulated textile wastewater.* Chemosphere, 2007. **66**(11): p. 2035-2043.

23.   Treimer, S.E., J. Feng, M.D. Scholten, D.C. Johnson, and A.J. Davenport, *Comparison of Voltammetric Responses of Toluene and Xylenes at Iron(III)-Doped, Bismuth(V)-Doped, and Undoped beta-Lead Dioxide Film Electrodes in 0.50 M H2SO4.* Journal of The Electrochemical Society, 2001. **148**(12): p. E459-E463.

24.   He, L., J.R. Anderson, H.F. Franzen, and D.C. Johnson, *Electrocatalysis of Anodic Oxygen-Transfer Reactions: Bi3Ru3O11 Electrodes in Acidic Media.* Chemistry of Materials, 1997. **9**(3): p. 715-722.

25.   Popović, N.D. and D.C. Johnson, *A Ring Disk Study of the Competition between Anodic Oxygen-Transfer and Dioxygen-Evolution Reactions.* Analytical Chemistry, 1998. **70**(3): p. 468-472.

26.   Cao, J., H. Zhao, F. Cao, J. Zhang, and C. Cao, *Electrocatalytic degradation of 4-chlorophenol on F-doped PbO2 anodes.* Electrochimica Acta, 2009. **54**(9): p. 2595-2602.

27.   Liu, Y., H. Liu, J. Ma, and J. Li, *Investigation on electrochemical properties of cerium doped lead dioxide anode and application for elimination of nitrophenol.* Electrochimica Acta, 2011. **56**(3): p. 1352-1360.

28.   Velichenko, A.B. and D. Devilliers, *Electrodeposition of fluorine-doped lead dioxide.* Journal of Fluorine Chemistry, 2007. **128**(4): p. 269-276.

29.   Yeh, C.-H., C.-C. Wan, and J.-S. Chen, *Physical and electrochemical characterization of PbO2 electrode prepared at different H2SO4/H2O/PbO ratios.* Journal of Power Sources, 2001. **101**(2): p. 219-225.

30.   Velichenko, A.B., D.V. Girenko, S.V. Kovalyov, A.N. Gnatenko, R. Amadelli, and F.I. Danilov, *Lead dioxide electrodeposition and its application: influence of*

fluoride and iron ions. Journal of Electroanalytical Chemistry, 1998. **454**: p. 203-208.

31. Recio, F.J., P. Herrasti, I. SirÈs, A.N. Kulak, D.V. Bavykin, C. Ponce-de-LeÛn, and F.C. Walsh, *The preparation of PbO2 coatings on reticulated vitreous carbon for the electro-oxidation of organic pollutants.* Electrochimica Acta, 2011. **56**(14): p. 5158-5165.

32. Zhu, X., M. Tong, S. Shi, H. Zhao, and J. Ni, *Essential Explanation of the Strong Mineralization Performance of Boron-Doped Diamond Electrodes.* Environmental Science & Technology, 2008. **42**(13): p. 4914-4920.

33. Zhu, X., J. Ni, H. Li, Y. Jiang, X. Xing, and A.G.L. Borthwick, *Effects of ultrasound on electrochemical oxidation mechanisms of p-substituted phenols at BDD and PbO2 anodes.* Electrochimica Acta, 2010. **55**(20): p. 5569-5575.

34. Dao, Y.H. and J. De Laat, *Hydroxyl radical involvement in the decomposition of hydrogen peroxide by ferrous and ferric-nitrilotriacetate complexes at neutral pH.* Water Research, 2011. **45**(11): p. 3309-3317.

35. Jörns, A., M. Tiedge, S. Lenzen, and R. Munday, *Effect of superoxide dismutase, catalase, chelating agents, and free radical scavengers on the toxicity of alloxan to isolated pancreatic islets in vitro.* Free Radical Biology and Medicine, 1999. **26**(9-10): p. 1300-1304.

36. Ma, J. and N.J.D. Graham, *Degradation of atrazine by manganese-catalysed ozonation--influence of radical scavengers.* Water Research, 2000. **34**(15): p. 3822-3828.

37. Davies, K.J., *Protein damage and degradation by oxygen radicals. I. general aspects.* The Journal of biological chemistry, 1987. **262**(20): p. 9895-9901.

38. Davies, K.J., M.E. Delsignore, and S.W. Lin, *Protein damage and degradation by oxygen radicals. II. Modification of amino acids.* Journal of Biological Chemistry, 1987. **262**(20): p. 9902-9907.

39. Hicks, M. and J.M. Gebicki, *Rate constants for reaction of hydroxyl radicals with Tris, Tricine and Hepes buffers.* FEBS Letters, 1986. **199**(1): p. 92-94.

40. Kocha, T., M. Yamaguchi, H. Ohtaki, T. Fukuda, and T. Aoyagi, *Hydrogen peroxide-mediated degradation of protein: different oxidation modes of copper- and iron-dependent hydroxyl radicals on the degradation of albumin.* Biochimica et Biophysica Acta (BBA) - Protein Structure and Molecular Enzymology, 1997. **1337**(2): p. 319-326.

Chapter 5. Electro-Fenton generation of hydroxyl radicals for use in the fragmentation of proteins

5.1. Introduction

5.1.1. Generation of hydroxyl radicals by the Fenton reaction

The Fenton reaction is fully described in section 1.6. H.J.H. Fenton discovered the Fenton reaction in the 1890s. In 1934 Haber and Weiss proposed that the active oxidant generated in the Fenton reaction was the hydroxyl radical.[1] The classical mechanism for the formation of hydroxyl radicals in acidic solution and in the absence of any organic compounds between hydrogen peroxide and an iron catalyst was proposed in 1949 by Barb et al.[2] Equations 1 and 2 show the key reactions for the electro-Fenton reaction.

$$(1)\ Fe^{2+} + H_2O_2 \rightarrow Fe^{3+} + OH\bullet + OH^-$$

$$(2)\ Fe^{3+} + H_2O_2 \rightarrow Fe^{2+} + OOH\bullet + H^+$$
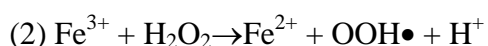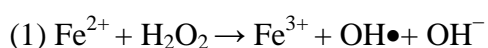
5.1.2. Electro-Fenton reaction

The Fenton reaction has been used for protein fragmentation to a small extent in previous work,[3-5] but no evidence of the electro-Fenton reaction's use for protein fragmentation could be found in the literature. The electro-Fenton reaction is a process in which one or

both of the species required for the Fenton reaction are electrochemically generated.[6-8] There are four different types of electro-Fenton system outlined in section 1.6.5. In this chapter two of these systems will be tested. In the first the H_2O_2 required for the reaction is generated electrochemically and the iron required for the reaction is added externally with no electrochemical regeneration of Fe(II). In the second, H_2O_2 will be electrochemically generated and the regeneration rate of Fe(II) will be increased by the reduction of Fe(III) on the working electrode. Equation 3 shows the target working electrode reaction for generating H_2O_2. A competitive reaction at the working electrode is shown in equation 4. Equation 5 shows the generation of protons on the counter electrode to supplement the loss of protons on the working electrode. Equation 6 shows the competitive reaction where H_2O_2 is consumed on the counter electrode.

$$(3) \qquad O_2 + 2H^+ + 2e^- \rightarrow H_2O_2$$

$$(4) \qquad 2H^+ + 2e^- \rightarrow H_2$$

$$(5) \qquad 2H_2O \rightarrow 4H^+ + O_2 + 4e^-$$

$$(6) \qquad H_2O_2 \rightarrow O_2 + 2H^+ + 2e^-$$
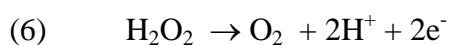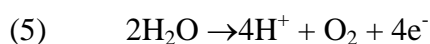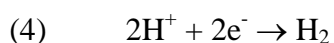
The working electrode (cathode) material used for electrochemical H_2O_2 production and regeneration of Fe(II) in this work was a woven carbon fibre electrode. This material was chosen, as it is a carbon based, low cost material with a high surface area. There are advantages and disadvantages for the use of both a divided cell and an undivided cell for the electro-Fenton process. The advantage of using an undivided cell is that the

consumption of H^+ by the cathode will be supplemented by the production of H^+ on the anode (equations 3 and 5). The disadvantage of an undivided cell is that H_2O_2 that is generated on the cathode can be consumed on the anode. For a divided cell the disadvantage is that the pH is not stable during production of H_2O_2, as protons consumed on the cathode are not replenished by the anode. The advantage is that H_2O_2 is not consumed on the anode. Both undivided and divided cells will be trialed in order to see which is most suitable for this system.

5.2. Experimental

Electrochemical cell configurations and the woven carbon fibre electrode working electrode used in this chapter are described in detail in section 2.2 and 2.3. The undivided cell configuration used for generation of H_2O_2 was simple beaker like cell with an electrolysis solution volume of 50 ml. The woven carbon fibre electrode and platinum counter electrode were the same as that described for the divided cell experiments. All potentials were measured vs. a Ag/AgCl reference electrode.

$FeSO_4.7H_2O$ and $CuSO_4$ provided the Fe(II) and Cu(II) respectively for electro-Fenton experiments unless stated otherwise. Analytical methods for the determination of H_2O_2 and Fe(II)/(III) are described in section 2.6.

5.3. Results and Discussion

5.3.1. Generation of H_2O_2 in a divided cell at varied applied currents.

There have been few reports of woven carbon fibre electrodes being used in the literature to produce H_2O_2, so an initial study was undertaken in order to find the most efficient conditions to use to generate H_2O_2. The effect of applied current on H_2O_2 production was evaluated by electrolysis of an aqueous solution of 0.1 M Na_2SO_4 at different applied currents in a cell divided by a porous frit. The H_2O_2 concentration was measured periodically throughout the electrolysis. The results showed that higher applied currents produced more H_2O_2 than lower applied currents over 2 hours. The current vs. time relationship (figure 5.1) is close to linear with evidence that over long electrolysis times, there would be a shift away from linearity, which might be expected on the basis that at higher H_2O_2 concentrations, the likelihood of a competing reaction such as equation 7 occurring at the working electrode increases; this removes H_2O_2 from the cathode compartments. After 120 min the amount of H_2O_2 produced at 100 mA and 50 mA was very similar. However at shorter electrolysis times, H_2O_2 production was faster when larger currents were applied. The pH at the beginning of these experiments was 3, but after 2 hours of electrolysis the pH was ~11. As the pH increases, formation of H_2O_2 is more difficult due to the decrease in availability of hydrogen ions, which are required for the production of H_2O_2. This could also eventually slow the production of H_2O_2. Low concentrations of H_2O_2 can be produced quickly at higher currents in this system but there is less benefit to using high currents if higher final concentrations of H_2O_2 are required.

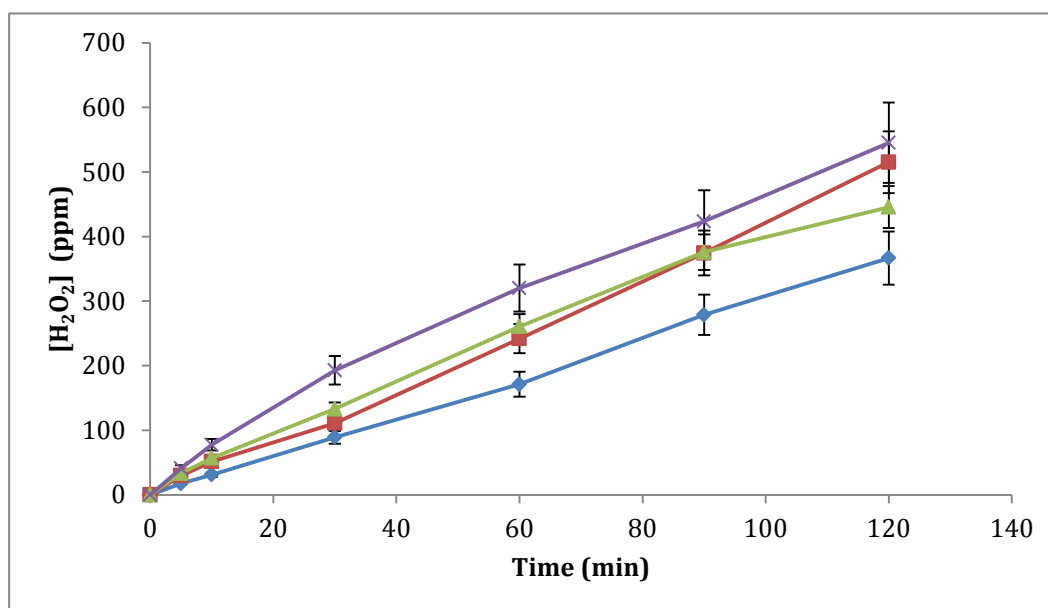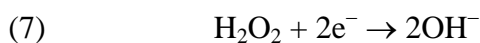(7) $\quad\quad\quad\quad\quad H_2O_2 + 2e^- \rightarrow 2OH^-$

Figure 5.1. Plot showing the effect of applied current on H_2O_2 production in a divided cell with a woven carbon fibre electrode. Blue line: 25 mA. Red line: 50 mA. Green line 75 mA. Purple line: 100 mA

5.3.2. Effect of pH adjustment on generation of H_2O_2 generation

The Fenton reaction is best performed at pH between 2 and 3 as ferric species begin to precipitate as insoluble oxy hydroxides above this pH. Furthermore, the target reaction shown in equation 1 is thermodynamically more favourable as pH decreases and hence it was assumed that continuously supplying H^+ by maintaining the pH between 2.8 and 3, would improve the production of H_2O_2. However, figure 5.2 shows that H_2O_2 generation is decreased at constant pH. This can be attributed to two competitive reactions occurring at the cathode and both of these are most favourable at low pH (equations 8 and 9). [9, 10]

(8) $\quad\quad H_2O_2 + 2H^+ + 2e^- \rightarrow 2H_2O$

(9) $\quad\quad 2H^+ + 2e^- \rightarrow H_2$
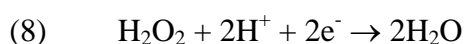
Equation 8 leads to the removal of H_2O_2 from the solution and equation 9 removes H^+ to produce H_2 gas. Both of the reactions slow the accumulation of H_2O_2 in solution.

In both of the experiments shown in figure 5.2, the pH was 3 at the beginning of the experiment. After 180 min, with no pH adjustment the solution pH was 12.4. For use in the Fenton reaction, the pH should be between 2.8 and 3. Hence after the cell was switched off, the pH was corrected to 3 by adding 1 M H_2SO_4. Based on the plot shown in figure 5.2, this method of correcting the pH after the required amount of H_2O_2 is produced, is an efficient route to generate high starting concentrations of H_2O_2 for Fenton reactions. However if lower concentrations of H_2O_2 are required, it makes little difference whether or not the pH is corrected during electrolysis, as shown by the early stages of the experiment with pH correction on figure 5.2.
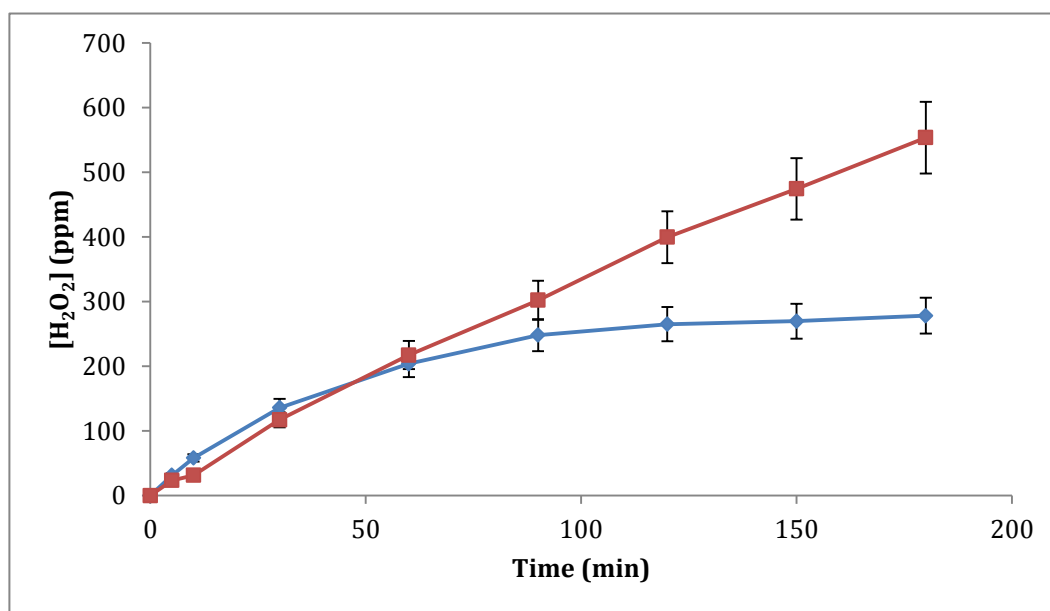

Figure 5.2. Plot showing the effect of maintaining the pH between 2.8 and 3 during production of H_2O_2 at an applied current of 50 mA with a woven carbon fibre electrode. Red line: no pH adjustment. Blue line: pH held at between pH 2.8 and 3 during experiment by addition of 1M H_2SO_4.

5.3.3. Effect of oxygen delivery method on H_2O_2 production

Reduction of O_2 at the cathode produces H_2O_2, hence maintaining a high concentration of dissolved O_2 in the electrolysis solution is important. Experiments were undertaken to investigate the effect of O_2 delivery method on H_2O_2 production. O_2 was delivered at 50 ml/min through a porous glass frit and through a 4-holed glass bubbler; in each experiment, O_2 was bubbled into solution for 15 minutes prior to electrolysis. Figure 5.3, blue line, shows that with the 4-hole bubbler, there is initially some H_2O_2 production in the O_2 saturated solution, but the rate at which this oxygen delivery system was able to replenish O_2 was too low to maintain significant H_2O_2 production. Figure 5.3, red line, shows that the glass frit was a very good oxygen delivery system. The frit produces much smaller O_2 bubbles that were much more readily dissolved into solution providing the O_2 required for good production of H_2O_2. The oxygen delivery system is therefore very important for the efficiency of this system.
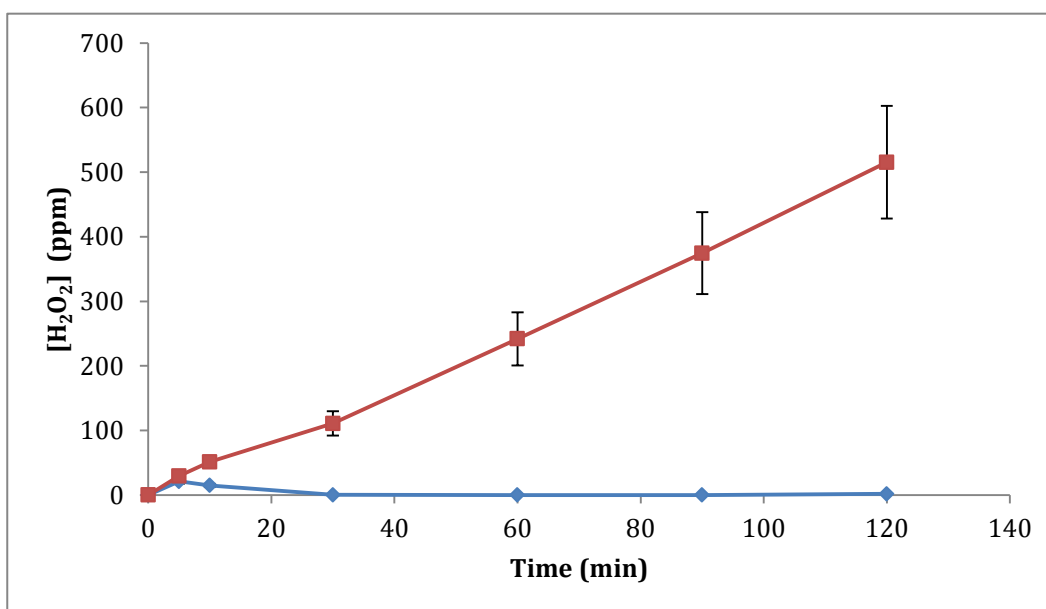

Figure 5.3. Plot showing the effect of the O_2 delivery system on production H_2O_2 at 50 mA and 50 ml/min O_2 in a 50ml solution of 0.1 M Na_2SO_4 with a woven carbon fibre electrode. Red line: Glass frit O_2 bubbler. Blue line: 4 hole glass bubbler.

5.3.4. Undivided cell production of H_2O_2

Production of H_2O_2 in an undivided cell was initially tested with a woven carbon fibre working electrode and a platinum mesh counter electrode. The benefits of this system are that the oxygen and hydrogen ions produced by the oxidation of water on the counter electrode (equation 5) can be used at the working electrode to produce H_2O_2. The disadvantage of this system is that H_2O_2 is also consumed on the counter electrode, suggesting that under some conditions the concentration of H_2O_2 may become limited.

5.3.5. Effect of applied current on H_2O_2 production in an undivided cell

The undivided cell configuration was tested at 200 mA, 100 mA, 50 mA and 25 mA currents for the production of H_2O_2. H_2O_2 concentration was measured periodically during electrolysis by UV-Vis spectroscopy using the iodide method (figure 5.4). For short times, up to 10 min, all currents produced similar concentrations of H_2O_2 at a similar rate, but the limiting concentration of H_2O_2 at longer times was higher for the lower applied currents except at 25 mA. At 25 mA the limiting concentration of H_2O_2 was lower, presumably a low rate of production meant that significant accumulation of H_2O_2 could not be achieved before the amount of H_2O_2 that is being generated at the cathode becomes equal to the rate at which it is being removed by oxidation at the anode. The steady state concentration at 50 mA is much higher than that at 100 mA and 200 mA. This can be explained by considering the potential required to maintain these applied currents. The cell potential was measured as -1 V, -1.8 V, -2.9 V and -5.1 V for 25 mA, 50 mA, 75 mA and 100 mA respectively. As the potential decreases, a 4 electron reduction of oxygen on the cathode becomes possible (equation 10). This reaction appears competitive with the formation of H_2O_2 at higher applied currents. Badellino et al

observed similar results with a reticulated vitreous carbon electrode when the potential was decreased below -1.7 V vs. SCE [9].

(10) $O_2 + 4e\text{-} + 4H^+ \rightarrow 2H_2O$
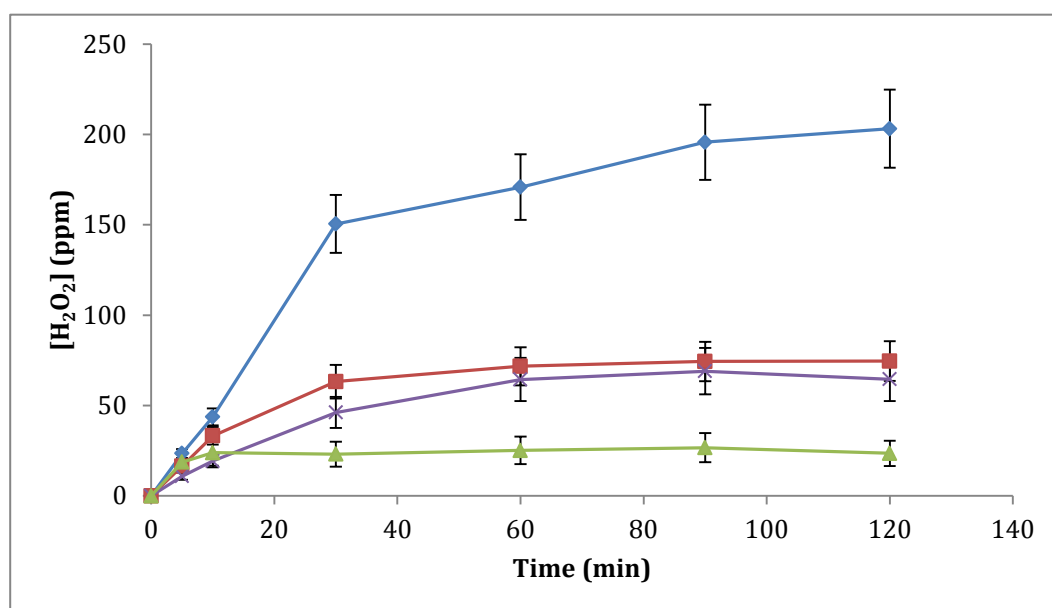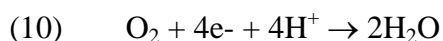
Figure 5.4. Plot showing the effect of current applied on H_2O_2 production in 50 ml of 0.1 M Na_2SO_4 in an undivided cell with a woven carbon fibre electrode. Purple line: 25 mA. Blue line: 50 mA. Red line: 100 mA. Green line: 200 mA.

5.3.6. Testing the regeneration of Fe(II) from Fe(III) in a divided cell

Based on the results of the previous section for the greatest production of H_2O_2, the divided cell configuration was used for all future work.

As discussed earlier, traditional Fenton processes are prone to producing iron sludge (ferric hydroxides) as a by-product. This insoluble sludge is a significant problem and

requires additional separation and disposal. In the electro-Fenton process Fe(III) can be continually cycled back to Fe(II) on the cathode, to avoid the build-up of iron sludge in the system. The ability of the woven carbon fibre electrode to regenerate Fe(II) from Fe(III) was tested in two ways; the first was the electrodes ability to reduce a 500 ppm solution of iron(III) ammonium sulfate to the iron(II) species. Figure 5.5 shows that at an applied current of 50 mA, there is a steady decline in Fe(III) concentration over the first 30 min. At 30 min a spike of iron(III) ammonium sulfate was added to the system giving an additional 500 ppm of Fe(III) in the cell. After the spike the concentration of Fe(III) continued to decrease slowly as the new Fe(III) addition continued to dissolve into solution while also being converted to Fe(II). After 40 min there was rapid removal of iron(III) from the solution. After 60 min of electrolysis the concentration of Fe(III) had been reduced from a total concentration of 1000 ppm to 220 ppm. The total concentration of Fe(III) in this solution was much higher than the catalytic amount of iron used in the electro-Fenton system, suggesting that the system should be capable of cycling Fe(III) to Fe(II) in the operating conditions required for the electro-Fenton system.
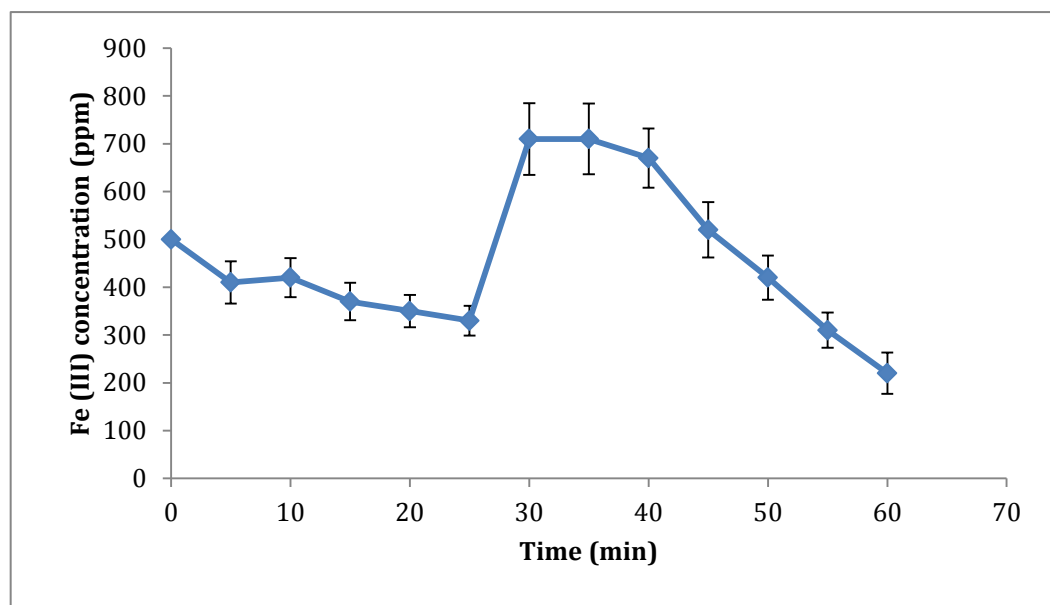
Figure 5.5. Plot showing the Fe(III) concentration against time for a woven carbon fibre electrode reducing Fe(III) to Fe(II) at an applied current of 50 mA. The starting Fe(III) concentration was 500 ppm and a spike of 500 ppm Fe(III) was introduced at 30 min. The pH was maintained between 2.8 and 3 with 1 M H_2SO_4 in a supporting electrolyte of 0.1 M Na_2SO_4 for the duration of the experiment.

The second method of testing the regeneration of Fe(II) from Fe(III) was an experiment that was more representative of the system used to fragment proteins. Initially the cell contained 1×10^{-3} M iron(II) sulfate with 0.1 M Na_2SO_4 as supporting electrolyte. H_2O_2 (0.02 M) was added to the system to initiate the Fenton reaction as the current to the electrodes was applied. The cell was thoroughly deoxygenated prior to the experiment to minimize the amount of H_2O_2 that the cell would produce.

It is expected that almost all of the Fe(II) in the system would be converted to Fe(III) immediately after the addition of the H_2O_2 at the beginning of the experiment (equation 1). Figure 5.6 shows that after 30 min, 0.8 % of the starting H_2O_2 remained in solution and there is good correlation between the drop in concentration of H_2O_2 and the rise in

Fe(II) concentration between 5 and 30 min. The system regenerates Fe(II) to approximately 60 % of its starting concentration after 90 minutes. This is an encouraging result as the working electrode is producing some extra H_2O_2 during the experiment, which is expected to slow the net rate at which Fe(III) is converted to Fe(II).

The conditions found to be most suitable for production of H_2O_2 with a woven carbon fibre electrode in this work, consist of a divided cell with a porous glass frit bubbler, an applied current of 50 mA and no pH adjustment during production of H_2O_2. These conditions will be used for the fragmentation of proteins in the remainder of this chapter.
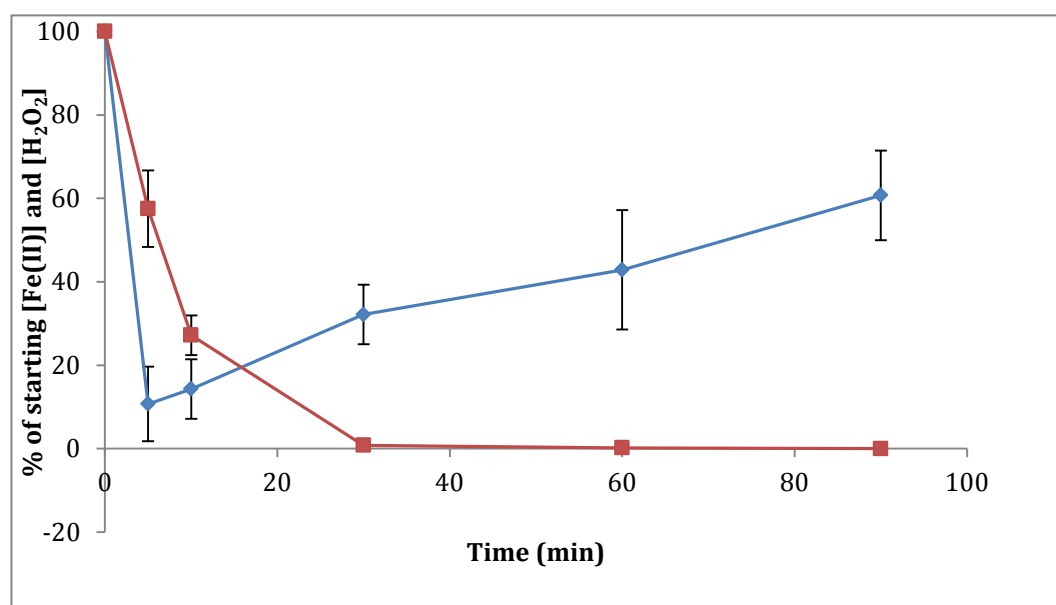
Figure 5.6. Plot of percentage starting concentrations of H_2O_2 and Fe(II) against time showing the ability of a woven carbon fibre electrode to regenerate Fe(II) during a Fenton reaction. 0.02 M H_2O_2 was added to 1×10^{-3} M $FeSO_4$ with 0.1 M Na_2SO_4 as supporting electrolyte, pH was maintained between 2.8 and 3 with 1 M H_2SO_4 at an applied current of 50 mA. Blue line: % of starting Fe(II) concentration. Red line: % of starting H_2O_2 concentration.

5.3.7. Fragmentation of proteins using the Fenton reaction

In terms of using the Fenton reaction as method for fragmenting proteins, the main challenge is achieving specific fragmentation in the protein as with PbO_2 electrodes in Chapter 4. Hydroxyl radicals react very quickly after they are generated so they will react in close proximity to where they are generated. In Chapter 4 the hydroxyl radicals were generated at an electrode, whereas in this chapter it is the interactions between the protein and the metal ion that is used to initiate the Fenton reaction. Controlling where the hydroxyl radicals are generated on the protein may provide a measure of control over where in the protein the radicals react. However, if there are no favourable binding opportunities or electrostatic interactions between the proteins and the metal ion used to initiate the Fenton reaction, then random fragmentation is also a possibility.

Initially, protein fragmentation experiments were conducted by generating H_2O_2 in the cathode compartment of the electrolysis cell until the desired concentration was reached, then the cell was turned off and the protein and iron(II) were added, no current was applied for regeneration of Fe(II) species. Regeneration of Fe(II) during the Fenton reaction is investigated later in this chapter. BSA was used initially to identify suitable conditions for the Fenton reaction that would produce specific fragmentation products. The reaction time was 10 min and the reaction was stopped by increasing the pH of the solution to 9 by addition of NaOH, Fe(III) species quickly become insoluble at this pH, stopping the regeneration of the required Fe(II) for the Fenton reaction. Figure 5.7 shows the fragmentation pattern of BSA when 50 μM Fe(II) and BSA were added to electrolysis solution containing 1 mM H_2O_2, some loss of the BSA protein band at ~66 kDa is apparent in lane 3 of figure 5.7, however no specific fragments are evident. The same

experiment as that shown in lane 3, except with an increased H_2O_2 concentration, was repeated. The results showed an increased loss of the starting protein material, however fragmentation was non-specific (results not shown). It was considered that disulfide bonds within the protein structure might be causing the protein to remain in a conformation that prevented hydroxyl radicals accessing a number of potential cleavage sites. For this reason 3 mM Dithiothreitol (DTT) was added at the beginning of an experiment (gel lane 4, figure 5.7) to remove the effect of the disulfide bonds using the same conditions. Addition of DTT gave an apparent increase in specific protein fragmentation, however the mechanism is unclear. DTT may have exposed new cleavage sites, but DTT is also an efficient hydroxyl radical scavenger, and might protect parts of the protein, so that only the most susceptible places on the protein are cleaved by hydroxyl radicals. This effect was also thought to be an important factor in specific protein fragmentation with PbO_2 electrodes in glycine/HCl buffer discussed in chapter 4 and may also be responsible for giving the specific fragmentation shown in lane 4 of figure 5.7. Figure 5.7, lane 2, shows the blank for Fe(II) and BSA without H_2O_2. Blanks were also run with DTT and BSA alone and also BSA, DTT and Fe(II). No fragmentation of BSA was evident in blanks (results not shown).
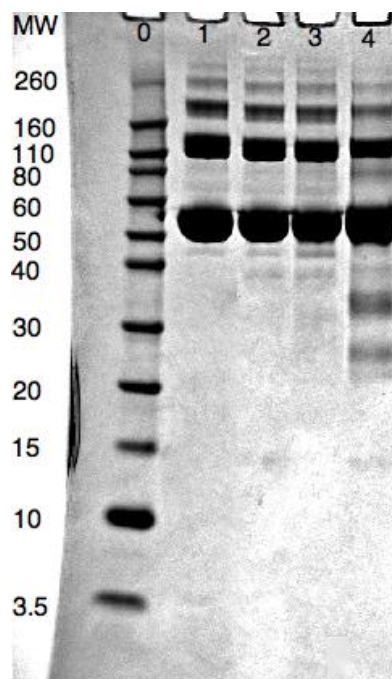
Figure 5.7. Electrophoresis gel image showing the effect of the Fenton reaction on the fragmentation of BSA in 0.1M Na_2SO_4. Reaction time: 10 min at pH 2.8 (adjusted with H_2SO_4) Reaction was stopped by adding NaOH to an aliquot of the electrolysis solution until pH 9. Lane 0: molecular mass markers. Lane 1: BSA control. Lane 2: 50 µM Fe(II). Lane 3: 50 µM Fe(II), 1 mM H_2O_2. Lane 4: 50 µM Fe(II), 1 mM H_2O_2, 3 mM DTT.

In order to investigate the influence of DTT on the system discussed above, two different buffers were used as the supporting electrolyte for the Fenton reaction. The buffers trialed were glycine/HCl and potassium hydrogen phthalate/HCl. Both buffers are capable of buffering the pH at 2.8. The electrophoresis gel image of the results of the two experiments with Fe(II), H_2O_2 and whey protein in the different buffers is shown in figure 5.8(a). Some visible specific fragmentation is apparent in Fe(II)/H_2O_2/glycine/HCl buffer system with one new band visible between the bands of β-lactoglobulin (~18 kDa) and α-lactalbumin (~14 kDa) and one below the band of α-lactalbumin (lane 2). No specific fragmentation is visible in potassium hydrogen phthalate/HCl however, so it appears that glycine/HCl plays a crucial role at some stage during the reaction and it is likely that the role of DTT in the earlier experiment is as a hydroxyl radical scavenger. In figure 5.8(b),

the effect of increasing the H_2O_2 concentration in the glycine/HCl system is shown.

Increasing H_2O_2 concentration provides more fuel for the Fenton reaction leading to

increased production of hydroxyl radicals. The concentration of the specific fragments

does not increase as more whey is fragmented. The fragments are also broken down

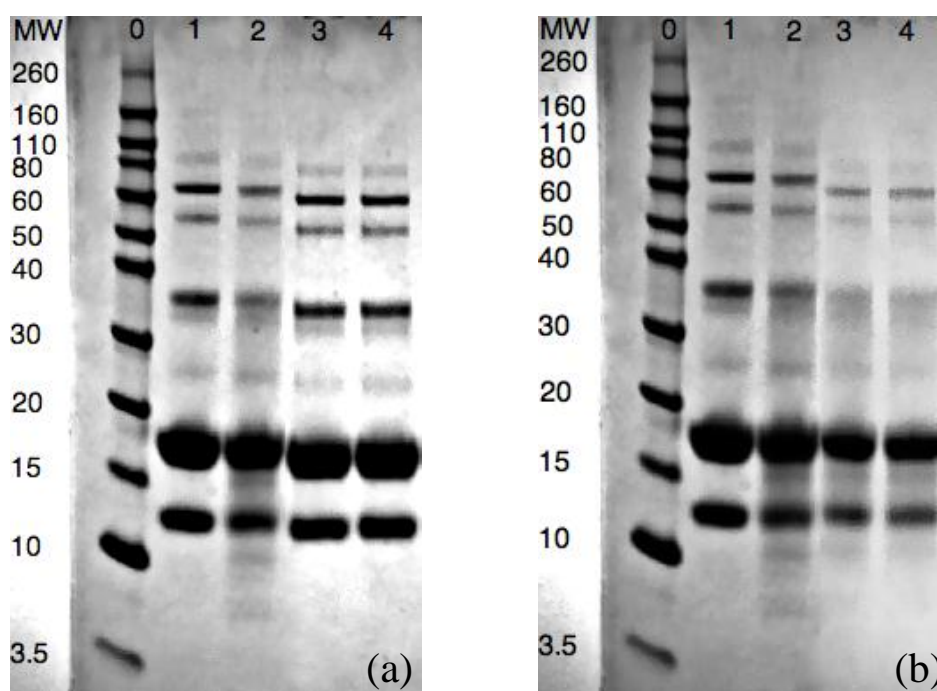during the reaction as evidenced by their disappearance at increased initial concentrations

of H_2O_2.

Figure 5.8.(a) Gel image showing the effect of using Fe(II) to initiate the Fenton reaction with H_2O_2 in different buffers at pH 2.8 on the fragmentation of whey. Lane 0: Molecular weight markers. Lane 1: 0.05 M glycine/HCl buffer control. Lane 2: 0.05 M glycine/HCl buffer, 50 μM Fe(II), 1 mM H_2O_2, 30 min reaction time. Lane 3: 0.05 M pH 2.8 potassium hydrogen phthalate/HCl buffer control. Lane 4: 0.05 M potassium hydrogen phthalate/HCl buffer, 50 μM Fe(II), 1 mM H_2O_2, 30 min reaction time. (b) Gel image showing the effect of increasing the H_2O_2 concentration on the fragmentation of whey in 0.05 M pH 2.8 glycine/HCl buffer for the Fenton reaction with 50 μM Fe(II). Lane 0: Molecular weight markers. Lane 1: Control. Lane 2: 1 mM H_2O_2. Lane 3: 2 mM H_2O_2. Lane 4: 4 mM H_2O_2.

The Fe(II)/H_2O_2/glycine/HCl buffer system was investigated for fragmentation of the

other proteins of interest. The results of these experiments are shown in figure 5.9. There

is some specific fragmentation evident with some light bands evident at ~22 kDa and ~18

kDa for β-casein (lanes 1-3), but there is also cross-linking evident with a strong increase in concentration of the band between 50 and 60 kDa in lanes 2 and 3. β-lactoglobulin (lanes 4-6) also gives some specific fragmentation, although the broad staining beneath the main band indicates that some of the fragmentation is also non-specific. Specific fragmentation is evident for BSA (lanes 7-8) with definite bands forming beneath the main band. Casein shows some reduction in intensity of the main protein bands and no significant evidence of an increase in higher molecular weight bands, so it is probable that some non-specific fragmentation of casein is occurring.
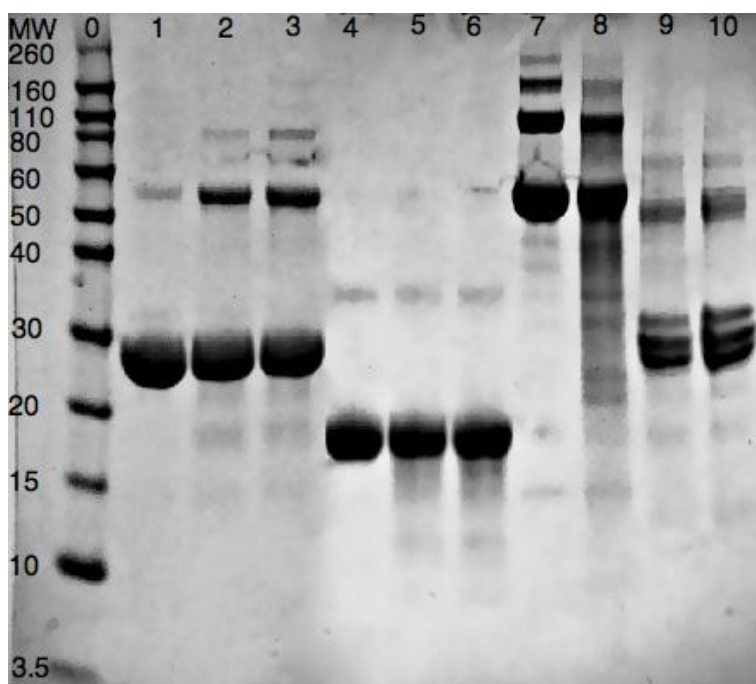
Figure 5.9. Gel image showing the effect of using Fe(II) to initiate the Fenton reaction with H_2O_2 in 0.05 M pH 2.8 glycine/HCl buffer on the fragmentation of the target proteins. Lane 0: molecular weight markers. Lane 1: β-casein control. Lane 2: β-casein, 1 mM H_2O_2, 50 μM Fe(II). Lane 3: β-casein, 2 mM H_2O_2, 50 μM Fe(II). Lane 4: β-lactoglobulin control. Lane 5: β-lactoglobulin, 1 mM H_2O_2, 50 μM Fe(II). Lane 6: β-lactoglobulin, 2 mM H_2O_2, 50 μM Fe(II). Lane 7: BSA control. Lane 8: BSA, 1 mM H_2O_2, 50 μM Fe(II). Lane 9: Casein, 1 mM H_2O_2, 50 μM Fe(II). Lane 10: Casein control.

5.3.8. Effect of electrochemical regeneration of Fe(II) from Fe(III) on protein fragmentation

The electro-Fenton system described to this point has only been used in the capacity of generating H_2O_2 before the protein and Fe(II) are added to initiate the Fenton reaction. H_2O_2 is not generated with Fe(II) and protein present in the system because H_2O_2 generation requires O_2 to be bubbled into the solution. Bubbling oxygen through a solution containing proteins causes excessive foaming, which is a problem.

Another way the electro-Fenton system can be used is to increase efficiency of the reaction by recycling Fe(II) from Fe(III) for reuse in the Fenton reaction. Fe(III) will be cycled back to Fe(II) without electrochemical regeneration upon reaction with H_2O_2, but the reaction is slow and consumes H_2O_2. In the electro-Fenton system, this can be achieved on the same electrode that is used to generate H_2O_2, so works well in the same divided cell used to generate H_2O_2.

Figure 5.10 (lanes 1-2) shows the results of an experiment in which H_2O_2 is generated until a concentration of 5 mM is reached in glycine/HCl buffer, in a divided cell with a woven carbon fibre electrode. The cell is then turned off before the pH is adjusted to 2.8 and BSA and Fe(II) are added to start the Fenton reaction. Some specific fragmentation of BSA occurs in this system. Lanes 3-7 in figure 5.10 show the difference in efficiency of the reaction when just the oxygen is switched off and the cell left on to recycle Fe(II) for use in the reaction. After just 5 minutes of reaction time almost all of the starting protein has been consumed. Clearly, having the cell on has significantly increased the speed of

fragmentation. One thing that must be kept in mind is that some further H_2O_2 will be produced on the working electrode, as there will likely be some residual oxygen left in the system from the initial generation of H_2O_2. Hence some of the increased fragmentation may be due to an increased H_2O_2 concentration. The fragmentation of BSA is not specific during this process; there is significant non-specific fragmentation that can be seen by the staining down the length of the gel lanes. Hence, even though there is a radical scavenger in the form of glycine/HCl buffer present, it is difficult to achieve specific fragmentation when the cell is running to regenerate Fe(II) from Fe(III).

Figure 5.10. Gel image showing the effect of the electrochemical regeneration of Fe(II) for use in the Fenton reaction on the fragmentation of BSA in 0.05 M pH 2.8 glycine/HCl buffer. H_2O_2 was generated until a concentration of 5 mM was reached prior to reaction on a woven carbon fibre electrode at 50 mA. Lane 0: Molecular weight markers. Lane 1: BSA control. Lane 2: 30 min reaction time, no electrochemical regeneration of Fe(II). Lane 3: BSA control. Lane 4-7: With electrochemical regeneration of Fe(II), 5 min, 10 min, 20 min and 30 min reaction time respectively.

The electrochemical regeneration of Fe(II) system was used on the target proteins whey and casein to effect fragmentation in glycine/HCl buffer. H_2O_2 was generated to a

concentration of 5 mM in glycine/HCl buffer before introduction of protein and Fe(II). BSA and whey were both extensively and non-specifically fragmented in these conditions (figure 5.11, lanes 1-4). The process was not as effective with casein, which only lost a small amount of intensity on the main protein bands on the gel in figure 5.15, lanes 5-6. Similar results with casein were also observed in chapter 4, the reason for the slower fragmentation when compared to the other proteins in this study could be due to the hydrophobic nature of casein meaning that it exists in aqueous solutions as a suspension of micelles. The micellar structure of casein in aqueous solution is likely to be keeping large hydrophobic areas of the protein inaccessible (and therefore unable to be cleaved) to hydroxyl radicals, which are generated in the aqueous solution.

Using electrochemical regeneration of Fe(II) on whey proteins leads to an increase in the speed of fragmentation (figure 5.11, lanes 3-4), but the fragmentation is largely non-specific. The reason for this remains unclear, however as found in earlier reactions with no regeneration of Fe(II) but at high H_2O_2 concentrations, it is possible that if the reaction progresses too far, specific fragments are also consumed in the process.
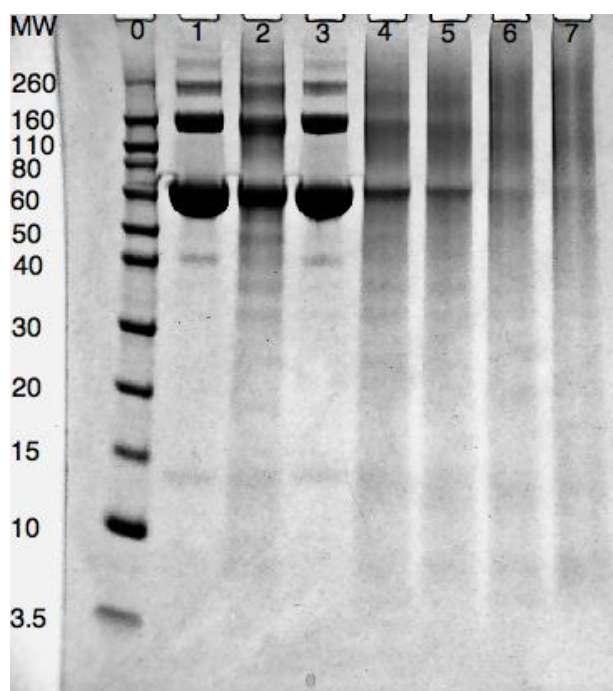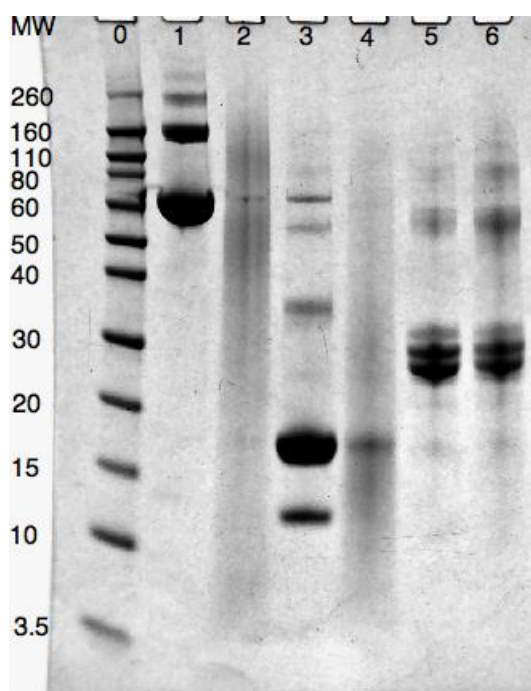
Figure 5.11. Gel image showing the effect of the electrochemical regeneration of Fe(II) for use in the Fenton reaction on the fragmentation of BSA, casein and whey in 0.05 M pH 2.8 glycine/HCl buffer. H_2O_2 was generated to a concentration of 5 mM prior to reaction on a woven carbon fibre electrode at 50 mA. Fe(II) was regenerated on the working electrode during the reaction in lanes 2, 4 and 6. Lane 0: molecular weight markers, Lane 1: BSA control. Lane 2: BSA, 30 min reaction time. Lane 3: Whey control. Lane 4: Whey, 30 min reaction time. Lane 5: Casein control. Lane 6: Casein, 30 min reaction time.

5.3.9. Copper initiated Fenton Reaction

The Fenton reaction can also be initiated by Cu(II) to produce hydroxyl radicals with H_2O_2. In order to investigate if the interactions between a different metal ion and the target proteins would have an effect on the fragmentation, experiments were conducted with Cu(II) in place of Fe(II) in the Fenton reaction.

BSA has been shown to bind to copper;[3] Cu(II) has been used previously with H_2O_2 to generate hydroxyl radicals to cleave BSA by Buranaprapuk et al in a non-electrochemical process.[4] Initially, the electrochemical system was used to generate the H_2O_2 required for the reaction with Cu(II) in order to try and reproduce the results of Buranaprapuk et al

134

with the electro-Fenton system. Cu(II) is able to be used at neutral pH, for this reason a 0.05 M pH 7 tris/HCl buffer system was used to provide the possibility of hydroxyl radical scavenging (as described in chapter 4). BSA was fragmented specifically (lane 2 figure 5.12). As a comparison pH 7 phosphate buffer, which lacks the ability to scavenge hydroxyl radicals, was also used as a reaction medium (lane 4, figure 5.12). Fragmentation of the main band of BSA was much more extensive in phosphate buffer, but it was also much less specific (as indicated by smearing in the gel lane). However there are some regions on lane 4 of the gel, of greater intensity and these correspond to the fragments seen in the tris system. This observation is most likely a result of copper ions binding to specific parts of the protein and fragmentation occurring nearby. However without a hydroxyl radical scavenger as in the tris system, some of the radicals diffuse away from the areas where the copper is bound and react with other parts of the protein giving less specific cleavage.
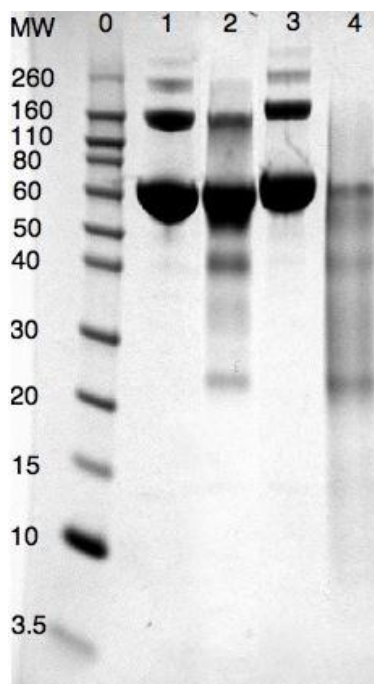
Figure 5.12. Gel image showing effect of buffer system on the fragmentation of BSA by hydroxyl radicals generated by 0.5 mM Cu(II) and 1 mM H_2O_2. Lane 0: molecular weight markers. Lane 1: 50 mM Tris/HCl buffer pH 7 control. Lane 2: 50 mM Tris/HCl buffer, pH 7, 30 min reaction time. Lane 3: 50 mM Phosphate buffer pH 7 control. Lane 4: 50 mM Phosphate buffer, pH 7, 30 min reaction time. The reaction was stopped by adding an aliquot of the reaction mixture to a mixture of DTT and SDS in preparation for electrophoresis.

The Cu(II)/H_2O_2 system of generating hydroxyl radicals was successful for use in fragmenting BSA, so it was applied to whey and casein. Unfortunately specific fragmentation did not occur when the system was used with casein and whey proteins (figure 5.13). β-lactoglobulin (lanes 1-2), a major fraction of whey, appears to have undergone fragmentation followed by cross linking of the smaller fragments and starting material to give higher molecular weight products, leaving no evidence of the smaller molecular weight fragments on the gel. The β-lactoglobulin (~18 kDa) fraction of whey (lanes 3-4) behaved in the same way as the isolated sample (lane 2) and there was some loss in intensity of α-lactalbumin (~14 kDa), but no evidence of specific fragmentation. Cross-linking was again the result when the Cu(II)/H_2O_2 system in tris/HCl buffer was

applied to β-casein, a major fraction of the casein proteins (lanes 5-6). In this case, based on the size of the fragments, it appears that protein units joined together to form trimers, tetramers and so on. The same was also true when the system was applied to whole casein (lanes 7-8). These results suggest that the target proteins do not have the same copper binding ability as BSA. There could also be free radical induced di-tyrosine cross-linking in the proteins in the presence of copper, which has been demonstrated in several studies[11-13]
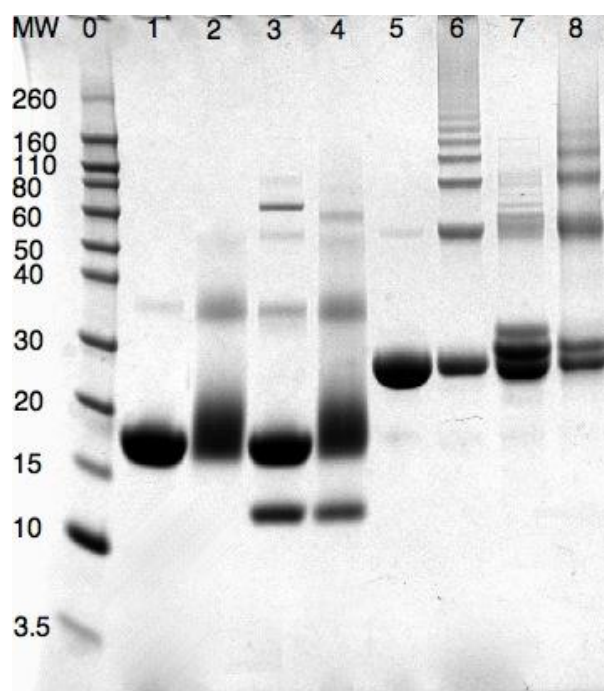
Figure 5.13. Effect of Cu^{2+}/H_2O_2 system on target proteins in 0.05 M pH 7 Tris/HCl buffer. 0.5 mM Cu(II) and 1 mM H_2O_2 were used for the Fenton Reaction in experiments represented by lanes 2, 4, 6, 8. Lane 0: Molecular mass markers. Lane 1: β-lactoglobulin control. Lane 2: β-lactoglobulin, 30 min reaction time. Lane 3: Whey control. Lane 4: Whey, 30 min reaction time. Lane 5: β-casein control. Lane 6: β-casein, 30 min reaction time. Lane 7: Casein control. Lane 8: Casein, 30 min reaction time. The reaction was stopped by adding an aliquot of the reaction mixture to a mixture of DTT and SDS in preparation for electrophoresis.

It has been reported that β-lactoglobulin has a hydrophobic pocket capable of binding small hydrophobic molecules.[14] In order to take advantage of this property, Cu(II) was complexed with a more hydrophobic ligand, 1,10 phenanthroline (figure 5.14(b)). The

goal was to bind copper to β-lactoglobulin at specific sites to induce specific cleavage. The gel image in figure 5.14(a) shows the results of the experiments with phenanthroline. Comparing lane 2 (no phenanthroline) and lane 3 (with phenanthroline), a small amount of specific fragmentation can be seen beneath the main β-lactoglobulin band in lane 3 but not in lane 2. These results suggest that the hydrophobic ligand increases specific fragmentation, but it also highlights another issue when using copper with β-lactoglobulin. Copper has been shown to catalyse dimer formation by way of a disulfide bridge between the free sulfhydral groups in the β-lactoglobulin monomers.[15] The thick bands at ~36 kDa in the gel lanes for the experiments that included copper clearly show that copper catalysed dimer formation is occurring. In order to combat this, DTT was also included in the reaction mixture giving the results shown in lanes 5 and 6. DTT had little effect on the formation of the dimer when phenanthroline was not present (lane 5), however DTT decreased dimer formation when phenathroline was present (compare lanes 6 and 3). Unfortunately, addition of DTT did not result in a higher concentration of specific fragments being visible by gel electrophoresis. The origin of this effect is not known and was not investigated.

As described above, Phenanthroline improved the specific fragmentation of β-lactoglobulin with Cu(II) and H_2O_2 to a small extent, possibly because the copper was able to bind in the hydrophobic binding pocket of β-lactoglobulin initiating a small site specific fragmentation, however the results were not considered sufficiently promising to warrant further work, especially considering the dimerisation problems that would need to be overcome.

Copper was effective at initiating the Fenton reaction to produce site-specific fragmentation of BSA, but was ineffective at causing specific fragmentation on casein and whey protein and mainly resulted in higher molecular weight products. For the target proteins casein and whey, Fe(II) is the more suitable metal ion to initiate the Fenton reaction.
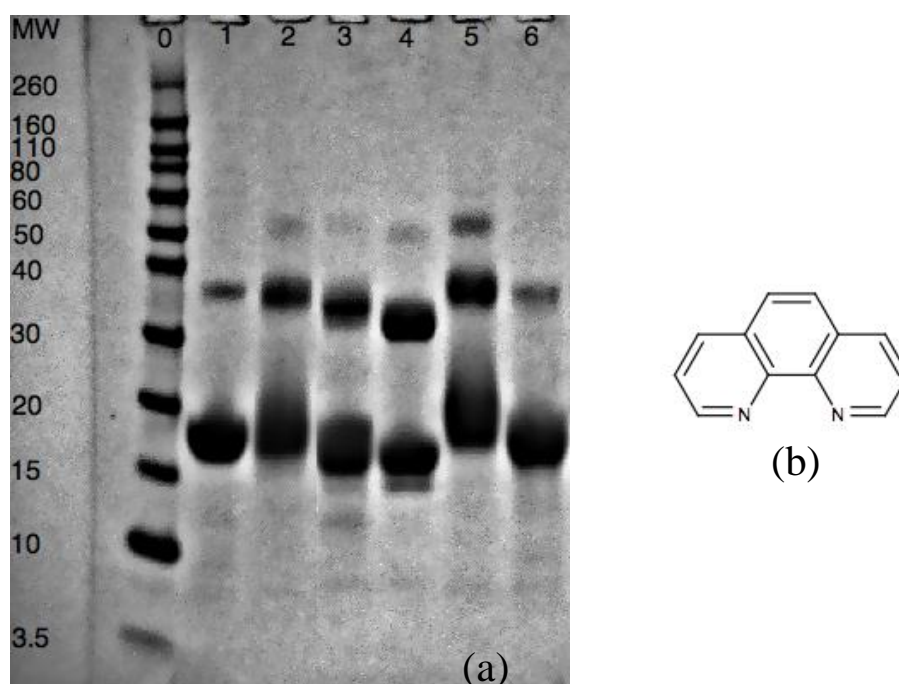
Figure 5.14. (a) Gel image showing the effect of Cu(II) complexed by a hydrophobic ligand 1,10 phenanthroline in the fragmentation of β-lactoglobulin in 50 mM pH 7 Tris HCl buffer induced by the Cu(II) initiated Fenton reaction. Lane 1: β-lactoglobulin control. Lane 2: 0.5 mM Cu^{2+}, 1 mM H_2O_2. Lane 3: 0.5 mM Cu^{2+}, 1 mM H_2O_2, 1 mM Phenanthroline Lane 4: Control, 0.5 mM Cu^{2+}, 1 mM Phenanthroline. Lane 5: 0.5 mM Cu^{2+}, 1 mM H_2O_2, 3 mM DTT Lane 6: 0.5 mM Cu^{2+}, 1 mM H_2O_2, 1 mM phenanthroline, 3 mM DTT. The reaction was stopped by adding an aliquot of the reaction mixture to a mixture of DTT and SDS in preparation for electrophoresis. (b) Structure of 1,10 phenanthroline.

5.4 Conclusion

In this work, the best system for generation of H_2O_2 with a woven carbon fibre electrode was a divided cell, so that the counter electrode did not remove the H_2O_2 from the system. The system produced H_2O_2 faster when the pH was not controlled, than when the pH was kept between 2.8 and 3 ready for the Fenton reaction. Higher applied currents on the working electrode produced H_2O_2 at a faster rate initially, but over time the concentration of H_2O_2 would stabilize due to the consumption of H_2O_2 on the working electrode at higher H_2O_2 concentrations. The method of delivery for oxygen was found to have a large influence on the production of H_2O_2: using a porous glass frit rather than a 4 hole glass bubbler to bubble oxygen produced smaller bubbles and substantially increased the efficiency for oxygen use for production of H_2O_2. The woven carbon fibre working electrode showed the ability to regenerate Fe(II) from Fe(III) improving the efficiency of the Fenton reaction by speeding up the recycling of Fe(II) for reaction with H_2O_2, and reducing the amount of H_2O_2 reacting with Fe(III).

Using pH 2.8 glycine/HCl buffer with Fe(II) to initiate the Fenton reaction led to visible fragmentation products in β-lactoglobulin, BSA, β-casein and the combination of whey proteins. There was evidence of specific fragmentation occurring, but it was not possible to increase the concentration of these products by adding more H_2O_2 to fuel the Fenton reaction. The fragmentation products were removed along with the starting protein material during this process.

When the electro-Fenton cell was used to generate H_2O_2 and also to regenerate Fe(II), an improved efficiency of fragmentation of the protein was achieved. This was likely due to the regeneration of Fe(II), but there is a possibility that a small amount of extra H_2O_2 was produced from dissolved oxygen in the system. The fragmentation of the proteins in this system was largely non-specific, so although the efficiency of fragmentation improved, the specificity of fragmentation decreased. The regeneration of Fe(II) during the Fenton reaction caused most of the starting protein material to be consumed during the reaction; this amount of fragmentation could also have caused the fragments to be consumed.

Cu(II) was trialed as a way to initiate the Fenton reaction as BSA has previously been reported to have the ability to bind Cu(II), therefore allowing site-specific production of hydroxyl radicals. This was shown to be the case with BSA and it was hoped that this principle could be applied to other proteins of interest. However, this approach was not successful for casein and whey and cross linking of the proteins was observed. β-lactoglobulin fragmentation was improved by a small extent when using Cu(II) complexed by hydrophobic phenanthroline ligands, presumably because copper bound in a hydrophobic pocket of β-lactoglobulin and produce hydroxyl radicals at that site.

While specific fragmentation of the target proteins was able to be achieved in the electro-Fenton system, the fragmentation was not as specific and the concentration of fragmentation products was not able to be increased to the same level as that produced with PbO_2 electrodes (chapter 4).

References

1.   Haber, F. and J. Weiss, *The Catalytic Decomposition of Hydrogen Peroxide by Iron Salts.* Proceedings of the Royal Society of London. Series A, Mathematical and Physical Sciences, 1934. **147**(861): p. 332-351.

2.   George, P., W.G. Barb, K.R. Hargrave, and J.H. Baxendale, *Reactions of Ferrous and Ferric Ions with Hydrogen Peroxide.* Nature (London), 1949. **163**(4148): p. 692-694.

3.   Kocha, T., M. Yamaguchi, H. Ohtaki, T. Fukuda, and T. Aoyagi, *Hydrogen peroxide-mediated degradation of protein: different oxidation modes of copper- and iron-dependent hydroxyl radicals on the degradation of albumin.* Biochimica et Biophysica Acta (BBA) - Protein Structure and Molecular Enzymology, 1997. **1337**(2): p. 319-326.

4.   Buranaprapuk, A., S.P. Leach, C.V. Kumar, and J.R. Bocarsly, *Protein cleavage by transition metal complexes bearing amino acid substituents.* Biochimica et biophysica acta, Protein structure and molecular enzymology, 1998. **1387**(1): p. 309-316.

5.   Choi, S.Y., H.Y. Kwon, O.B. Kwon, W.S. Eum, and J.H. Kang, *Fragmentation of human ceruloplasmin induced by hydrogen peroxide.* Biochimie, 2000. **82**(2): p. 175-180.

6.   Oturan, M.A., I. Sirés, N. Oturan, S. Pérocheau, J.-L. Laborde, and S. Trévin, *Sonoelectro-Fenton process: A novel hybrid technique for the destruction of organic pollutants in water.* Journal of Electroanalytical Chemistry, 2008. **624**(1-2): p. 329-332.

7.   Panizza, M. and M.A. Oturan, *Degradation of Alizarin Red by electro-Fenton process using a graphite-felt cathode.* Electrochimica Acta, 2011. **56**(20): p. 7084-7087.

8.   Zhang, H., D. Zhang, and J. Zhou, *Removal of COD from landfill leachate by electro-Fenton method.* Journal of Hazardous Materials, 2006. **135**(1-3): p. 106-111.

9.   Badellino, C., C.A. Rodrigues, and R. Bertazzoli, *Oxidation of pesticides by in situ electrogenerated hydrogen peroxide: Study for the degradation of 2,4-dichlorophenoxyacetic acid.* Journal of Hazardous Materials, 2006. **137**(2): p. 856-864.

10.   Ozcan, A., Y. Sahin, A. Savas Koparal, and M.A. Oturan, *Carbon sponge as a new cathode material for the electro-Fenton process: Comparison with carbon felt cathode and application to degradation of synthetic dye basic blue 3 in aqueous medium.* Journal of Electroanalytical Chemistry, 2008. **616**(1-2): p. 71-78.

11.   Balasubramanian, D. and R. Kanwar, *Molecular pathology of dityrosine cross-links in proteins: Structural and functional analysis of four proteins.* Molecular and Cellular Biochemistry, 2002. **234-235**(1): p. 27-38.

12.   Pacifici, R.E., *Protein damage and degradation by oxygen radicals*, in *ProQuest Dissertations and Theses*. 1991, University of Southern California: United States -- California. p. 1.

13.   Huggins, T.G., M.C. Wells-Knecht, N.A. Detorie, J.W. Baynes, and S.R. Thorpe, *Formation of o-tyrosine and dityrosine in proteins during radiolytic and metal-catalyzed oxidation.* The Journal of biological chemistry, 1993. **268**(17): p. 12341-12347.

14.   Brownlow, S., J.o.H.M. Cabral, R. Cooper, D.R. Flower, S.J. Yewdall, I. Polikarpov, A.C.T. North, and L. Sawyer, *Bovine β-lactoglobulin at 1.8Å resolution - still an enigmatic lipocalin.* Structure, 1997. **5**(4): p. 481-495.

15.   Saïd, B., H. Gwénaële, C. Florence, C. Thomas, F. Jacques, and M. Daniel, *Copper-catalyzed formation of disulfide-linked dimer of bovine β-lactoglobulin.* Lait, 2004. **84**(6): p. 517-525.

Chapter 6. Conclusions and future work

This thesis investigated the use of electrochemistry as a method to fragment whey and casein proteins. Direct electrochemical oxidation, electrochemical generation of hydroxyl radicals and electro-Fenton chemistry were each investigated as methods to achieve protein fragmentation. A key aim of this project was to achieve specific fragmentation meaning that fragmentation would only occur at specific sites on each protein molecule in the hope that this process may provide a new pathway to producing useful protein fragments.

Direct electrochemical oxidation of the target proteins was studied at a graphite rod electrode in a solution containing acetonitrile, water and formic acid. β-lactoglobulin was able to be fragmented in this solution, as evidenced by mass spectroscopy, but specific fragmentation products only occurred in low concentrations. Most of the electrolysis products appeared to be non-cleavage oxidation products. β-lactoglobulin was fragmented to a greater extent than β-casein and BSA. The smaller size of β-lactoglobulin may account for this. Acetonitrile is not desirable for use in an industrial setting, so attempts were made to lower its concentration in solution, however this resulted in a decreased amount of both protein fragmentation and non-cleavage oxidation products. The proteins were much more soluble when acetonitrile was present and this is thought to be playing a role in preventing protein adsorption to the electrode surface. Protein adsorption results in

decreased electron transfer from the electrode surface to the protein in solution and therefore less efficient electrochemical oxidation of the proteins.

Protein adsorption on electrode surfaces was demonstrated with glassy carbon electrodes. Modification of the glassy carbon surface with PEG films led to decreased protein adsorption, however electron transfer through the film to the protein was unable to be observed with cyclic voltammetry. Future work could focus on the optimisation of PEG films to improve the electron transfer through the film while maintaining its anti-fouling properties.

The use of PbO_2 electrodes to generate hydroxyl radicals was the main focus of this work, as initial indications were that this method is effective at generating hydroxyl radicals, whilst not being as complicated as the electro-Fenton reaction. For the first time, specific fragmentation of proteins has been achieved by electrochemical generation of hydroxyl radicals. The pH and chemical environment of the protein solutions were found to be crucially important to the process; this was investigated by using a range of different buffers and reagents at varied pH. Non-specific fragmentation was observed using phosphate buffer as the supporting electrolyte. To achieve specific protein fragmentation, three factors were found to be essential. These were low pH, a chemical environment that contained a primary amine based radical scavenger and the presence of HCl. Glycine/HCl buffer has all of these properties and was found to give the best results for specific fragmentation. No other additives were necessary to achieve specific protein fragmentation with PbO_2 electrodes.

As lead is a toxic metal the stability of the electrodes is very important. Accelerated lifetime testing and SEM analysis were conducted to assess PbO_2 film stability. Electrode preparation conditions were varied, including deposition rate of PbO_2 and deposition bath additives. The most stable PbO_2 films produced on a platinum substrate were prepared in the presence of the surfactant Triton X-100 at a deposition rate of 60 mA/cm^2, where the surface area is based on the geometric area of the platinum mesh. The optimum deposition rate will depend on the total active surface area of the platinum mesh electrode, and in future work, the relationship between PbO_2 stability and current density (based on the active electrode area) should be established.

Future work in this area would involve stability testing of PbO_2 electrodes in a range of different solutions and conditions. If the leaching of lead is a problem, boron doped diamond electrodes could be a viable alternative, as they have been shown to produce hydroxyl radicals in a very similar manner to PbO_2 electrodes. Boron doped diamond electrodes are extremely stable and do not release toxic components, however their high cost would have to be measured against the value of the protein fragments produced.

All of the target proteins were fragmented specifically with PbO_2 electrodes. Casein and whey proteins are very different in structure and properties, however both of these types of proteins were specifically fragmented with a PbO_2 electrode. Hence this process has the potential to produce fragmentation in a wide range of proteins. Important future work would involve investigating the fragmentation of many more proteins. Further work is also required to identify the protein fragments produced in this work and gain a better

understanding of the amino acid residues where fragmentation is occurring. If the fragmentation is found to occur in a predictable pattern it could become a fast, inexpensive and robust alternative to many of the enzymic and chemical methods currently used to achieve this. Optimisation of the current density during fragmentation would provide reduced costs if the process was to be scaled up for industrial applications.

Electro-Fenton chemistry was investigated using a woven carbon fibre electrode to produce H_2O_2 and regenerate Fe(II) from Fe(III). Electrochemical cell conditions including use of a single or double compartment format, oxygen delivery method and applied current were optimised for the production of H_2O_2 while still maintaining the ability to regenerate Fe(II) from Fe(III). As pH 2.8 glycine/HCl buffer was the best medium for production of hydroxyl radicals at PbO_2 electrodes, it was used with the electro-Fenton system, with and without electrochemical regeneration of Fe(II). Fragmentation products were produced for β-lactoglobulin, BSA, β-casein and the combination of whey proteins. There was evidence of specific fragmentation occurring, but it was not possible to increase the concentration of these products by adding more H_2O_2 to fuel the Fenton reaction. The fragmentation products were further fragmented along with the starting protein material upon increasing the H_2O_2 concentration. Electrochemical regeneration of Fe(II) increased the rate of fragmentation, however it was largely non-specific. The difference in the amount of specific fragmentation in the electro-Fenton and PbO_2 electrode systems highlights the importance of the hydroxyl radicals being physisorbed to the PbO_2 electrodes as this property is likely to account for the difference in the amount of specific fragmentation produced in the two systems.

Of the three methods of electrochemical fragmentation examined in this work, electrochemical production of hydroxyl radicals with PbO_2 electrodes was the most successful in producing specific protein fragmentation and is most applicable to further study and possible scaling up to an industrial level. This work has the potential to have an impact on several important areas: it could be used for hydrolysis of proteins required for nutrition and medical purposes and could also be used as a fast method for protein identification analysis with mass spectroscopy, in a similar way that trypsin is currently used for protein digestion before tandem mass spectroscopy. Clearly, identification of the protein fragments generated under different conditions is required before specific applications can be proposed.

As a final consideration, a cost benefit analysis for the PbO_2 system is important. The PbO_2 electrochemical fragmentation process uses only mild reagents; glycine/HCl buffer is the only reagent necessary for protein fragmentation. The process is environmentally clean as lead leaching into solution can be kept to a very low level when the electrodes are prepared by the methods outlined in this work. Electrolysis consumes electricity and hence in future work, a full cost assessment of the PbO_2 electrochemical fragmentation method should be undertaken to assess the potential of the method to be applied industrially.